

*ISSN 0970-5953*

*Volume 36. No. 3*

*July - September 2020*



# PHYSICS EDUCATION

THE NOBEL PRIZE  
IN PHYSICS 2020



Roger Penrose

Reinhard  
Genzel

Andrea  
Ghez

*[www.physedu.in](http://www.physedu.in)*

**Volume 36, Number 3****In this Issue**

- ❖ **A Simple Scale Factor in the Light of the Recent Planck Satellite Data Analysis** 08 Pages  
Robin Francis, C Sivakumar and E M Mohammed
  
- ❖ **Using Classical Collisions to Conceptualize High-Energy Physics Scattering Outcomes at Introductory Physics Level** 12 Pages  
V. Shekoyan, R. Armendariz, S. Dehipawala, G. Tremberger Jr, D. Lieberman, and T. Cheung
  
- ❖ **Why We Need Ensembles in Statistical Mechanics?** 09 Pages  
Prasath P, Reshma P and Udayanandan K M
  
- ❖ **BCS Theory in ( 2 × 2 ) Matrix Way** 16 Pages  
Debnarayan Jana
  
- ❖ **Spin Inequality for Energy Computation of Heisenberg Spin Hamiltonian** 07 Pages  
Debnarayan Jana
  
- ❖ **Revisiting Lees and Chorlton Disc Experiment** 10 Pages  
Deepak Jain
  
- ❖ **Elements of Electrical Safety for Physics Students** 08 Pages  
Emanuel Gluskin
  
- ❖ **Graphical Pedagogy Of Teaching Reciprocal Space** 08 Pages  
Adarsh Singh and Mitushi Gupta

# A Simple Scale factor for a curved Universe in the light of the recent Planck satellite data analysis

ROBIN FRANCIS, C SIVAKUMAR and E M MOHAMMED

Department of Physics, Maharaja's college, Ernakulam, Kerala, India

(Affiliated to M.G. University, Kottayam, Kerala)

thrisivc@yahoo.com

*Submitted on 10-May-2020*

## Abstract

The Standard Cosmology states that ours is a flat Universe of about 5% baryonic matter, 25% dark matter and 70% dark energy and is presently accelerating. But the analysis of the data released last year of the Planck satellite mission requires a reconsidering of these more or less established matters. Space-time could be positively curved and it may not be accelerating presently as it was five billion years back or so owing to dark matter. If that is the case, we need a new scale factor to explicate the fundamental features of the Universe and this paper suggests a simple scale factor for the Universe which is closed and having accelerated expansion for a definite period in the past consistent with the Friedman equations.

**Keywords:** Standard model of cosmology; Flat Universe; Baryonic matter; Dark matter; Dark energy; Planck satellite mission; Space time; Scale factor; Friedman

equations.

## 1.Introduction

If the Universe is isotropic and homogeneous on a large scale and space-time trajectories of the building blocks of the Universe are non-intersecting and orthogonal to a set of space-like surfaces of constant time, then Robertson-Lemaitre-Walker metric can be assumed for space-time and Einstein's gravitational field equations reduce to the Friedmann equations [1] which are the fundamental equations of standard cosmology:

$$\left(\frac{dR}{dt}\right)^2 + \frac{kc^2}{R^2} - \frac{8\pi G\rho}{3} = 0 \quad (1)$$

$$\left(\frac{dR}{dt}\right)^2 + \frac{kc^2}{R^2} + \frac{8\pi GP}{c^2} + 2\left(\frac{d^2R}{dt^2}\right) = 0 \quad (2)$$

where  $R$  is the scale factor of the Universe,  $\frac{dR}{dt} = H$  is the Hubble number and  $k$  is the curvature parameter which can take

any of the three values:  $+1$ ,  $0$ ,  $-1$ . Curvature parameter is  $+1$  for closed Universe or positively curved Universe,  $0$  for flat Universe and  $-1$  for open Universe or negatively curved Universe. Also,  $G$  is the Newton's constant of gravitation,  $c$  is the speed of light in vacuum,  $P$  is the uniform pressure and  $\rho$  the uniform mass density of the Universe which includes the density  $\rho_r$  of radiation,  $\rho_m$  of matter (baryonic plus dark) and  $\rho_d$  of dark energy of the cosmic fluid which are respectively 0%, 30% & 70% approximately in the present Universe [2].

Equations (1) and (2) together give,

$$\left(\frac{d^2R}{dt^2}\right) = -\frac{4\pi G\rho}{3}(1 + 3W) \quad (3)$$

where  $W = \frac{P}{\rho c^2}$  is the equation of state parameter.

Universe has decelerated expansion when  $W > -\frac{1}{3}$  and accelerated expansion when  $W < -\frac{1}{3}$ . The acceleration rate of expansion of the universe is quantified using the deceleration parameter  $q$ ;

$$q = -\frac{\frac{d^2R}{dt^2}}{H^2R} \quad (4)$$

where positive and negative  $q$  refers to deceleration and acceleration in the expansion of the universe. According to General Relativity, the source of gravity is  $S$ :

$$S = 3P + \rho c^2 \quad (5)$$

When  $S > 0$ , gravity sucks and when  $S < 0$ , instead of sucking gravity blows. In

other words, positive  $S$  has the tendency of stopping the Universe and making it contract while negative  $S$ , of forcing it to expand with acceleration [3].

The brightest microwave background fluctuations measured by the *Wilkinson Microwave Anisotropy Probe (WMAP)* to the accuracy of 0.004 are about one degree across [4] and it points to  $k = 0$ . The results of *Supernova Cosmology Project (SCP)* show that Universe is presently accelerating when measured accurately the redshifts produced by the standard candles that lie at a distance around 5 billion light years [5,6]. Also, the present Hubble number as obtained by WMAP is near 71 km/s/ Mpc [7].

The paper is organized as follows. Section 2 discusses the new model, section 3 describes the results we obtained and finally section 4 the conclusions.

## 2 The model

Based on the *Cosmic Microwave Background Radiation Gravitational Lensing Data* collected by the *Planck satellite* of the *European Space Agency*, Universe cannot be flat as WMAP declared. According to an international team of astronomers led by Eleonora Di Valentino this calls for a rethinking of the Standard model of Cosmology. Planck collaboration call this anomaly  $A_{lens}$ , a parameter which rescales the amplitude of

the lensing potential to smooth the power spectrum and a possible explanation for it could be the positive curvature of the Universe [8, 9, 10, 11, 12].

If  $k$  is  $+1$ , Universe has to stop at some stage in future and start contracting as in the Friedmann model of closed Universe [13]. This paper presents the simplest closed model of a Universe that has acceleration as required by SCP around the time of 8.7 billion years from Big Bang, which is believed to have occurred 13.7 billion years back and consistent with the other proven features of the Universe.

Let the scale factor is

$$R \approx B \sin^2 \Theta, \Theta = \omega t \quad (6)$$

for sufficiently large  $t$  with  $\omega$  as a constant. This is the simplest periodic function that grows from zero when  $t$  rises from zero having second derivative positive in the early phase.

Then, Hubble number

$$H = \frac{2\omega}{\tan \Theta} \quad (7)$$

Acceleration

$$\frac{d^2 R}{dt^2} = 2\omega^2 B \cos 2\Theta \quad (8)$$

Pressure by equation (2)

---


$$P = -\left(\frac{c^2}{8\pi G B^2 \sin^4 \Theta}\right)(c^2 + 4\omega^2 B^2 \sin^2 \Theta \cos 2\Theta + 4\omega^2 B^2 \sin^2 \Theta \cos^2 \Theta) \quad (9)$$

Density by equation (1)

$$\rho = \left(\frac{3}{8\pi G B^2 \sin^4 \Theta}\right)(c^2 + 4\omega^2 B^2 \sin^2 \Theta \cos^2 \Theta) \quad (10)$$

From the ratio between equation (9) and equation (10), the equation of state parameter

$$W = -\frac{\left(\frac{1}{3}\right)(c^2 + 4\omega^2 B^2 \sin^2 \Theta \cos 2\Theta + 4\omega^2 B^2 \sin^2 \Theta \cos^2 \Theta)}{(c^2 + 4\omega^2 B^2 \sin^2 \Theta \cos^2 \Theta)} \quad (11)$$

Equation (4) provides the deceleration parameter

$$q = -\frac{\cos 2\Theta}{2 \cos^2 \Theta} \quad (12)$$

And the source of gravity by equation (5) is

$$S = -\frac{3\omega^2 c^2 \cos 2\Theta}{2\pi G \sin^2 \Theta} \quad (13)$$


---

### 3 Discussion and Results

The most important aspect of the model is that it fits into the standard equations of cosmology without any friction.

Solving equation (7) numerically using  $t = 13.7$  billion years  $= 4.32 \times 10^{17}$ s and  $H = 71$ km/s/Mpc  $= 2.302 \times 10^{-18}$ /s, we get the frequency as  $\omega = 2.705 \times 10^{-18}$ /s

Since presently, the Galaxies have redshift, it needs the current value of  $\omega t$  to lie between 0 and  $\frac{\pi}{2}$  and it is so according to the model;

presently  $\omega t$  is 1.169 which is less than  $\frac{\pi}{2}$ .  $R$  has an accelerated evolution in  $[0, \frac{\pi}{4}]$  of  $\Theta$  and universe has expanded with acceleration for 9.202 billion years from Big Bang or it was accelerating around 5 billion years in the past from now (4.499 billion years exactly and let us call it  $T$ ). Since the SCP measurements were around the past 5 billion years, the model agrees with it.

Note that  $W = -\frac{1}{3}$  at  $\Theta = \frac{\pi}{4}$ ,  $W < -\frac{1}{3}$  for  $\Theta < \frac{\pi}{4}$  and  $W > -\frac{1}{3}$  when  $\Theta > \frac{\pi}{4}$  to have consistency between equations (3) and (11).

$\Theta$	$W$
$\pi/6$	$[(-1/3)(c^2 + (5\omega^2 B^2/4))]/[c^2 + (3\omega^2 B^2/4)]$
$\pi/4$	$-1/3$
-	-
$\pi/2$	$[(-1/3)(c^2 - 4\omega^2 B^2)]/c^2$

Table 1:  $W(\Theta)$

Time to the fully grown universe,  $T' = (1.570 - 1.169)/\omega = 4.7$  billion years.

Time between Big Bang and Big Crunch,  $\tau = (13.7 + 4.7) * 2 = 36.8$  billion years.

The present value of  $R = 0.847B$ , 84.7% of the maximum size of the universe and the order of size of the present universe [14] which is  $10^{26}$  is same as the order of  $B$  to give  $\frac{c^2}{B^2} \approx 4\omega^2 \approx 10^{-35}$ .

So,  $B \approx \frac{c}{2\omega}$

There must be a reason for this equality and is clear from equation (2) that  $B = \frac{c}{2\omega}$  needs  $P = 0$  at  $\Theta = \frac{\pi}{2}$ .

$$\left(\frac{2}{B}\right)(-2\omega^2 B) + 0 + \frac{8\pi GP}{c^2} + \frac{kc^2}{B^2} = 0 \text{ at } \Theta = \frac{\pi}{2}$$

When  $P = 0$ ,

$$\frac{kc^2}{B^2} = 4\omega^2 \text{ or } B = \frac{c}{2\omega} \tag{14}$$

Note also that the equation implies  $k = +1$  since  $\omega$  cannot be 0 or imaginary.

So using  $c$  and the well-fixed  $\omega$ ,  $B = 5.545 \times 10^{25} \text{ m}$ .

As Universe expands, magnitude of the negative pressure of dark energy may possibly be decreasing while that of dark matter, increasing or only one of them changing so that an equilibrium is achieved between the two when the size of the Universe rises to  $B$ .

**Parameters of the present Universe as per the model:**

Scale factor =  $4.697 \times 10^{25} \text{ m}$

Hubble number =  $+2.302 \times 10^{-18} / \text{s}$

Pressure =  $-1.187 \times 10^{-9} \text{ Pa}$

Density =  $8.255 \times 10^{-26} \text{ kg/m}^3$

Equation of state parameter =  $-0.016$

Density parameter = 8.701 (critical density is  $9.487 \times 10^{-27} \text{ kg/m}^3$ )

Deceleration parameter =  $+2.269$

Source of gravity =  $+3.869 \times 10^{-9} \text{ Pa}$

$\Theta$	$R * 10^{25} \text{ m}$	$H * 10^{-18} / \text{s}$	$\rho * 10^{-26} \text{ kg/m}^3$	$P * 10^{-9} \text{ Pa}$	$S * 10^{-10} \text{ Pa}$	$q \text{ m/s}^2$
$\pi/12$	0.372	20.190	1240.150	-392.580	-608.050	-0.464
$\pi/6$	1.386	9.370	99.514	-75.460	-94.200	-0.330
$\pi/4$	2.773	5.410	26.188	-7.864	0	0
$\pi/3$	4.159	3.124	11.057	-2.278	+31.400	+1.000
$5\pi/12$	5.174	1.450	6.393	-0.461	+43.703	+6.464
$\pi/2$	5.545	0	5.237	0	+47.100	$\infty$

Table 2: Evolution of cosmological parameters

Universe, according to the model, is now slowing down by the high density of matter which is currently about 9 times the critical density, the reason for the large curvature of the universe. This is indicated by the positive value of the source of gravity.

The modelling can be done using higher even powers of sine also. Time  $T$  to the accelerating phase from now decreases with the power of sine, a desired result in the light of SCP measurements to have

acceleration for some more time after 8.7 billion years.

So generally, let

$$R = B \sin^n \Theta \tag{15}$$

Finding  $\frac{d^2R}{dt^2}$  and equating it to zero,  $\tan \Theta = \sqrt{n - 1}$

Therefore,

$$T = 4.32 \times 10^{17} - \left(\frac{1}{\omega}\right) \tan^{-1} \sqrt{n - 1} \tag{16}$$

where  $\omega$  is to be obtained from  $2.302 \times 10^{-18} \tan(4.32 \times 10^{17} \omega) - n\omega = 0$ .

Also,

$$T' = \frac{1.57}{\omega} - 4.32 \times 10^{17} \quad (17)$$

$$\frac{\tau}{2} = \frac{1.57}{\omega} \quad (18)$$

$$\omega = \frac{c}{B\sqrt{2n}} \quad (19)$$

$n$	$\omega(/s)$	$T'(by)$	$\tau/2(by)$	$T(by)$
2	$2.705 \times 10^{-18}$	4.700	18.400	4.499
4	$3.226 \times 10^{-18}$	1.730	15.430	3.412
6	$3.373 \times 10^{-18}$	1.062	14.762	2.890
8	$3.445 \times 10^{-18}$	0.755	14.455	2.572
—	—	—	—	—

Table 3: Different even powered sine models

Going to higher powers but reduces  $B$  as

shown below; it would not be good to compromise  $B$  much.

$n$	$B * 10^{25}m$
2	5.545
4	3.288
6	2.568
8	2.177
—	—

Table 4:  $B(n)$

## 4 Conclusions

When Alexander Friedmann proposed his models, he was worried about only matter as it was shown that the effect of radiation on the dynamics of the universe lasted only for a small time, about 50,000 years from

Big Bang. He called the present time the matter era that followed the radiation era. He put  $W = 0$  in the equations so that in his models [15], the Universe can have only a decelerated expansion by equation (3) since  $W\rho = W_r\rho_r + W_m\rho_m$  with  $W_m \approx 0$ ,  $W_r = \frac{1}{3}$ , the equation of state parameter for radiation

and  $W_m$ , that for matter which he assumed 0. In 1998, when Perlmutter et.al announced the accelerated expansion of the universe, the present time became the dark era, under control of dark energy [4,5].

But the recent studies on the Planck data which inspired this article make us re-think about the role of dark matter which might have a strong command over the evolution of  $W$ :

$$W\rho = W_r\rho_r + W_{mn}\rho_{mn} + W_{md}\rho_{md} + W_d\rho_d, \rho_r \approx 0, W_{md} \neq 0 \quad (20)$$

where  $W_{mn}$  is the equation of state parameter for normal matter,  $W_{md}$  that for dark matter and  $W_d$  for dark energy.

If we assume the simplest form of dark energy, the cosmological constant (of equation of state parameter  $-1$ ) as introduced by Einstein in 1917 to counterbalance the effects of gravity to achieve a static universe [16],

$$W\rho \approx W_{md}\rho_{md} - \rho_d \quad (21)$$

This gives the current value  $+2.736$  for  $W_{md}$  from the current value of  $-0.016$  of the equation of state parameter  $W$  and the current amounts of dark matter and dark energy in the Universe. This high value of the dark matter equation of state parameter could be an indicator of the positive curvature of the Universe.

The proposed model might be an over simplified one for a positively curved Universe. But since the underlying science of the Universe must be simple and a cyclic universe would be a permanent solution to

the problem of the Creation, the model with modifications could be considered to study the evolution of the universe. A model using the evolution of dark matter equation of state parameter is another possible way of doing it and it will be attempted in our next paper. We suspect that the key role is played by dark matter and not dark energy in the dynamics of the Universe.

## References

- [1] M Charles, Kip S Thorne, J A Wheeler, Gravitation, (W H Freeman, San Francisco, 1973)
- [2] C L Bennet et.al. (2013), ApJS, 208(20B), 1
- [3] P J Steinhardt, Neil Turok, Endless Universe: Beyond the Big Bang, (Broadway Books, 2007)
- [4] G F Hinshaw et.al. (2013), ApJS, 208(19H), 1
- [5] S Perlmutter et.al. (1999), The As-

trophys. J., 517, 565

[6] A G Riess et.al. (1998), The Astron. J., 116, 1009

[7] <https://map.gsfc.nasa.gov/universe/bbtestsexp.html>

[8] <http://www.sciencealert.com>>Wild New Study Suggests The Universe Is a Closed Sphere, Not Flat-Science Alert

[9] E D Valentino, A Melchiorri, J Silk (2020), Nature Astronomy 4, 196

[10] G Efstathiou, S Gratton, A Detailed Description of the Cam Spec Likelihood Pipeline and a Reanalysis of the Planck High Frequency Maps (2020), arXiv:1910.00483v2[astro-ph.CO]

[11] [www.forbes.com](http://www.forbes.com), Ask Ethan:

Could The Shape Of Our Universe Be Closed Instead Of Flat?

[12] <https://wwwmpa.mpa-garching.mpg> > Planck legacy results and tensions-MPA

[13] A Friedmann (1999), General Rel and Gr., 31, 1991

[14] <https://en.wikipedia.org/wiki/Observableuniverse>

[15] J. V. Narlikar, An Introduction to Cosmology, (Cambridge University Press, Cambridge, 2002)

[16] [blogs.scientificamerican.com](https://blogs.scientificamerican.com), Einstein's Greatest Blunder?

---

# Using classical collisions to conceptualize high-energy physics scattering outcomes at introductory physics level

V. Shekoyan, R. Armendariz, S. Dehipawala, G. Tremberger Jr, D. Lieberman, and T. Cheung

Department of Physics  
Queensborough Community College Bayside New York USA.

TCheung@qcc.cuny.edu

*Submitted 28-12-2017*

## Abstract

Collisions between objects moving translationally is a topic covered in typical introductory physics courses. When one of the objects has a rolling motion, the outcomes depend on the ratio of the impact parameter to the radius of rotation. The decrease in the translational object's energy depends on the degrees of freedom associated with the rolling object's energy. The scattered translational object's energy change can be used to characterize a collision outcome. The classical collision outcomes would resemble the possible outcomes in high-energy scattering experiments. For the case of an observer moving at an angle relative to the lab frame, the  $\sqrt{E}$  description of a lab frame 1-Dim collision in matrix notation has semblance with the Weinberg angle description of the electroweak interaction. Numerical matrix examples are presented for flexible implementation of exercise in introductory physics courses.

to the environment, while an explanation of the material deformation of the objects would include the reference to a restitution coefficient. This paper discusses the momentum transfer or generation of internal impulses in a collision using numerical simulations. The numerical results showed that the energy loss to the environment in a collision of objects moving translationally would approach zero as the magnitude of the generated impulse pair reached a maximum.

When the target object has a rotational degree of freedom, the energy transfer process would mimic an energy loss to the environment when the collision is modelled with the target moving only in translation. The impacting object's energy would decrease and depend on the rolling constraints. Similarly, the impacting electron's energy loss in a deep inelastic scattering experiment would depend on the quark's constraints inside a hadron [1]. The association of the classical case with the high-energy case would help to initiate an interest in high-energy physics for first semester physics students.

---

## 1. Introduction

The physics of collisions in a college introductory course usually would cover elastic collisions with translational energy conservation and inelastic collisions with energy loss to the environment. The sound generated during a collision has been an intuitive explanation often given for the energy loss

## 2. Simulation

The simulation of a collision was performed with the following classroom problem. A 4-kg mass at 17 m/s acting as an impacting object collides with a 2-kg stationary target mass in a laboratory frame. The initial linear momentum equals 68 kg m/s and the initial total translational energy equals 578

Joules. The zero-momentum frame of reference would be a 4-kg impacting object moving 5.67 m/s rightward and a 2-kg target moving 11.33 m/s leftward. After the collision, the 4-kg mass would recoil at 5.67 m/s leftward and the 2-kg target at 11.33 m/s rightward in the zero-momentum frame. The transformation to the lab frame would give the target a rightward speed of 22.67 m/s and the scattered impactor 5.67 m/s rightward. These are calculations that students can perform easily without solving the quadratic energy and linear momentum equations containing velocity variable.

Using the energy conservation concept, students can construct a circle with diameter equal to the value of the square root of the total translational system energy of 578 Joules for the 1-D elastic collision. The diameter has a magnitude of about 24 in the unit of  $\sqrt{\text{Joules}}$ , which is carried by the impactor mass before the collision and shared between the impactor mass and target mass after the collision. The diameter would correspond to the hypotenuse of a 90-degree triangle with  $\sqrt{\text{Energy}}$  variables or states as the other two sides of the triangle, shown in Figure 1. The 90-degree angle has a unique

vertex that can be visualized with angle  $\theta$  with respect to the diameter. The angle  $\theta$  lies between the impactor's initial  $\sqrt{\text{Energy}}$  value and final  $\sqrt{\text{Energy}}$  value, shown in Figure 1. In the case of inelastic collision, the diameter represents the final total  $\sqrt{\text{Energy}}$  of the translational system because of the energy lost to the environment during collision. There is still an angle between the impactor's final  $\sqrt{\text{Energy}}$  variable and total final  $\sqrt{\text{Energy}}$  variable of the translational system, in a smaller circle when compared to the larger circle in the elastic collision case, as shown in Figure 2. Note that a  $\sqrt{\text{Energy}}$  variable is also an adjusted-momentum variable when defined as  $p / \sqrt{(2m)}$  where  $p$  is the momentum and  $m$  is the mass. In comparison, the Landau and Lifshitz text on Mechanics at the graduate level also uses diagrams with circles containing real physical angles for the description of 2-D elastic scattering [2]. This paper discusses the application of circle geometry in the  $\sqrt{\text{Energy}}$  variable for the description of 1-D elastic collision. The observable final velocity values of the target can be studied in a simulation.

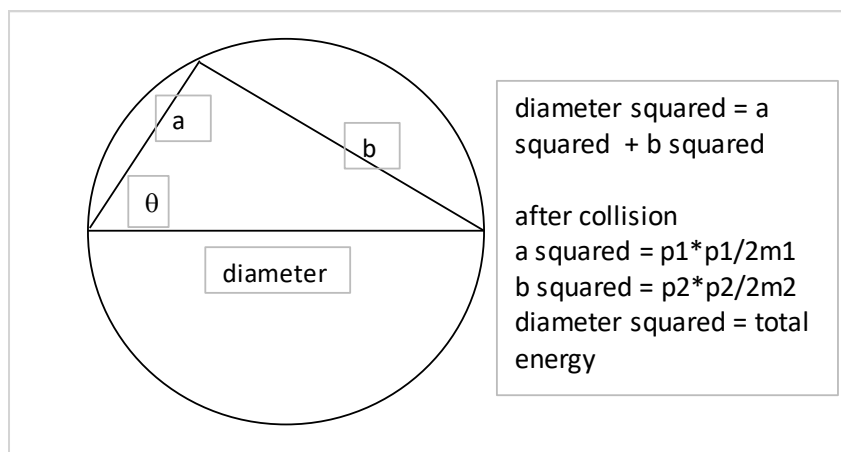


FIG 1: Diagram showing collision variables  $\sqrt{\text{Energy}}$  or  $p/\sqrt{(2m)}$  after the 1-Dim collision. The impactor mass ( $m_1$ ) equals 4 kg. The target mass ( $m_2$ ) equals 2 kg. The diameter equals 24 in the unit of  $\sqrt{\text{Joules}}$  for elastic collision.

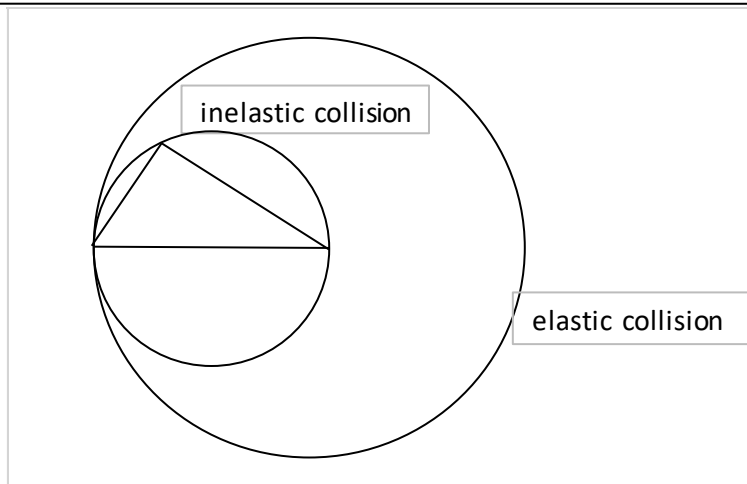


FIG 2: Diagram showing collision variables  $\sqrt{\text{Energy}}$  after the 1-Dim collision for inelastic collision with diameter equals the square root of total final translational system energy. The elastic collision circle of Figure 1 is shown with the maximum diameter, 24 in the unit of  $\sqrt{\text{Joules}}$  for elastic collision, for comparison.

The simulation was performed using Microsoft Excel. Different momentum transfer values were used in the simulation, shown in Column-D, Figure 3. The completely inelastic collision case would correspond to a momentum transfer value of about 23 kg m/s. The results for various observable target final velocity values are shown in Column-B, Figure 3. The energy lost to the environment, defined as

final energy – initial energy, is shown in Column-K as a fraction of the total initial energy. An elastic collision with zero energy loss to the environment and maximum momentum transfer (Column-D) is shown in Row-12. The graph of the fraction of energy lost versus transferred momentum is shown in Figure 4.

	A	B	C	D	E	F	G	H	I	J	K	L
1	total-p	v2 zero-p-frame	v2-lab- frame	p2=impulse	2*m2	2*m1	p2/sqrt2m2	p1/sqrt2m1	inv-tan	angle	energy loss fraction	
2	68	8	16	32	4	8	16	12.72792206	0.898808	51.4978	-0.27681661	
3	68	8.3333	16.6666	33.3332	4	8	16.6666	12.25656468	0.936707	53.66923	-0.25951742	
4	68	8.6666	17.3332	34.6664	4	8	17.3332	11.7852073	0.973674	55.78726	-0.23991188	
5	68	8.9999	17.9998	35.9996	4	8	17.9998	11.31384992	1.009645	57.84828	-0.218	
6	68	9.3332	18.6664	37.3328	4	8	18.6664	10.84249254	1.044572	59.84944	-0.19378178	
7	68	9.6665	19.333	38.666	4	8	19.333	10.37113516	1.078418	61.78864	-0.16725721	
8	68	9.9998	19.9996	39.9992	4	8	19.9996	9.899777779	1.111158	63.6645	-0.1384263	
9	68	10.3331	20.6662	41.3324	4	8	20.6662	9.428420399	1.142778	65.47623	-0.10728904	
10	68	10.6664	21.3328	42.6656	4	8	21.3328	8.957063019	1.173276	67.22363	-0.07384544	
11	68	10.9997	21.9994	43.9988	4	8	21.9994	8.485705638	1.202657	68.90699	-0.0380955	
12	68	11.333	22.666	45.332	4	8	22.666	8.014348258	1.230932	70.52703	-3.9215E-05	

FIG 3: Results for various target final velocity values. Column-K values represent (final energy value – initial energy value of 578 Joules)/ 578 Joules. The Row-12 angle value listed in Column-J is the angle  $\theta$  denoted in Figure 1 for an elastic collision.

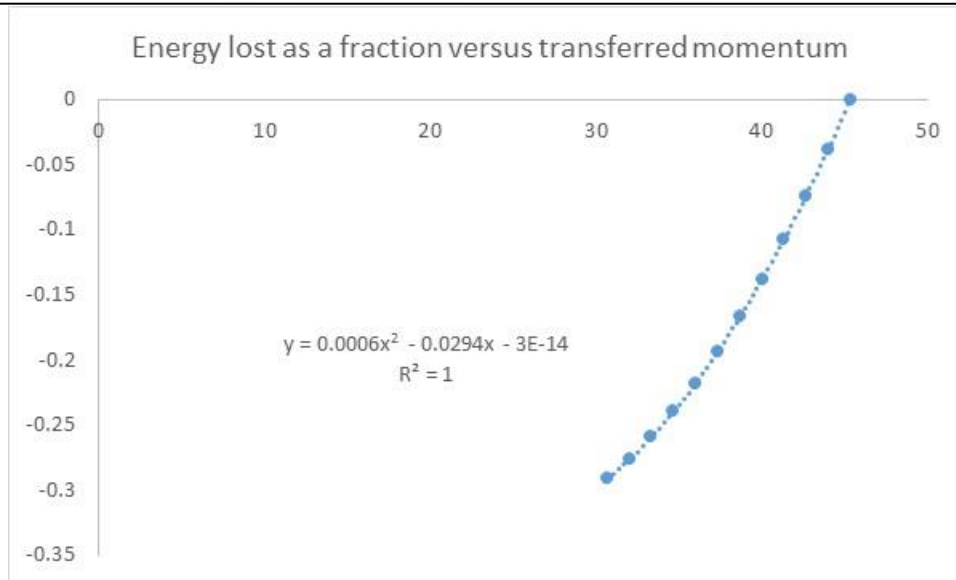


FIG 4: Graph of final energy lost as a fraction (y-axis) versus transferred momentum in kg m/s (x-axis).

### 3. Rotational Energy add-on

The remodeling of the energy lost arising from a rotational energy degree of freedom, in the case of a rolling target, would be easily understood by students using the inelastic cases shown in Figures 3 and 4. From the perspective of the system’s translational energy, a transformation of the elastic collision case to the inelastic one requires the inclusion of sound energy or rotational energy. A target object with a rolling structure is illustrated in Figure 5. A collision would generate an impulse pair and different momentum transfer values were

discussed in Section-2 without the rotation degree of freedom. With a rolling target, the received energy would be the sum of linear momentum induced energy and angular momentum induced energy. The rotational energy expression,  $L^2/(2I)$ , where  $L$  is the angular momentum and  $I$  is the moment of inertia at the center of mass, would be the energy lost as shown in Figures 3 and 4. The adjustable parameter,  $b^2/\alpha R$ , could be made to match the energy lost as a fraction in the simulation results shown in Figures 3 and 4.

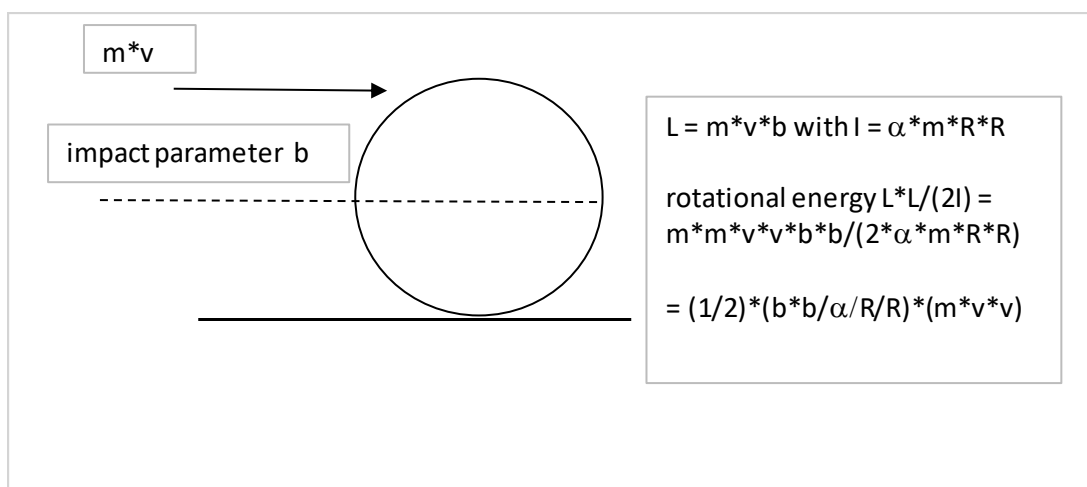


FIG 5: A target object with rolling structure. The circle has a radius  $R$

The collision problem illustrated in Figure 1 and Figure 2 would strengthen a student's spatial reasoning and its learning, which is an essential cognitive process in physics education. Furthermore, the emphasis on momentum transfer, the generation of a pair of impulses at the time of contact, would remind students about Newton's Third Law. The linear impulse pair in the lab frame is an invariant in other frames including the zero momentum frame would be another fact to highlight the Newton's Third Law. The decreasing impulse, from its maximum in elastic collision, to smaller values in inelastic collision is another such fact. The post-collision steady state solution of the rolling target object after receiving an impulse has been covered in the MIT Lectures [3]. The MIT presentation used angular momentum conservation and showed that the steady state velocity would be  $(9/7) \cdot (\text{collision-induced velocity})$ , where the impact parameter equals  $0.8 \cdot \text{radius}$  for a solid sphere rolling on a surface exerting a frictional force. The emphasis on the generated impulse pair could help students perform better in assessment tools, such as the Force Concept Inventory FCI multiple-choice question test, without teaching to the test, and further physics education research studies could verify the usefulness of emphasizing impulse pair in collision problems in terms of FCI test results.

Returning to the collision aspect illustrated in Figure 5 with an applied impulse ( $m \cdot v$  or  $F \cdot \Delta t$ ), the rotational energy carries an expression,  $(1/2) \cdot (b \cdot b / \alpha / R / R) \cdot m \cdot v \cdot v$ , such that the impactor's scattered energy will become less than it is in the case of the collision with translational energy only. In other words the exchange interaction between the impactor and target via the  $F \cdot \Delta t$  impulse pair would depend on the degrees of freedom of the target. The case of minimum friction to support rolling is discussed in Appendix-A for instructors who are interested in using a rolling-with-slipping target as a demonstration of extra energy transfer mechanism, from the viewpoint of an impactor's scattered energy in their classrooms. The energy transfer during the scattering of very short wavelength electrons from a quark could be illustrated using the

model described above. The scattered short wavelength electron would lose energy due to the interaction with the hadron's internal structure, depending on the initial quark parameter values in deep inelastic scattering experiments. By the same token, a classically scattered impactor would lose more energy due to the rolling structure of the target object, depending on the ratio of the impact parameter to the radius of rotation.

#### 4. Collision Matrices & Moving Observer Frame

In terms of generating numerical exercises from the perspective of teaching, it would be effective to have a matrix approach where numerical values can be generated using Excel. In fact numerical matrix manipulation can also be taught directly. Elementary matrix computation is a topic covered in the US College Board SAT Math and the UK GCSE Math review materials for high school students UK [4, 5]. It is interesting to point out that the topic of matrix arithmetic on the UK GCSE Math review materials can be taught effectively [6]. The presentation of collision using matrices would reinforce the teaching of matrix arithmetic where physical data is analyzed beyond straight forward numerical manipulation. The  $2 \times 2$  collision matrix in 1-Dim has been published [6]. The numerical matrix operation details are shown in the Appendix-B with the impactor  $m = 4$  kg at 17 m/s and target  $M = 2$  kg at 0 m/s.

It is interesting to note that a moving observer with two orthogonal velocity components would report a 2-Dim collision for the lab frame 1-Dim elastic collision between the 4 kg impactor and the 2 kg target at a total initial energy of 578 Joules. A tree would be seen as moving in the NW direction relative to an observer moving along in the SE direction, a common sense notion even for students having majors in various technology curriculums. Such a moving observer could adjust his/her velocity such that the total initial kinetic energy equals to 578 Joules, the same value observed by the lab frame observer. A mental construct of the

$\sqrt{\text{Energy}}$  variables based on the moving observer's data is shown in Figure 6. The “e” parameter, which is the height of the 90-degree triangle in the direction of the perpendicular line to the hypotenuse, is shared by both the impactor and the target  $\sqrt{\text{Energy}}$  variables through the angle  $\theta$ , shown in Figure 6. The Excel Solver, based on the perspective of running simulations, can be used to find a solution with the constraint of 578 Joules as the total initial kinetic energy. The introduction of a “constraint perspective” could help those students planning to study Lagrangian Mechanics. The Excel Solver showed that a moving observer in the direction of (-50 degrees) with (9.3653 m/s, -11.1611 m/s) would report a total energy of 578 Joules. The moving observer would report an impactor with velocity component of (7.6347 m/s, 11.1611 m/s) and target with velocity component of (-9.3653 m/s, 11.1611 m/s), given the lab frame of impactor velocity component of (17 m/s, 0 m/s) and target velocity component of (0 m/s, 0 m/s). Instead of using a simulation perspective via the Excel Solver, the moving frame answers could be simply obtained by vector subtraction principle for relative velocity calculation by first year physics students. There are advantages in the using of matrix multiplication instead of using vector subtraction. Matrix multiplication has an advantage of representing cause and effect in the notion of  $F = ma$  with a multiplicative perspective including the generation of new unit. Numerical matrix multiplication methodology in classical collision has a semblance to the matrix methodology in high energy physics. After the collision, the lab frame of impactor velocity component (5.667 m/s, 0 m/s) and target velocity component (22.67 m/s, 0 m/s) would transform accordingly for the moving observer.

Note that the “e” parameter would be conserved in a collision when an observer moved in a direction of (-45 degree) with (11.333 m/s, -11.333 m/s). The Excel Solver simulation results are shown in Figure 7. A graph of the initial and final “e” parameter values versus moving frame angle is shown in Figure 8, in which a vertical shift represents a change of the “e” parameter due to collision. The

moving frame direction of (-45 degree) calculation shown in Figure 9 shows that the “e” parameter is conserved when the  $\theta$  angle of Figure 6 equals 41.8101 degrees. A student planning for a major in physics major would ask for the interpretation of the “e” parameter while most engineering major students would not be curious for further questioning. One acceptable answer for beginning physics majors could be the following. The created “e” parameter in the  $\sqrt{\text{Energy}}$  mathematical space is the result of doing an extension to higher dimension in matrix notation such that an additional parameter could be found to be associated with a 1-Dim collision in the lab frame. In other words, the “e” parameter can be artificially-mathematically created in the  $\sqrt{\text{Energy}}$  mathematical space with trigonometry expressions of “ $e = a \cdot \sin \theta = b \cdot \cos \theta$ ”, shown in Figure 6. The “e” parameter conservation case when the observer moved at -45 degrees direction has a drawing semblance to the Weinberg angle illustration depicted in a particle physics text [7] and in open access webpage [8]. The electric charge  $e$  could be represented as the perpendicular height of a 90-degree triangle with the weak isospin coupling  $g$  and weak hypercharge coupling  $g'$  as its two shorter sides with  $\theta$  being the Weinberg angle in trigonometry expression of “ $e = g \cdot \sin \theta = g' \cdot \cos \theta$ ”. The created “e” parameter in this collision example is related to the  $\theta$  angle in Figure 6. The right angled triangle in the context of “ $\sqrt{\text{Energy}}$  mathematical space with matrix multiplication” is a unique perspective. The Weinberg angle depicted as an angle in a right-angled triangle in the context of “weak isospin coupling and weak hypercharge coupling” is a unique perspective. A higher 2-D dimension would carry the  $\theta$  interaction angle parameter due to an extra demission with new degree of freedom, similar to a target carrying rolling as the add-on degree of freedom discussed in Section 3.

The  $\theta$  angle can be described in the following way. The  $\theta$  angle, about 41.8 degrees in the above example, is different from the physical angle of a tilted moving observer at -45 degrees. The  $\theta$  angle has an associated  $\theta$  rotation matrix. The (0,

$\sqrt{\text{Energy}}$ ) vector has a physical meaning in the lab frame motion for a stationary target at zero energy initially. The 41.8 degrees  $\theta$  rotation matrix multiplication to the  $(0, \sqrt{\text{Energy}})$  vector would transform the vector to the  $(\sqrt{\text{Energy-target}}, \sqrt{\text{Energy-impactor}})$  vector, which is an invariant vector for the pre-collision and post-collision observed in a moving frame at -45 degrees, shown in Appendix-C. When the “e” parameter and the  $\theta$  rotation angle are not conserved, the  $(\sqrt{\text{Energy-target}}, \sqrt{\text{Energy-impactor}})$  vector would not an invariant but change. For the case of a 50-degree tilted moving observer shown in Appendix-C, the transformations of the  $(\sqrt{\text{Energy-target}}, \sqrt{\text{Energy-impactor}})$  vector in the pre-collision and post-collision are shown to be different in the matrix multiplications. For an individual analyzing the motions in the two reference frames and taking a transformation perspective, the special case of “e” parameter conservation ensures that the  $\theta$  angle rotation matrix in the multiplication transformation of the  $(\sqrt{\text{Energy-target}}, \sqrt{\text{Energy-impactor}})$  vector is identical for the pre-collision and post-collision. In other words, the elastic collision would reverse the horizontal velocity values with zero total horizontal momentum, but keep the energy constant, in a special moving frame shown in Appendix-C. The (16.0277 m/s, -45 degrees) is a special moving frame for “e” and  $\theta$  angle conservation. The numerical example shows that the 41.8 degrees  $\theta$  angle rotation matrix transformation, which can generate the  $(\sqrt{\text{Energy-target}}, \sqrt{\text{Energy-impactor}})$  invariant vector, has an origin in the zero total horizontal momentum, with or without a collision. On one hand, an individual may complain that the (16.0277 m/s, -45 degrees) moving frame observation is an unnecessary complication of the obvious, in this case a simple 1-D collision; and that the creation of “e” and 41.8 degrees  $\theta$  angle

conservation is just an academic curiosity for rotation matrix transformation with minimal meaning. On the other hand, another individual may be interested in the generation of new conserved parameters, perhaps with some parallelism to the use of higher dimensions via matrix language in particle physics theories for the explanation of high energy physics data.

Continuing with the matrix multiplication perspective, the  $\theta$  angle rotation matrix transformation can generate an invariant  $(\sqrt{\text{Energy-target}}, \sqrt{\text{Energy-impactor}})$  vector, when the  $\theta$  angle is conserved. Such a transformation perspective has a matrix semblance to high energy physics studying electroweak interaction. The Weinberg angle rotation matrix multiplication to the (B-boson, W-boson) vector would transform the vector to the (photon, Z boson) observable vector mathematically in the electroweak interaction model including Weinberg angle conservation. On one hand, the question of why using the related  $\theta$  rotation matrix in the transformation, and not any other matrices generated by the  $\theta$  angle, is a graduate school level question. On the other hand, a student familiar with geometry and linear algebra would recognize that the  $\theta$  rotation matrix multiplication is simply mathematically associated with a rotation transformation of reference axes, shown in Figure 9. The  $(\sqrt{\text{Energy-target}}, \sqrt{\text{Energy-impactor}})$  vector would contribute new projections in the new X'Y' coordinates generated by the  $\theta$  rotation angle. In any event, the exposure to numerical matrix manipulation in physics would also be beneficial to engineering students when MATLAB is an expected topic in first year curriculum such as biomedical engineering [9].

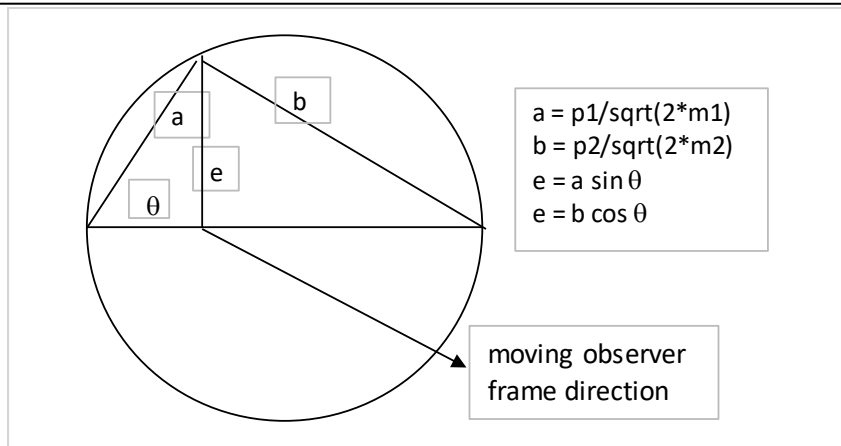


FIG 6: Diagram showing collision variables  $\sqrt{\text{Energy}}$  or  $p / \sqrt{(2m)}$  before the collision from the viewpoint of a moving observer.

CO	CP	CQ	CR	CS	CT	CU
direction(deg)	speed m/s	init-angler(deg)	init-e (sqrt(J))	final-angle(deg)	final-e (sqrt(J))	change-e (sqrt(J))
-55	13.0010242	32.7360846	10.93606701	50.56122636	11.79502047	0.858953463
-50	14.56981704	37.30251272	11.58950243	46.23919641	12.00956905	0.420066621
-45	16.02772426	41.81012301	11.94637789	41.81031123	11.94638666	8.77552E-06
-40	17.36365025	46.23901199	12.00957239	37.30270383	11.58952371	-0.420048679
-35	18.56742778	50.5610472	11.79503498	32.73627781	10.93610067	-0.858934311

FIG 7: Results for the final change of “e” values in an Excel simulation.

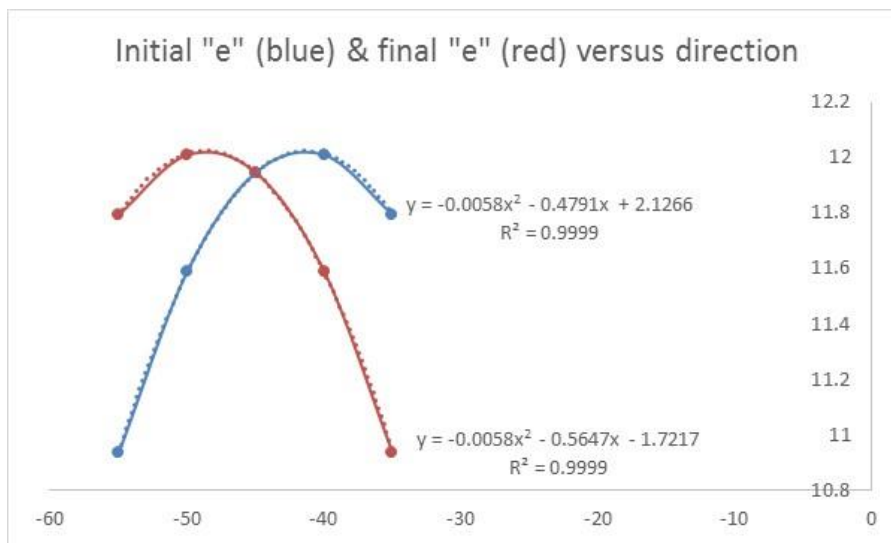


FIG 8: Graph of initial and final “e” values in  $\sqrt{\text{Joules}}$  (y-axis) versus moving frame direction in degrees (x-axis).

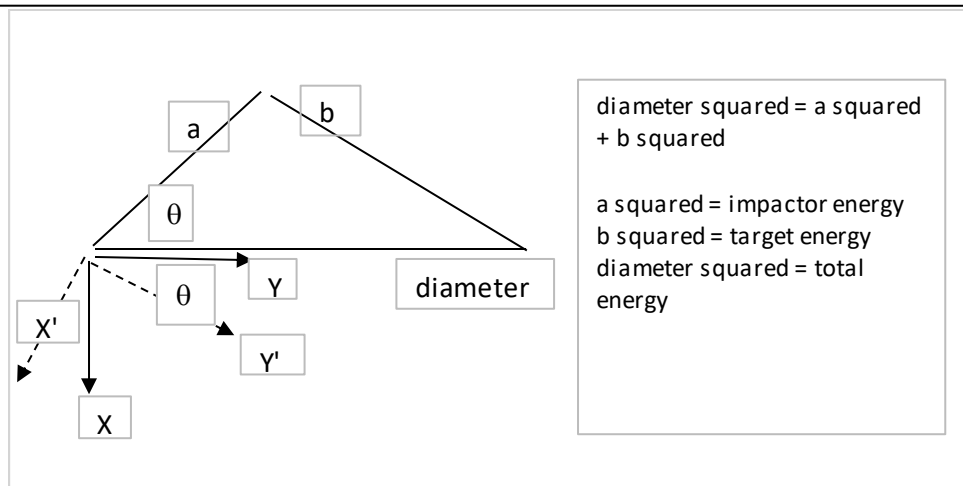


FIG 9: Diagram showing the  $\theta$  clockwise rotation of reference axes in  $\sqrt{\text{Energy}}$  mathematical space with the new X'-Y' coordinates.

### 5. Discussion

Altogether, the richness of the classical collision phenomenon in the context of “ $\sqrt{\text{Energy}}$  mathematical space with matrix multiplication” enables mechanism associations to modern physics from Weinberg angle in electroweak theory to deep inelastic scattering in high energy physics experiments. The artificially-mathematically created “e” parameter in the  $\sqrt{\text{Energy}}$  mathematical space when the 1D collision was observed by a 2D observer could be used to echo what Einstein had said: The problems that exist in the world today cannot be solved by the level of thinking that created them [10]. The Einstein’s quote could be used to echo the perspective of transforming a problem to a higher dimension, although the problem was created in 1D. The level of thinking for a 2D observer is more involved as discussed above. An extra dimension can hold extra information in which precise mathematical tools may be able to generate meaningful insights. The consideration of extra dimensions in String Theory is one example. There were instances that enthusiastic first year physics students asked about the universe dimensions after watching “The Elegant Universe” shown on USA Public Television NOVA Program [11, 12]. The perspective discussed above would offer an illustrative mechanism beyond just using English words. In the above simulation results, the 2D

observer would discover that the “e” parameter was conserved for 41.81 degrees, shown in Figure 8.

The inelastic collision outcomes due to the target rolling condition in classical mechanics can be used to conceptualize high energy physics scattering with several outcomes. Of course, the energy quantization gives rise to particle creation in terms of  $E = mc^2$  in high-energy physics and there is no analogy in classical mechanics. This shortcoming in the analogy would be of minimal significance when explaining to students what a high-energy physics career would demand, since the equation representing the mass-energy conversion mechanism is not intimidating. The richness of a high-energy scattering association that builds on the inclusion of rotational energy in a classical collision problem is reflected in the Excel simulation where the numerical values can be adjusted easily from one semester to another. When a learnable mechanism is available, those students who take shortcuts in the memorization of facts would likely become deficient in reasoning skills. After all, the learning of an answer may not be identical to the learning of the associated investigative process in pedagogy. A discussion of high-energy physics scattering at the introductory physics level beyond fact memorization, such as what happen in the particle decay processes with branching fractions, would help to inspire A-level high school and first year

university students interested in high-energy physics.

## 6. Conclusions

The several outcomes of a classical collision between an object moving translationally and a rolling object were demonstrated through numerical simulation. The scattered object's energy transfer would become the rotational energy of the rolling object initially at rest. The outcomes of classical collision carry resemblances to the possible outcomes found in high-energy deep inelastic collision of electrons with quarks inside a hadron. It would be useful to show that the transformation of a 1-Dim collision in the lab frame to a 2-Dim collision seen by a moving observer with two orthogonal velocity components has a semblance to the Weinberg angle in high energy physics in terms of numerical matrix multiplication. Future studies could include the collision of two rolling objects that may have resemblances to other high-energy physics scattering experiments for first year physics students.

## 7. Appendix

The details of the numerical matrix operation are given below for easy Excel implementation.

### Appendix-A

Rolling under minimum friction condition would be accompanied by slipping. The following situation can be used as a classroom example. A collision would generator an impulse pair. A sphere of mass  $M$  kg and radius  $R$  meter resting on a rough horizontal table received an applied force of  $F$  in magnitude at the center of mass for  $\Delta t$  sec from a collision. The friction $\cdot R \cdot \Delta t$  would generate an angular momentum at the center of mass which would be  $0.4 \cdot M \cdot R \cdot R \cdot (\text{angular velocity})$ . The  $F \cdot \Delta t \cdot R$  would generate an angular momentum  $L$  at the sphere surface which would be  $1.4 \cdot M \cdot R \cdot R \cdot (\text{angular velocity})$ . Solving the above two equations would give friction =  $F \cdot 0.4 / 1.4$ . The received energy would the sum of linear momentum induced energy and angular momentum induced

energy, which would be  $(p\text{-net}) \cdot (p\text{-net}) / 2M + L \cdot L / 2I$  at sphere surface. The p-net would be  $(F\text{-friction}) \cdot \Delta t$  and I-sphere-surface would be the moment of inertia taking the sphere surface contact point to the table as the pivot. The p-net induced energy would all become heat energy eventually while the  $(L \cdot L / 2I$  at sphere surface) rolling energy would continue forever in this model. A cube of mass  $M$  with length  $2R$  could only acquire the  $(p\text{-net}) \cdot (p\text{-net}) / 2M$  energy when receiving an identical  $F \cdot \Delta t$  impulse. The rotation degree of freedom of the target would affect the impactor's scattered energy.

### Appendix-B

The numerical matrix is shown below with the impactor  $m = 4$  kg at 17 m/s and target  $M = 2$  kg at 0 m/s. The matrix multiplication would give the final velocities of 5.67 m/s for the 4 kg and 22.67 m/s for the 2 kg.

In matrix presentation,  $AX = Y$ ; A the collision matrix, X the initial velocity vector, Y the final velocity vector.

$$\frac{1}{(m+M)} * \begin{pmatrix} m - M & 2M \\ 2m & M - m \end{pmatrix} * \begin{pmatrix} 17 \text{ m/s} \\ 0 \text{ m/s} \end{pmatrix}$$

$$= \frac{1}{(6)} * \begin{pmatrix} 2 & 4 \\ 8 & -2 \end{pmatrix} * \begin{pmatrix} 17 \text{ m/s} \\ 0 \text{ m/s} \end{pmatrix} = \begin{pmatrix} 5.67 \text{ m/s} \\ 22.67 \text{ m/s} \end{pmatrix}$$

The time reversal collision where -5.67 m/s for the 4 kg and -22.67 m/s for the 2 kg are used in a collision would give -17 m/s for the 4 kg and 0 m/s for the 2kg.

$$\frac{1}{(m+M)} * \begin{pmatrix} m - M & 2M \\ 2m & M - m \end{pmatrix} * \begin{pmatrix} -5.67 \text{ m/s} \\ -22.67 \text{ m/s} \end{pmatrix}$$

$$= \frac{1}{(6)} * \begin{pmatrix} 2 & 4 \\ 8 & -2 \end{pmatrix} * \begin{pmatrix} -5.67 \text{ m/s} \\ -22.67 \text{ m/s} \end{pmatrix}$$

$$= \begin{pmatrix} -17 \text{ m/s} \\ 0 \text{ m/s} \end{pmatrix}$$

The inverse of the 2 x 2 collision matrix A would also give the same final vector upon multiplication with the vector elements (17 m/s, 0). The inverse of any 2 x 2 matrix is simply obtained by interchanging the diagonal elements and multiplying -1 to the two off-diagonal elements, and multiplied by the determinant of A. A keen student would realize that the 1-dim matrix is an involutory matrix where a matrix has its own inverse.

$$\frac{(m+M)}{\det-A} * \begin{pmatrix} M - m & -2M \\ -2m & m - M \end{pmatrix} * \begin{pmatrix} 17 \text{ m/s} \\ 0 \text{ m/s} \end{pmatrix}$$

$$= \frac{6}{(-36)} * \begin{pmatrix} -2 & -4 \\ -8 & 2 \end{pmatrix} * \begin{pmatrix} 17 \text{ m/s} \\ 0 \text{ m/s} \end{pmatrix}$$

$$= \begin{pmatrix} 5.67 \text{ m/s} \\ 22.67 \text{ m/s} \end{pmatrix}$$

**Appendix-C**

In the case of a -45 degree moving observer, the Excel Solver showed that a moving observer of (16.0277 m/s, -45 degrees) or (11.3332 m/s, -11.3332 m/s) would report a total energy of 578 Joules or 24.0416 √Joules. The moving observer would report a 4-kg impactor with initial velocity component of (5.6667 m/s, 11.3332 m/s) while carrying 17.9196 √Joules, and a 2-kg target with initial velocity component of (-11.3332 m/s, 11.3332 m/s) while carrying 16.0277 √Joules; given the lab frame of impactor velocity component of (17 m/s, 0 m/s) and target velocity component of (0 m/s, 0 m/s). Note that the total horizontal momentum is zero because 4kg\*5.67 m/s + 2kg\*(-11.333m/s) = 0 kg m/s. After the collision, the horizontal momentum is still zero. The moving observer would report an impactor with velocity component of (-5.6667 m/s, 11.3332 m/s) while carrying 17.9195 √Joules and target with velocity component of (11.3333 m/s, 11.3333 m/s) while carrying 16.0277 √Joules such that the “e” parameter and

41.8 degrees θ angle are conserved in the elastic collision for the moving observer.

The transformation of the (0, √Energy) vector is illustrated below when the rotation matrix operates on the (0, √578 Joules) vector.

$$\begin{pmatrix} \cos 41.8101 & \sin 41.8101 \\ -\sin 41.8101 & \cos 41.8101 \end{pmatrix} * \begin{pmatrix} 0 \\ 24.04163 \text{ sqrt - J} \end{pmatrix}$$

$$= \begin{pmatrix} 16.0277 \text{ sqrt - J} \\ 17.9195 \text{ sqrt - J} \end{pmatrix}$$

The multiplication result would yield the (√Energy-target, √Energy-impactor) vector for θ = 41.8101 degrees in Figure 6 where the observer moved in the direction of -45 degrees. The initial and final (√Energy-target, √Energy-impactor) vectors are identical and the “e” parameter and 41.8 degrees θ angle are conserved. (Note that if the target mass becomes 4 kg, the collision with the 4 kg impactor also gives an “e” parameter conservation for an observer moving at -50 degrees.)

The transformation of the (0, √Energy) vector is illustrated below when the pre-collision rotation matrix operates on the (0, √578 Joules) for an observer moving with ( 14.5698 m/s , -50 degrees). Note that the impactor would carry 19.1238 √Joules and the target 14.5698 √Joules before the elastic collision.

$$\begin{pmatrix} \cos 37.3025 & \sin -37.3025 \\ -\sin 37.3025 & \cos 37.3025 \end{pmatrix} * \begin{pmatrix} 0 \\ 24.04163 \text{ sqrt - J} \end{pmatrix} = \begin{pmatrix} 14.5698 \text{ sqrt - J} \\ 19.1238 \text{ sqrt - J} \end{pmatrix}$$

The multiplication result would yield the initial (√Energy-target, √Energy-impactor) vector for θ = 37.3025 degrees in Figure 6 where the observer moved in the direction of -50 degrees.

The transformation of the (0, √Energy) vector is illustrated below when the post-collision rotation matrix operates on the (0, √Joules) for an observer

moving with (14.5698 m/s, -50 degrees). Note that the impactor would carry 16.6283  $\sqrt{\text{Joules}}$  and the target 17.3637  $\sqrt{\text{Joules}}$  after the elastic collision with an increase of “e” parameter value of about 0.4  $\sqrt{\text{Joules}}$ , show in Figures 9 and 10.

$$\begin{pmatrix} \cos 46.2391 & \sin 46.2391 \\ -\sin 46.2391 & \cos 46.2391 \end{pmatrix} *$$

$$\begin{pmatrix} 0 \\ 24.04163 \text{ sqrt} - J \end{pmatrix}$$

$$= \begin{pmatrix} 17.3637 \text{ sqrt} - J \\ 16.6283 \text{ sqrt} - J \end{pmatrix}$$

The multiplication result would yield the final ( $\sqrt{\text{Energy-target}}$ ,  $\sqrt{\text{Energy-impactor}}$ ) vector for  $\theta =$

### References:

- [1] Barr, A.J. 2014 B2.IV Nuclear and Particle Physics Lecture Notes Oxford University Merton College UK <http://www-pnp.physics.ox.ac.uk/~barra/teaching/subatomic.pdf>
- [2] L.D.Landau and E.M.Lifshitz, 1960 Mechanics, pp44 Addison-Wesley, Reading, Massachusetts
- [3] MIT 2007 Physics 8.01 Mechanics Problem Set 10 Problem 3 Billiards Challenge [http://web.mit.edu/8.01t/www/materials/ProblemSets/Raw/old\\_files\\_fall07/ps10sol.pdf](http://web.mit.edu/8.01t/www/materials/ProblemSets/Raw/old_files_fall07/ps10sol.pdf)
- [4] College Board Math Review 2017 <https://collegereadiness.collegeboard.org/sat-subject-tests/subjects/mathematics/mathematics-1>
- [5] projectGCSE 2017 Matrices Review [http://www.projectgcse.co.uk/gcse\\_maths/matrices](http://www.projectgcse.co.uk/gcse_maths/matrices)
- [6] Carter, J, Lieber, M (2007) Matrix analysis of classical elastic collisions, American Journal of Physics, Vol 75, pp758 <http://aapt.scitation.org/doi/full/10.1119/1.2742395>

46.2391 degrees in Figure 6 where the observer moved in the direction of -50 degrees.

The Excel files are located on CUNY Queensborough Community College website (<http://www.qcc.cuny.edu/physics/faculty-research.html>) for download when the article is published.

### Acknowledgment

The authors thank researchers for sharing their work in open access platforms. The authors thank Alexei Kisselev for maintaining the Excel download webpage. The anonymous review suggestions are gratefully acknowledged.

- [7] Lee T.D. 1981 Weinberg Angle Diagram. Particle Physics and Introduction to Field Theory, pp 681, Figure 22.3, Harwood Academic
- [8] [https://en.wikipedia.org/wiki/Weinberg\\_angle](https://en.wikipedia.org/wiki/Weinberg_angle)
- [9] Stony Brook University Biomedical Engineering BME 120 Programming Fundamentals in Biomedical Engineering <http://sb.cc.stonybrook.edu/bulletin/current/academicprograms/bme/>
- [10] Prensky, Marc (2009) "H. Sapiens Digital: From Digital Immigrants and Digital Natives to Digital Wisdom," Innovate: Journal of Online Education ISSN 1552-3233: Vol. 5 : Issue 3 , Article 1. <https://nsuworks.nova.edu/innovate/vol5/iss3/1/>
- [11] Groleau, Rick. Imagining Other Dimensions. NOVA Program PBS USA Oct 2003 <https://www.pbs.org/wgbh/nova/article/imagining-other-dimensions/>
- [12] NOVA Program. The Elegant Universe. Oct 2003 <https://www.pbs.org/wgbh/nova/series/the-elegant-universe/>

# Why we need ensembles in statistical mechanics?

Prasanth. P.<sup>1</sup>, Reshma. P<sup>2</sup> and K. M. Udayanandan<sup>3</sup>

<sup>1</sup>Department of Physics, Government Engineering College  
Thrissur 680 009, Kerala.

<sup>2</sup>Department of Physics, S N Polytechnic College  
Kanhangad, Kerala.

<sup>3</sup>Former HOD, Department of Physics, Nehru Arts and Science College  
Kanhangad, Kerala.

udayanandan@gmail.com

*Submitted on 16-May-2020*

## Abstract

Freshers undertaking a course in statistical mechanics find it very difficult to understand the logic behind the introduction of the ensemble method. For many, it takes days or months or years to digest the concepts of ensemble. In this article we attempt to justify the necessity of ensembles and highlight the easiness of the ensemble technique in finding the thermodynamics compared to the computation via time average, using some examples.

## 1 Introduction

The macroscopic thermodynamic properties like energy, pressure etc in materials are due to the microscopic behavior of constituent particles. It is the aim of statistical mechan-

ics to answer the question, how the microscopic behavior of particles or small constituents, lead to a particular macroscopic property of the material[1]. Any macroscopic quantity of the system which we wish to find is measured over a finite time, which is very long compared to the time-scale of motion of the particles of the system. So, the measured quantity is actually a time-averaged quantity. In this article in Section 2 we show that finding the time average for any system is very difficult. In Section 3 we give a brief description about the background of ensemble theory and different types of ensembles commonly used. In Section 4 we show that the examples of systems we tried to find thermodynamics using time average method in section 2 can be easily solved using ensemble method.

## 2 Time Average

Let us find how a time averaged quantity can be theoretically calculated. Consider a system with a collection of N interacting or non interacting atoms or molecules or any other particles and we are interested in finding an observable quantity like temperature which is the effect of the motion of these particles. Temperature can be determined by performing the average over the time trajectory of each particle, and then average over all the particles[2] at equilibrium. Time average of velocity is defined for a particle as

$$\langle v \rangle = \lim_{T_t \rightarrow \infty} \frac{1}{T_t} \int_0^{T_t} v(t) dt$$

where  $T_t$  is the total time. We know, according to the equipartition theorem

$$\frac{1}{2} m v^2 = \frac{3}{2} k T_{temp}$$

where  $T_{temp}$  is the temperature, k is the Boltzmann constant and m is the mass of the particle. So for N particles the temperature is

$$T_{temp} = \frac{m}{3k} \frac{1}{N} \sum_{i=1}^N \lim_{T \rightarrow \infty} \frac{1}{T} \int_0^{T_t} v_i^2(t) dt$$

To get the velocity, the equation of motion of the system must be solved.

As an example let us find how the temperature of a system of harmonic oscillators is obtained. The differential equation for a harmonic oscillator is

$$m \frac{d^2 q}{dt^2} + \omega^2 q = 0$$

where 'm' is the mass, 'q' is the displacement and ' $\omega$ ' is the angular frequency. The solution of the above second order differential equation is

$$q(t) = a \cos \omega t + b \sin \omega t$$

Differentiating

$$\frac{dq(t)}{dt} = -a\omega \sin \omega t + b\omega \cos \omega t$$

and hence velocity

$$v(t) = -a\omega \sin \omega t + b\omega \cos \omega t$$

We can find the value of the constants 'a' and 'b' by applying the initial conditions.

Let at  $t = 0, q(t) = q_0$  and  $v(t) = v_0$ . Then  $a = q_0$  and  $b = \frac{v_0}{\omega}$ . The instantaneous displacement

$$q(t) = q_0 \cos \omega t + \frac{v_0}{\omega} \sin \omega t \quad (1)$$

and instantaneous velocity

$$v(t) = -\omega q_0 \sin \omega t + v_0 \cos \omega t \quad (2)$$

Substituting in the equation for  $T_{temp}$ , the temperature for a collection of harmonic oscillators is given by

$$T_{temp} = \frac{m}{3Nk} \frac{1}{N} \sum_{i=1}^N \lim_{T \rightarrow \infty} \frac{1}{T} \int_0^{T_t} (v(t))^2 dt$$

Solving we get

$$T_{temp} = \frac{m}{6Nk} \frac{1}{N} \sum_{i=1}^N (v_{0i}^2(t) + \omega^2 q_{0i}^2)$$

Can we get this temperature by substituting the unknown values?. Look at  $v_0$  and  $q_0$ .

They are the amplitudes of velocity and displacement. We have  $N$  number of particles with different values for the amplitudes of velocity and displacement and have to use molecular dynamics simulation method to find these values. But it will be a laborious process to calculate this. Thus it is, practically impossible to generate a long time trajectory of a macroscopic system consisting of a large number of atoms or molecules. Even with the help of the fastest computers, it is hard to simulate the time trajectory of more than a few tens of thousands of molecules more than a few hundred nano seconds. Second reason for no possibility of finding time average is that solving equation of state of many systems is in many cases very difficult. To support and justify our arguments we give two simple examples of trying to find the time average.

## 2.1 Two examples of finding the time average of energy

### 2.1.1 Free particle

Consider a free particle of mass  $m$ . It will be governed by the equation

$$m \frac{d^2 q}{dt^2} = 0$$

So

$$\frac{dq}{dt} = \text{a constant}$$

Then momentum,  $p = \text{a constant} = p_0$ .  
Then the time average of energy is

$$\langle E \rangle = \frac{p_0^2}{2m} \quad (3)$$

For  $N$  particles the calculation of average energy will be very difficult because of the same arguments given in the previous section.

### 2.1.2 A particle in a gravitational field

Consider a particle with mass  $m$  moving in a gravitational field and let the motion be one dimensional. Then

$$q(t) = q_{max} - \frac{1}{2}gt^2$$

where  $q(t)$  is the instantaneous displacement measured from the ground,  $q_{max}$  is the initial height and  $g$  is the acceleration due to gravity. Let at  $t = 0$ ,  $q(t) = q_{max} = h$ . So

$$v(t) = \frac{dq}{dt} = -gt$$

where  $v(t)$  is the instantaneous velocity which is zero at  $t = 0$ . Then

$$p(t) = -mgt$$

where  $p(t)$  is the instantaneous momentum.

$$\langle p^2 \rangle = \frac{1}{T_t} \int_0^{T_t} p^2 dt = \frac{m^2 g^2 T_t^2}{3}$$

Then the time average of the kinetic energy is

$$\langle \frac{p^2}{2m} \rangle = \frac{mg^2 T_t^2}{6} \quad (4)$$

Average displacement

$$\begin{aligned} \langle q(t) \rangle &= \frac{1}{T_t} \int_0^{T_t} (q_{max} - \frac{1}{2}gt^2) dt \\ &= q_{max} - \frac{gT_t^2}{6} \end{aligned}$$

The time average of potential energy is

$$\langle mgq(t) \rangle = mgq_{max} - \frac{mg^2 T_t^2}{6} \quad (5)$$

Adding equations (4) and (5) gives

$$\langle \frac{p^2}{2m} \rangle + \langle mgq(t) \rangle = mgq_{max}$$

But

$$q_{max} = h = \frac{1}{2} g T_t^2$$

Simplifying the time average of energy

$$\langle E \rangle = \frac{mg^2 T_t^2}{2} \quad (6)$$

This is an impractical equation since  $T_t$  will be different and summing for  $N$  particles will result in a large value. All these show that finding the thermodynamics using time average is not a practical method in statistical mechanics.

### 3 Introduction of ensemble theory

The above issue of the difficulty of computing the time average was faced by the founder of statistical mechanics Ludwig Boltzmann. To counter this, Boltzmann used a hypothesis, accordingly a system in free evolution and waiting for a sufficiently long time, will pass through all the states consistent with its general conditions with the given value of the total energy. This hypothesis, later known as the Ergodic hypothesis, can be found more or less explicitly in all of Boltzmann's work on this subject. Actually, the ergodic hypothesis assumed a central role, above all due to J. Willard Gibbs

work in 1902. Gibbs[3] proposed an alternative to avoid time averaging in order to obtain equilibrium properties of macroscopic objects. He introduced and developed the concept of ensemble and used a set of postulates to formulate an entire theoretical scheme where equilibrium properties of the system can be obtained as an ensemble average. This method is given below.

Let us consider any observable property, say  $X$ . The ensemble average is a simple average over all the members of the ensemble.

$$\langle X \rangle = \lim_{N \rightarrow \infty} \frac{1}{N} \sum_{i=1}^N n_i X_i$$

Taking  $\frac{n_i}{N} = p_i$

$$\langle X \rangle = \lim_{N \rightarrow \infty} \sum_{i=1}^N p_i X_i$$

where  $p_i$  is the probability of a member of the ensemble to be in the  $i^{th}$  microscopic state. A virtual, mentally constructed replica or collection of thermodynamically identical systems is called an ensemble, or a statistical ensemble[4]. Three important thermodynamic ensembles were defined by Gibbs. They are

**Micro canonical ensemble(MCE):** A statistical ensemble where the total energy, volume and the number of particles in the system are fixed, which means it is a completely isolated system with no exchange of energy and particles with the surroundings allowed.

**Canonical ensemble(CE) :** A statistical ensemble where temperature, volume and the

number of particles are fixed. It is not an isolated system but can be considered as a system in contact with a heat bath, so that energy is exchanged but temperature, volume and number of particles remains constant.

**Grand canonical ensemble(GCE)** : A statistical ensemble where the temperature, volume and chemical potential are fixed. Here the system is considered to be in contact with a heat and a particle bath.

All ensembles give the same result but we will take canonical ensemble for further discussion because of its simplicity.

### 3.1 Canonical Ensemble

The thermodynamics of systems can be obtained if we introduce the concept of probability[5, 6]. Let  $p_i$  be the probability of the subsystem being in state  $i$  and it is equal to the fraction of the total number of states (of system plus reservoir) in which the subsystem is in the state  $i$ .(with energy  $E_i$ )

$$p_i = \frac{\Omega_{res}(E_{tot} - E_i)}{\Omega_{tot}(E - tot)}$$

$E_{tot}$  is the energy of the system plus reservoir, and  $\Omega_{tot}$  is the total number of states of the system plus reservoir.  $\Omega_{res}(E_{tot} - E_i)$  is the number of states available to the reservoir when the subsystem is in the state  $i$ . Our system does have only a measurable average energy and let us represent it by  $U$ . From the additive property of entropy

$$S_{tot}(E_{tot}) = S(U) + S_{res}(E_{tot} - U)$$

The other details of calculations are given Reference [5]. Finally using Boltzmann re-

lation

$$S = k \ln \Omega$$

we get

$$p_i = e^{\beta(U-TS)} e^{-\beta E_i}$$

Thus we get the probability as proportional to a thermodynamic quantity- Helmholtz free energy  $A = U - TS$ . Then

$$p_i = \frac{e^{-\beta E_i}}{Q}$$

where  $Q$  is called the partition function given by

$$Q = \sum_i e^{-\beta E_i}$$

### 3.2 Thermodynamics

In canonical ensemble we measure only average properties. This is because the energy is varying and hence we can measure only average energy. Other thermodynamic quantities like pressure and entropy depends on energy. So let us find expressions for these thermodynamic quantities. We want to make sure all thermodynamic quantities that we get in canonical ensemble is average.

#### 3.2.1 Average pressure

So average pressure

$$\langle P \rangle = \sum_i P_i p_i$$

From basic mechanics we know that  $P_i = -\frac{\partial \epsilon_i}{\partial V}$ . Substituting

$$\langle P \rangle = - \sum_i \frac{\frac{\partial \epsilon_i}{\partial V} e^{\beta \epsilon_i}}{Q}$$

Rearranging

$$\langle P \rangle = -\frac{1}{\beta Q} \left( \frac{\partial Q}{\partial V} \right)_{T,N}$$

which can be written in the popular form as

$$\langle P \rangle = - \left( \frac{\partial A}{\partial V} \right)_{T,N} \quad (7)$$

where  $A = -kT \ln Q$  [1, 4].

### 3.2.2 Average energy

$$\langle E \rangle = U = \sum_i \frac{\epsilon_i n_i}{N}$$

$$\langle E \rangle = \sum_i \epsilon_i p_i$$

But  $p_i = \frac{e^{\beta \epsilon_i}}{Q}$ . Substituting

$$\langle E \rangle = \sum_i \frac{\epsilon_i e^{\beta \epsilon_i}}{Q} = -\frac{1}{Q} \left( \frac{\partial Q}{\partial \beta} \right)_{V,N}$$

This can be written in the popular form as

$$\langle E \rangle = - \left( \frac{\partial \ln Q}{\partial \beta} \right)_{V,N} \quad (8)$$

## 4 Thermodynamics using ensemble method

### 4.1 Classical systems

In this section we will show that the thermodynamics of systems we tried to find using the time average can be easily calculated using ensemble method.

#### 4.1.1 Free particles

The time evolution of a classical system can be represented as a path, or trajectory, through phase space, the region of allowed states in the space defined by the  $2N$  independent coordinates  $q$  and  $p$ . As time passes, the particles make a trajectory in the phase space. Since our particles possess both kinetic energy due to momentum and potential energy due to position a space is imagined with momentum and position as coordinates. Such a space is called phase space. It will be a  $6N$  dimensional space. Any point in this space will be called a representative point and it represents a state or a component of the ensemble. For a single particle, let the energy be

$$E_r = \frac{p_r^2}{2m}$$

in three dimensions, where  $r$  represents a momentum state. The partition function

$$Q_1 = \sum_r e^{-\beta E_r}$$

For a classical system momentum varies continuously and hence,

$$\begin{aligned} Q_1 &= \int_0^\infty g(p) dp e^{-\beta E_r} \\ &= \frac{4\pi V}{h^3} \int_0^\infty p^2 e^{-\beta \frac{p^2}{2m}} dp \end{aligned}$$

We used the concept that in phase space the number of states between  $p$  and  $p+dp$  is

$$g(p)dp = \frac{\text{Volume of phase space}}{\text{minimum volume}}$$

$$g(p)dp = \frac{\int \int d^3 p d^3 q}{h^3}$$

where  $h^3$  in the minimum volume.

Solving

$$Q_1 = \frac{V}{h^3} (2\pi mkT)^{\frac{3}{2}}$$

N particle partition function,

$$Q_N = \frac{(Q_1)^N}{N!}$$

where the previous value of the partition function was divided by  $N!$  to avoid Gibbs paradox[7]. Using equation(8) we get

$$\langle E \rangle = U = \frac{3}{2} NkT$$

Similarly any thermodynamic quantity can be easily found.

#### 4.1.2 Particle in a gravitational field

For a single particle of mass  $m$  in a gravitational field

$$E = \frac{p^2}{2m} + mgq$$

with  $q$  one dimensional. Single particle partition function is

$$Q_1 = \int_0^\infty \int_0^\infty \frac{d^3p d^3q}{h^3} e^{-\beta \left( \frac{p^2}{2m} + mgq \right)}$$

Solving

$$Q_1 = \frac{(2\pi mkT)^{\frac{3}{2}}}{h^3} \frac{AkT}{mg}$$

Here  $A$  is the cross sectional area. As before  $Q_N$  can be found and we get

$$\langle E \rangle = \frac{5NkT}{2}$$

#### 4.1.3 Harmonic oscillators

Now we take a harmonic oscillator with energy

$$E = \frac{p^2}{2m} + \frac{1}{2} m\omega^2 q^2$$

The single particle partition function is

$$Q_1 = \int_0^\infty \int_0^\infty \frac{d^3p d^3q}{h^3} e^{-\beta \left( \frac{p^2}{2m} + \frac{1}{2} m\omega^2 q^2 \right)}$$

Solving

$$Q_1 = \left( \frac{1}{\beta \hbar \omega} \right)^3$$

N particle partition function is

$$Q_N = [Q_1]^N = \left[ \frac{1}{\beta \hbar \omega} \right]^{3N}$$

From this partition function we can find all thermodynamics. The average energy is

$$\langle E \rangle = 3NkT$$

Thus the ensemble method is a very comfortable technique to find the thermodynamic properties associated with a system. For classical systems the particle will be traversing a trajectory in phase space with each point representing a component of the ensemble. In canonical ensemble when the particle moves in phase space, each representative point is at constant temperature, volume and the number of particles and hence we call it as an ensemble.

### 4.2 Discrete system- A Toy model

Next we can deal with a system which possess discrete type of energy. It can have only some particular energy values. This example will give more insight into what an ensemble is. A typical Hamiltonian is taken as

$$H = -JS_1(S_2 + S_3)$$

where J is a constant and  $S_1, S_2,$  and  $S_3$  are spins which can take value  $\pm 1$ . Our system is having a fixed volume V, number of particles N is constant and temperature T is constant. Ensemble theory say that the system will pass through different available states before it reaches equilibrium. Now let us find out the available or possible states and how much energy they will contribute.

No	$S_1$	$S_2$	$S_3$	Energy
1	+1	+1	+1	-2J
2	+1	+1	-1	0
3	+1	-1	+1	0
4	+1	-1	-1	+2J
5	-1	+1	+1	+2J
6	-1	+1	-1	0
7	-1	-1	+1	0
8	-1	-1	-1	-2J

So we have a system with only 8 possible states. Our constituent particles can have only these possible states. Ensemble theory says that as time passes particles will have all these states. Each state is a component of the ensemble with fixed N, T and V. In reality all the systems will have infinite possible states. So we can say our system is a collection of such states which constitute an

ensemble.

Now let us calculate the average energy. We see that there are 3 types of energies +2j, -2J and 0 with multiplicities 2, 2 and 4. So the average energy is

$$\langle E \rangle = \frac{\sum_i E_i g_i e^{\beta E_i}}{\sum_i g_i e^{\beta E_i}}$$

where  $g_i$  is the degeneracy. Substituting the values and simplifying we get

$$\langle E \rangle = -\frac{2J \sinh 2\beta J}{1 + \cosh 2\beta J}$$

Thus finding average energy of a system is not difficult using ensemble method for discrete energy systems also.

## 5 Conclusions

In statistical mechanics classrooms, many teachers simply say that finding the time average is very difficult and hence we use ensemble method, without justifying it with arguments or examples. This article intends to discuss the issues behind the difficulties faced by the time average method in finding the thermodynamics of systems and understanding of the concepts of ensemble theory. Both classical and discrete energy systems are used for demonstrating what an ensemble is. We hope our examples in the article will help the readers visualize what an ensemble is!

## References

- [1] Huang K, Statistical Mechanics, Second Edition, John Wiley and Sons (1987).

- [2] Biman Bagchi, *Statistical Mechanics for Chemistry and Materials Science*, CRC Press (2018).
- [3] Gibbs, Josiah Willard, *Principles in Statistical Mechanics*. New York: Charles Scribner's Sons (1902).
- [4] R. K. Pathria and P. D. Beale, *Statistical Mechanics*, Butterworth (2009).
- [5] K. M. Udayanandan, R. K. Sathish and Augustine. A, *Physics Education* 30(1), (2014).
- [6] Daniel C. Mattis, *Statistical Mechanics made simple*, Daniel C. Mattis, World Scientific(2003).
- [7] T. P. Suresh, Lisha Damodaran and K. M. Udayanandan, *Physics Education*, 32(3), (2016)

# BCS Theory in $(2 \times 2)$ Matrix Way

Debnarayan Jana

Department of Physics, University of Calcutta  
92 A P C Road, Kolkata- 700 009, West Bengal, India.  
djphy@caluniv.ac.in

*Submitted on 10-Jul-2020*

## Abstract

In this paper, we present a very simple way of solving the Nobel prize winning work of superconductivity due to Bardeen-Cooper-Schrieffer (BCS) via  $(2 \times 2)$  matrix formulation. This alternative, intuitive original formulation of the approach is due to P. W. Anderson. The algebra of basic Pauli spin matrix are used to get the energy gap equation and the average number particles in the ground state. This formulation is used to obtain the finite temperature energy gap equation and universal signature of BCS type of superconductor. For completeness, we also include  $(4 \times 4)$  formulation in the single electron Fock space yielding the same energy eigenvalues.

---

**Keywords:** Superconductivity, BCS theory, Pseudo-spin analog

## 1. Introduction

Cooper pairs [1] are the electrons having equal and opposite momentum and spin

and behave approximately as bosons. They are indeed quasi-particles having zero spin. The superconductivity of a material occurs [2] because of formation of the Cooper pairs indirectly supported by phonons, the quantized quasi-particles of lattice vibrations. This pairing opens up a gap at the Fermi surface. Moreover, it has been demonstrated by Saraiva and collaborators [3] the formation of photonic Cooper-like pairs in transparent media in general via the virtual Stokes and Anti-stokes (SAS) processes in Raman spectroscopy. In such a case, although the photons are bosons but the photon pairs exchange virtual vibrations in transparent media, leading to an effective photon-photon interaction identical to that for electrons in the BCS theory of superconductivity.

This pairing problem in superconductivity cannot be formally attacked by the perturbation theory because of the emergence of an intriguing non-analytic ground state of the Cooper pairs. This non-

perturbative condensed state was correctly described by Bardeen-Cooper-Schrieffer (BCS) theory [4]. In this many body approach, the orbital part of the wave function however can have angular momentum state such  $l = 0$  ( $s$  state), 1 ( $p$  state), 2 ( $d$  state), 3 ( $f$  state). For an effective attraction between the electrons in Cooper pair, it can be argued that the singlet spin state will give the lowest ground state energy. If the spin part of the wave function is antisymmetric (Singlet), then the orbital part of the wave function has to be even ( $= 0, 2, 4, \dots$ ). The normal BCS Cooper pair correspond to  $s$  ( $l = 0$ ) wave superconductor while the high temperature superconductors fall into the category of  $d$  wave superconductors with  $l = 2$ . The wave function in case of  $l = 0$  state is spherically symmetric like the  $s$ -states of hydrogen atom. Although the theory of Cooper pairs is quite successful in the normal type of superconductor, however, it seems not quite adequate enough to explain the features of high temperature superconductivity.

Matrix formulation always gives one a simple way of calculating the relevant physical quantities easily. The simplest examples are the matrix formulation of simple harmonic oscillator and spin algebra in quantum mechanics. We will adopt the spin- $\frac{1}{2}$  algebra to solve a quantum many body problem. Recently, this kind of formulation has been used to extract the effective mass and excitation spectra of Dirac materials [5, 6].

In this pedagogic approach, we will fol-

low the Anderson's pseudo-spin formulation [7] to recast the BCS Hamiltonian in terms of pseudo-spin variables. As a consequence, we will be able to write down the ground state of BCS theory in a very transparent and suggestive way. In this formulation we will be able to compute the energy gap and its temperature variation in a very easy way without going into the rigorous second quantized operator calculation. The basic ( $2 \times 2$ ) spin matrix algebra will be sufficient enough to draw the major results of BCS theory.

## 1 Pair operators and spin operators

To proceed further, first we have to identify the second quantized operators used in BCS theory with the appropriate spin operators. The BCS annihilation and creation operators [2] for the electron pairs at  $\mathbf{k}$  space are defined respectively as

$$\begin{aligned} b_{\mathbf{k}} &= C_{-k\downarrow} C_{k\uparrow} \\ b_{\mathbf{k}}^{\dagger} &= C_{k\uparrow}^{\dagger} C_{-k\downarrow}^{\dagger} \end{aligned} \quad (1)$$

where the  $C_{k\sigma}, C_{k\sigma}^{\dagger}$  are one-particle fermion operators. These operators however satisfy the anticommutation relations consistent with Pauli exclusion principle given by

$$\begin{aligned} \{C_{k\sigma}, C_{q\sigma'}^{\dagger}\} &= \delta_{kq} \delta_{\sigma\sigma'} \\ \{C_{k\sigma}, C_{q\sigma'}\} &= 0 \\ \{C_{k\sigma}^{\dagger}, C_{q\sigma'}^{\dagger}\} &= 0 \end{aligned} \quad (2)$$

At this junction, let us check the commutation or anticommutation relations among

the pair creation and annihilation operators. It is clear from the above anticommutation relation that the number operator  $n_{\mathbf{k}\sigma}$  does indeed satisfy the relation  $n_{\mathbf{k}\sigma}^2 = n_{\mathbf{k}\sigma}$ . This indicates that at any state either zero or one electron is occupied. We also note that  $C_{k\sigma}^2 = 0 = (C_{k\sigma}^\dagger)^2$ . This implies also  $(b_{\mathbf{k}})^2 = 0 = (b_{\mathbf{k}}^\dagger)^2$ . With these information, we explicitly try to know the nature of these pair creation and annihilation operators via the commutation/anti-commutation relation.

It is easy to visualize that the pair creation and annihilation operators satisfy the following set of rules:

$$\begin{aligned} [b_{\mathbf{k}}, b_{\mathbf{q}}] &= 0 = [b_{\mathbf{k}}^\dagger, b_{\mathbf{q}}^\dagger] \\ [b_{\mathbf{k}}, b_{\mathbf{q}}^\dagger] &= (1 - n_{\mathbf{k}\uparrow} - n_{-\mathbf{k}\downarrow}) \delta_{\mathbf{k}\mathbf{q}} \\ \{b_{\mathbf{k}}, b_{\mathbf{q}}\} &= 2b_{\mathbf{k}}b_{\mathbf{q}}(1 - \delta_{\mathbf{k}\mathbf{q}}) \\ \{b_{\mathbf{k}}, b_{\mathbf{q}}^\dagger\} &= (n_{\mathbf{k}\uparrow} - n_{-\mathbf{k}\downarrow}) \delta_{\mathbf{k}\mathbf{q}} \end{aligned} \quad (3)$$

It is clear that the new paired quasi-electrons neither obey commutation nor anticommutation relations. So, we call them composite quasi particles. With the help of these commutation relations we would like to identify the appropriate spin operators equivalent to fermionic states. The fermionic states could of either occupied or empty. Can we design spin operators which can identify these two states?

Let us denote the fermionic empty and occupied state by  $|0_{\mathbf{k}\uparrow}0_{-\mathbf{k}\downarrow}\rangle$  and  $|1_{\mathbf{k}\uparrow}1_{-\mathbf{k}\downarrow}\rangle$

respectively. Then, we note that

$$\begin{aligned} \frac{1}{2}(n_{\mathbf{k}\uparrow} + n_{-\mathbf{k}\downarrow} - 1)|0_{\mathbf{k}\uparrow}0_{-\mathbf{k}\downarrow}\rangle \\ = -\frac{1}{2}|0_{\mathbf{k}\uparrow}0_{-\mathbf{k}\downarrow}\rangle \\ \frac{1}{2}(n_{\mathbf{k}\uparrow} + n_{-\mathbf{k}\downarrow} - 1)|1_{\mathbf{k}\uparrow}1_{-\mathbf{k}\downarrow}\rangle \\ = +\frac{1}{2}|1_{\mathbf{k}\uparrow}1_{-\mathbf{k}\downarrow}\rangle \end{aligned} \quad (4)$$

Noting down the similarity with the well-known spin algebra ( in units of  $\hbar = 1$ )  $S_{\mathbf{k}}^z|\uparrow\rangle = +\frac{1}{2}|\uparrow\rangle$  and  $S_{\mathbf{k}}^z|\downarrow\rangle = -\frac{1}{2}|\downarrow\rangle$ , we identify

$$\begin{aligned} S_{\mathbf{k}}^z &= \frac{1}{2}(n_{\mathbf{k}\uparrow} + n_{-\mathbf{k}\downarrow} - 1) \\ |0_{\mathbf{k}\uparrow}0_{-\mathbf{k}\downarrow}\rangle &= |\downarrow\rangle \\ |1_{\mathbf{k}\uparrow}1_{-\mathbf{k}\downarrow}\rangle &= |\uparrow\rangle \end{aligned} \quad (5)$$

Similarly, we also visualize

$$\begin{aligned} C_{k\uparrow}^\dagger C_{-k\downarrow}^\dagger |1_{\mathbf{k}\uparrow}1_{-\mathbf{k}\downarrow}\rangle &= 0 \\ C_{k\uparrow}^\dagger C_{-k\downarrow}^\dagger |0_{\mathbf{k}\uparrow}0_{-\mathbf{k}\downarrow}\rangle &= |1_{\mathbf{k}\uparrow}1_{-\mathbf{k}\downarrow}\rangle \end{aligned} \quad (6)$$

In this way, we can identify the pair creation operator and annihilation operator at  $\mathbf{k}$  space as

$$\begin{aligned} b_{\mathbf{k}}^\dagger &= S_{\mathbf{k}}^x + iS_{\mathbf{k}}^y = S_{\mathbf{k}}^+ \\ b_{\mathbf{k}} &= S_{\mathbf{k}}^x - iS_{\mathbf{k}}^y = S_{\mathbf{k}}^- \end{aligned} \quad (7)$$

Let us verify whether the above identification is correct or not by looking into the stan-

standard spin algebra. It is easy to check that

$$\begin{aligned}
 [S_{\mathbf{k}}^+, S_{\mathbf{k}}^-] &= [b_{\mathbf{k}}^{\dagger}, b_{\mathbf{k}}] \\
 &= 2 \times \frac{1}{2} (n_{\mathbf{k}\uparrow} + n_{-\mathbf{k}\downarrow} - 1) \\
 &= 2S_{\mathbf{k}}^z \\
 [S_{\mathbf{k}}^+, S_{\mathbf{k}}^z] &= \frac{1}{2} [b_{\mathbf{k}}^{\dagger}, n_{\mathbf{k}\uparrow}] + \frac{1}{2} [b_{\mathbf{k}}^{\dagger}, n_{-\mathbf{k}\downarrow}] \\
 &= -b_{\mathbf{k}}^{\dagger} = -S_{\mathbf{k}}^+ \\
 [S_{\mathbf{k}}^-, S_{\mathbf{k}}^z] &= \frac{1}{2} [b_{\mathbf{k}}, n_{\mathbf{k}\uparrow}] + \frac{1}{2} [b_{\mathbf{k}}, n_{-\mathbf{k}\downarrow}] \\
 &= b_{\mathbf{k}}^{\dagger} = S_{\mathbf{k}}^- \quad (8)
 \end{aligned}$$

Out of four terms in each commutator in raising and lowering spin operators, only one term will survive because of the restriction that  $C_{k\sigma}^2 = 0 = (C_{k\sigma}^{\dagger})^2$ . Thus, the pseudo-spin (because of its definition in  $\mathbf{k}$  space) operators satisfy the  $SU(2)$  spin algebra with the restriction that  $(S_{\mathbf{k}}^+)^2 = 0 = (S_{\mathbf{k}}^-)^2$ . As a result, we can find the spin length as follows:

$$\begin{aligned}
 (S_{\mathbf{k}}^{tot})^2 &= (S_{\mathbf{k}}^z)^2 + \frac{1}{2} (S_{\mathbf{k}}^+ S_{\mathbf{k}}^- + S_{\mathbf{k}}^- S_{\mathbf{k}}^+) \\
 &= \frac{1}{4} (b_{\mathbf{k}}^{\dagger} b_{\mathbf{k}} - b_{\mathbf{k}} b_{\mathbf{k}}^{\dagger})^2 + \frac{1}{2} (b_{\mathbf{k}}^{\dagger} b_{\mathbf{k}} + b_{\mathbf{k}} b_{\mathbf{k}}^{\dagger}) \\
 &= \frac{1}{2} (n_{\mathbf{k}\uparrow} - n_{-\mathbf{k}\downarrow}) \quad (9)
 \end{aligned}$$

If the pairs are either empty or occupied, we find  $S_{\mathbf{k}}^{tot} = 0$ . Thus we have shown that one pseudospin for each pair of electron states. The situation in which both states are unoccupied is represented by a pseudo-spin in the positive  $z$  direction, while occupation of both states is represented by a pseudo-spin in the negative  $z$  direction; other pseudo-spin orientations correspond to a superposition of the two possibilities.

## 2 BCS Hamiltonian in ( $4 \times 4$ ) Matrix form

The BCS Hamiltonian for quasi-electrons [4] interacting via an effective attractive phonon mediated interaction is

$$\begin{aligned}
 H_{BCS} - \mu N &= \sum_{\mathbf{k}} (\epsilon_{\mathbf{k}} - \mu) (n_{\mathbf{k}\uparrow} + n_{\mathbf{k}\downarrow}) \\
 &\quad - \frac{V_0}{\Omega} \sum'_{\mathbf{k}, \mathbf{q}} b_{\mathbf{k}}^{\dagger} b_{\mathbf{q}} \quad (10)
 \end{aligned}$$

The first part of the BCS Hamiltonian is the sum of the non-interacting single particle energy  $\epsilon_{\mathbf{k}}$  with respect to the Fermi energy  $\mu$ . Here  $\Omega$  is the volume,  $V_0 (> 0)$  is the strength of the interaction and the sum  $\sum'$  runs over momenta  $\mathbf{k}$  and  $\mathbf{q}$  such that  $|\epsilon_{\mathbf{k}(\mathbf{q})} - \mu| < \epsilon_c$  where  $\epsilon_c = \hbar\omega_D$  is the characteristic energy cut-off of the interaction. Thus, this is a short range interaction. Before proceeding for pseudospin transformation, we would like to transform the above BCS Hamiltonian to ( $4 \times 4$ ) matrix in the electron's annihilation and creation operator's Fock space using the inherent anticommutation algebra.

In the mean field level [2, 8, 9], the above Hamiltonian can be written as

$$\begin{aligned}
 H_{eff-BCS} - \mu N &= \sum_{\mathbf{k}} (\epsilon_{\mathbf{k}} - \mu) (n_{\mathbf{k}\uparrow} + n_{\mathbf{k}\downarrow}) \\
 &\quad + \Delta \sum_{\mathbf{k}} (c_{\mathbf{k}\uparrow}^{\dagger} c_{\mathbf{k}\downarrow}^{\dagger} + c_{\mathbf{k}\uparrow} c_{\mathbf{k}\downarrow}) \quad (11)
 \end{aligned}$$

Here,  $\Delta = -\frac{V_0}{\Omega} \sum_{\mathbf{q}} \langle c_{\mathbf{q}\downarrow} c_{\mathbf{q}\uparrow} \rangle$  and consequently, the original BCS Hamiltonian which was quadratic in pairing operators has now become *linear* in pairing operator.

Using the anticommutation relation between the fermionic operator ( $c_{\mathbf{k}}^{\dagger} c_{\mathbf{k}} = 1 - c_{\mathbf{k}} c_{\mathbf{k}}^{\dagger}$ ;  $c_{\mathbf{k}\uparrow} c_{\mathbf{k}\downarrow} = -c_{\mathbf{k}\downarrow} c_{\mathbf{k}\uparrow}$  etc), we first rewrite the above Hamiltonian in the following form as

$$\begin{aligned}
 H_{eff-BCS} - \mu N &= \frac{1}{2} \left\{ \sum_{\mathbf{k}} 2(\epsilon_{\mathbf{k}} - \mu) (n_{\mathbf{k}\uparrow} + n_{\mathbf{k}\downarrow}) + 2\Delta \sum_{\mathbf{k}} (c_{\mathbf{k}\uparrow}^{\dagger} c_{\mathbf{k}\downarrow}^{\dagger} + c_{\mathbf{k}\uparrow} c_{\mathbf{k}\downarrow}) \right\} \\
 &= \frac{1}{2} \left\{ \sum_{\mathbf{k}} (\epsilon_{\mathbf{k}} - \mu) \left[ n_{\mathbf{k}\uparrow} + (1 - c_{\mathbf{k}\uparrow} c_{\mathbf{k}\uparrow}^{\dagger}) + n_{\mathbf{k}\downarrow} + (1 - c_{\mathbf{k}\downarrow} c_{\mathbf{k}\downarrow}^{\dagger}) \right] \right. \\
 &\quad \left. + \Delta \sum_{\mathbf{k}} (c_{\mathbf{k}\uparrow}^{\dagger} c_{\mathbf{k}\downarrow}^{\dagger} - c_{\mathbf{k}\downarrow}^{\dagger} c_{\mathbf{k}\uparrow}^{\dagger} + c_{\mathbf{k}\uparrow} c_{\mathbf{k}\downarrow} - c_{\mathbf{k}\downarrow} c_{\mathbf{k}\uparrow}) \right\} - \sum_{\mathbf{k}} (\epsilon_{\mathbf{k}} - \mu) \\
 &= \frac{1}{2} \left\{ \sum_{\mathbf{k}} (\epsilon_{\mathbf{k}} - \mu) (c_{\mathbf{k}\uparrow}^{\dagger} c_{\mathbf{k}\uparrow} - c_{\mathbf{k}\uparrow} c_{\mathbf{k}\uparrow}^{\dagger} + c_{\mathbf{k}\downarrow}^{\dagger} c_{\mathbf{k}\downarrow} - c_{\mathbf{k}\downarrow} c_{\mathbf{k}\downarrow}^{\dagger}) \right. \\
 &\quad \left. + \Delta \sum_{\mathbf{k}} (c_{\mathbf{k}\uparrow}^{\dagger} c_{\mathbf{k}\downarrow}^{\dagger} - c_{\mathbf{k}\downarrow}^{\dagger} c_{\mathbf{k}\uparrow}^{\dagger} + c_{\mathbf{k}\uparrow} c_{\mathbf{k}\downarrow} - c_{\mathbf{k}\downarrow} c_{\mathbf{k}\uparrow}) \right\} - \sum_{\mathbf{k}} (\epsilon_{\mathbf{k}} - \mu)
 \end{aligned} \tag{12}$$

Now, it is easy to recast the above Hamiltonian ignoring the last constant term in equation (12) in the following  $(4 \times 4)$  matrix form with  $\tilde{\zeta}_{\mathbf{k}} = \epsilon_{\mathbf{k}} - \mu$  as:

$$\begin{aligned}
 &H_{eff-BCS} - \mu N \\
 &= \sum_{\mathbf{k}} \frac{1}{2} \begin{pmatrix} c_{\mathbf{k}\uparrow}^{\dagger} & c_{\mathbf{k}\downarrow} & c_{\mathbf{k}\downarrow}^{\dagger} & c_{\mathbf{k}\uparrow} \end{pmatrix} \begin{pmatrix} \tilde{\zeta}_{\mathbf{k}} & \Delta & 0 & 0 \\ \Delta & -\tilde{\zeta}_{\mathbf{k}} & 0 & 0 \\ 0 & 0 & \tilde{\zeta}_{\mathbf{k}} & -\Delta \\ 0 & 0 & -\Delta & -\tilde{\zeta}_{\mathbf{k}} \end{pmatrix} \begin{pmatrix} c_{\mathbf{k}\uparrow} \\ c_{\mathbf{k}\downarrow}^{\dagger} \\ c_{\mathbf{k}\downarrow} \\ c_{\mathbf{k}\uparrow}^{\dagger} \end{pmatrix}
 \end{aligned} \tag{13}$$

Considering just the upper block, we may write the part of the matrix as  $(2 \times 2)$  below

$$\begin{pmatrix} c_{\mathbf{k}\uparrow}^{\dagger} & c_{\mathbf{k}\downarrow} \end{pmatrix} \begin{pmatrix} \tilde{\zeta}_{\mathbf{k}} & \Delta \\ \Delta & -\tilde{\zeta}_{\mathbf{k}} \end{pmatrix} \begin{pmatrix} c_{\mathbf{k}\uparrow} \\ c_{\mathbf{k}\downarrow}^{\dagger} \end{pmatrix} \tag{14}$$

The trace of this matrix ( $M_1$ ) is zero while the determinant being  $-(\tilde{\zeta}_{\mathbf{k}}^2 + \Delta^2)$ . As a result, the eigenvalues are simply  $\pm \sqrt{\tilde{\zeta}_{\mathbf{k}}^2 + \Delta^2}$ . In the same way, the lower block also can be seen as

$$\begin{pmatrix} c_{\mathbf{k}\downarrow}^{\dagger} & c_{\mathbf{k}\uparrow} \end{pmatrix} \begin{pmatrix} \tilde{\zeta}_{\mathbf{k}} & -\Delta \\ -\Delta & -\tilde{\zeta}_{\mathbf{k}} \end{pmatrix} \begin{pmatrix} c_{\mathbf{k}\downarrow} \\ c_{\mathbf{k}\uparrow}^{\dagger} \end{pmatrix} \tag{15}$$

It is evident that the trace of this matrix ( $M_2$ ) is zero while the determinant being  $-(\xi_{\mathbf{k}}^2 + \Delta^2)$ . Consequently, the eigenvalues are simply  $\pm\sqrt{\xi_{\mathbf{k}}^2 + \Delta^2}$  like the upper block matrix  $M_1$ .

### 3 BCS Hamiltonian as a pseudo-spin Hamiltonian

Noting down the spin algebra in the previous section we can recast the above BCS Hamiltonian in the pseudo-spin formulation [7, 8] as

$$\begin{aligned} H_{BCS} - \mu N &= \sum_{\mathbf{k}} \left[ \frac{2(\epsilon_{\mathbf{k}} - \mu)}{1} \right. \\ &\quad \left. - \frac{V_0}{\Omega} \Theta(\epsilon_c - |\epsilon_{\mathbf{k}(q)} - \mu|) \right] S_{\mathbf{k}}^z \\ &\quad - \frac{V_0}{\Omega} \sum_{\mathbf{k}, \mathbf{q}} \left( S_{\mathbf{k}}^x S_{\mathbf{q}}^x + S_{\mathbf{k}}^y S_{\mathbf{q}}^y \right) + \sum_{\mathbf{k}} (\epsilon_{\mathbf{k}} - \mu) \\ &= - \sum_{\mathbf{k}} \vec{\mathcal{H}}_{\mathbf{k}} \cdot \vec{S}_{\mathbf{k}} \end{aligned} \quad (16)$$

In the last equation we have thrown away the constant term  $\sum_{\mathbf{k}} (\epsilon_{\mathbf{k}} - \mu)$  without any loss of physics involved in further discussion. Now, we can indeed think of  $\mathbf{k}$ -space as a lattice (it is discretized after all, due to the boundary conditions), and put a  $S = 1/2$  (pseudo-) spin on each lattice site. The above Hamiltonian effectively describes a system of interacting spins on a lattice. The local effective magnetic field acting on each lattice point is simply  $\vec{\mathcal{H}}_{\mathbf{k}}$ . The components of this pseudo-magnetic field are given by

$$\begin{aligned} \mathcal{H}_{\mathbf{k}}^x &= \frac{V_0}{\Omega} \sum_{\mathbf{q}} S_{\mathbf{q}}^x \\ \mathcal{H}_{\mathbf{k}}^y &= \frac{V_0}{\Omega} \sum_{\mathbf{q}} S_{\mathbf{q}}^y \\ \mathcal{H}_{\mathbf{k}}^z &= -\frac{2(\epsilon_{\mathbf{k}} - \mu)}{1} + \frac{V_0}{\Omega} \Theta(\epsilon_c - |\epsilon_{\mathbf{k}(q)} - \mu|) \end{aligned} \quad (17)$$

Thus, the  $z$ -component of  $\mathcal{H}_{\mathbf{k}}$  gives the kinetic energy, while the  $xy$ -component is the potential energy.

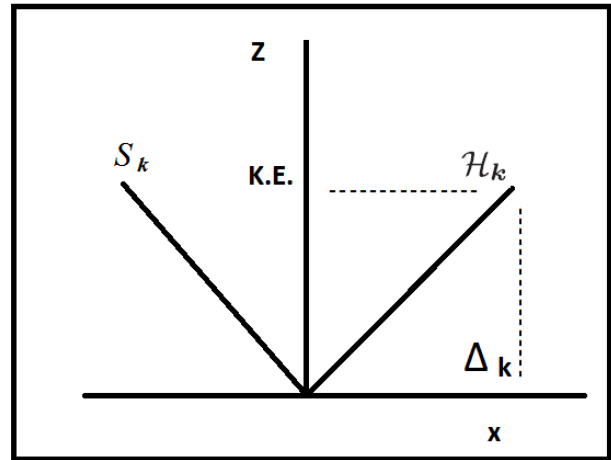


Figure 1: A schematic illustration of the vectors  $\mathcal{H}_{\mathbf{k}}$  and  $S_{\mathbf{k}}$  in the  $x - z$  plane. At equilibrium,  $\mathcal{H}_{\mathbf{k}}$  and  $S_{\mathbf{k}}$  should point in the same direction.

The reduction of this Hamiltonian in this form is equivalent of Anderson's pseudo-spin formulation [7]. Hence, the system is a kind a magnet resides in momentum space.

In figure 1, we show the directions of the pseudo magnetic field and the spin.

Apart from the study of magnetization at finite temperature at mean field level, there is one interesting application of the above equation (17) regarding spin dynamics. Using Heisenberg equation we note that

$$\frac{d}{dt}\vec{S}_{\mathbf{k}} = \vec{S}_{\mathbf{k}} \times \vec{\mathcal{H}}_{\mathbf{k}} \quad (18)$$

The coupled non-linear ordinary differential equation (18) can be solved at the semiclassical level with appropriate boundary conditions. The ground state is the configuration that each spin is parallel to its own local magnetic field.

Under time-reversal symmetry operator  $T_R$ , the states are transformed accordingly from  $|\mathbf{k}, \uparrow\rangle \rightarrow |-\mathbf{k}, \downarrow\rangle$ . Under the operation of parity, it is seen that  $P|\mathbf{k}, \uparrow\rangle = |-\mathbf{k}, \uparrow\rangle$ . Thus under joint operation of parity and time reversal operator, we note that  $PT_R|\mathbf{k}, \uparrow\rangle = |\mathbf{k}, \downarrow\rangle$ . Again the spin-operators are transformed  $T_R\vec{S}_{\mathbf{k}}T_R^{-1} = -\vec{S}_{-\mathbf{k}}$ . As result,  $S_{\mathbf{k}}^z$ ,  $S_{\mathbf{k}}^+$  and  $S_{\mathbf{k}}^-$  will transform respectively as  $S_{-\mathbf{k}}^z$ ,  $S_{-\mathbf{k}}^+$  and  $S_{-\mathbf{k}}^-$ . Note that the kinetic energy being proportional to  $k^2$ , it is invariant under time reversal symmetry. Consequently, the BCS Hamiltonian remains invariant under time reversal symmetry. It is interesting to point out that although the non-interacting part of the Hamiltonian is invariant under parity but the interacting part is not.

Two fold degeneracy is always present in a system with time-reversal symmetry known as Kramer's degeneracy. Interaction

with a **real** magnetic field can destroy the time-reversal symmetry. In s-wave superconductor, the pairing (or the critical transition temperature) is not affected by time-reversal invariant impurities (non-magnetic) as long as the the impurities are not strong enough to cause localization. This is one of the Anderson's theorem in condensed matter physics [10]. In other word, disorder does not affect  $T_C$  as well as the energy gap. But the magnetic impurity scattering can lead to spin-flips which destroy BCS like pairing of time reversal symmetry.

It is interesting to note that for non-interacting case ( $V_0 = 0$ ), the eigenvalues of the above Hamiltonian

$$(E - \mu N)_{non} = \pm \frac{1}{2} \sum_{\mathbf{k}} (\epsilon_{\mathbf{k}} - \mu) \quad (19)$$

To find the nature of the magnet, we find that the non-interacting state is the paramagnet one having positive susceptibility but independent of temperature because of the Pauli exclusion principle at the Fermi energy [ $\chi \propto \frac{1}{T} \times \frac{T}{T_F} \propto T^0$ ]. Now, once we switch on the interaction, there will be alignment of spins with the direction of the magnetic field. Hence, the rotation of spins will take place forming a domain wall. Without the interaction, metal has a sharp domain wall but the superconducting state will have a soft Bloch domain wall as indicated in figure 2. Here, the pseudo-spins rotate *continuously* from down (full) to up (empty) state. In this sense, BCS ground

state is understood as a kind of formation of soft Bloch domain wall at the Fermi surface.

Now we would like to discuss the broken

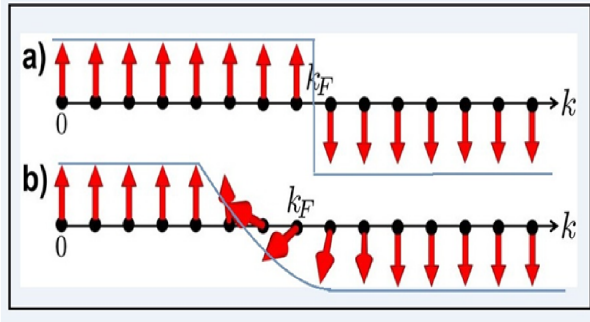


Figure 2: (a) A normal metal with sharp domain wall (b) Superconductor with soft domain wall

symmetry in this Hamiltonian. Since, in the non-interacting case, the Hamiltonian is invariant under rotation about the z-axis due to the conservation of number of particle in the Hamiltonian (Fig 2(a)). However, ground state in Fig. 2(b) breaks the symmetry of the pseudospin Hamiltonian with respect to rotation about the z axis. Because of this symmetry a degenerate set of ground states exists, in which the pseudospins can lie in any plane through the z axis. The angle  $\Phi$  which this plane makes with the xz plane plays an important key role in Josephson effect [11].

Now, if we assume that the pseudospins are lying in the xz plane so that all  $S_{\mathbf{k}}^y$  and  $S_{\mathbf{q}}^y$  are set equal to zero, then we can recast the BCS Hamiltonian into  $(2 \times 2)$  simple Hamiltonian given by

$$H - \mu N = \sum_{\mathbf{k}} \begin{pmatrix} \tilde{\zeta}_{\mathbf{k}} & \Delta_{\mathbf{k}} \\ \Delta_{\mathbf{k}} & -\tilde{\zeta}_{\mathbf{k}} \end{pmatrix} \quad (20)$$

where  $\tilde{\zeta}_{\mathbf{k}} = \epsilon_{\mathbf{k}} - \mu$  and  $\Delta_{\mathbf{k}} = \frac{V_0}{2\Omega} \sum_{\mathbf{q}} S_{\mathbf{q}}^x$ . The above Hamiltonian is the simple BogolibovdeGennes (BdG) Hamiltonian [2] as

$$H_{BdG} = \sum_{\mathbf{k}} [\tilde{\zeta}_{\mathbf{k}} \tau_z + \Delta_{\mathbf{k}} \tau_x] \quad (21)$$

This Hamiltonian matrix has zero trace and its determinant is  $-(\tilde{\zeta}_{\mathbf{k}}^2 + \Delta_{\mathbf{k}}^2)$ . And as a result the energy eigenvalues are  $E_{\mathbf{k}} = \pm \sqrt{\tilde{\zeta}_{\mathbf{k}}^2 + \Delta_{\mathbf{k}}^2}$ . As has been indicated that in the ground state, the spin  $\vec{S}_{\mathbf{k}}$  lies along the magnetic field  $\vec{\mathcal{H}}_{\mathbf{k}}$  giving an energy  $-E_{\mathbf{k}}$ . If the spin is reversed, this costs  $2E_{\mathbf{k}}$ , not  $E_{\mathbf{k}}$ . This reversal corresponds to  $\theta_{\mathbf{k}} \rightarrow \pi - \theta_{\mathbf{k}}$ ,  $\phi_{\mathbf{k}} \rightarrow \pi + \phi_{\mathbf{k}}$ . Thus, the minimum energy required for excitation at the Fermi energy ( $\tilde{\zeta}_{\mathbf{k}} = 0$ ) is  $2\Delta_{\mathbf{k}}$ . The above derivation is valid for any spin-singlet superconducting order parameter including d-wave. For s-wave superconductor, the energy gap  $\Delta_k$  is real and independent of  $k$ .

Finally, one interesting comment about pseudo-spin follows like this. It is clear from the above discussion although algebra of pseudospin is same as that real spin, but it is not linked with the internal magnetic moment of an electron. Hence, they cannot be detected by the Stern-Gerlach type experiments.

## 4 BCS variational wavefunction and expectation values of the operators

To formulate the BCS variational states in the non-interacting case ( $V_0 \neq 0$ ), we proceed in the the basis of spin eigenstates in a factorized form, namely in the form given by

$$|\Psi_0\rangle = \prod_{\mathbf{k}} |\theta_{\mathbf{k}}, \phi_{\mathbf{k}}\rangle \quad (22)$$

Let the polar and azimuthal angle that characterize a unit vector  $\hat{n}$  be  $\theta_{\mathbf{k}}$  and  $\phi_{\mathbf{k}}$  respectively. We rotate the y-axis by angle  $\theta_{\mathbf{k}}$  and subsequently rotate by angle  $\phi_{\mathbf{k}}$  about the z-axis. How does the spin up state  $\chi_1 = \begin{bmatrix} 1 \\ 0 \end{bmatrix}$  transform under the above rotation? This is important because we have pointed out that the local effective magnetic field will rotate continuously the spin up and down states. Let us evaluate it explicitly.

$$\begin{aligned} |\theta_{\mathbf{k}}, \phi_{\mathbf{k}}\rangle &= U_2 U_1 \chi_1 \\ &= \exp(-i\sigma_3 \phi_{\mathbf{k}}/2) \exp(-i\sigma_2 \theta_{\mathbf{k}}/2) \begin{bmatrix} 1 \\ 0 \end{bmatrix} \\ &= [\cos(\phi_{\mathbf{k}}/2) - i\sigma_3 \sin(\phi_{\mathbf{k}}/2)] \\ &\quad \times [\cos(\theta_{\mathbf{k}}/2) - i\sigma_2 \sin(\theta_{\mathbf{k}}/2)] \begin{bmatrix} 1 \\ 0 \end{bmatrix} \\ &= \begin{bmatrix} \cos(\theta_{\mathbf{k}}/2) e^{-i\phi_{\mathbf{k}}/2} \\ \sin(\theta_{\mathbf{k}}/2) e^{+i\phi_{\mathbf{k}}/2} \end{bmatrix} \\ &= \cos(\theta_{\mathbf{k}}/2) e^{-i\phi_{\mathbf{k}}/2} \begin{bmatrix} 1 \\ 0 \end{bmatrix} \\ &\quad + \sin(\theta_{\mathbf{k}}/2) e^{+i\phi_{\mathbf{k}}/2} \begin{bmatrix} 0 \\ 1 \end{bmatrix} \end{aligned} \quad (23)$$

This form of the state will help us to compute the expectation values of the spin operators in the BCS Hamiltonian. But before that we pause for a while to connect this state with the usual BCS variational wavefunction written in second quantized form.

Note that the true vacuum states are those in which all pairs are empty (spin down). To generate a state with the spin in the xz plane and quantized at an angle  $\theta_{\mathbf{k}}$  with the z axis, we have the unitary rotation matrix

$$\begin{aligned} U_1 &= [\cos(\theta_{\mathbf{k}}/2) - i\sigma_2 \sin(\theta_{\mathbf{k}}/2)] \\ &= [\cos(\theta_{\mathbf{k}}/2) - \frac{1}{2}(S_{\mathbf{k}}^+ - S_{\mathbf{k}}^-) \sin(\theta_{\mathbf{k}}/2)] \end{aligned} \quad (24)$$

Note that  $S_{\mathbf{k}}^-$  operates on the vacuum gives zero contribution and as a result

$$\begin{aligned} |\Psi_0\rangle &= \prod_{\mathbf{k}} |\theta_{\mathbf{k}}, \phi_{\mathbf{k}}\rangle \\ &= \prod_{\mathbf{k}} [\cos(\theta_{\mathbf{k}}/2) - S_{\mathbf{k}}^+ \sin(\theta_{\mathbf{k}}/2)] |0\rangle \\ &= \prod_{\mathbf{k}} (u_{\mathbf{k}} + v_{\mathbf{k}} b_{\mathbf{k}}^+) |0\rangle \end{aligned} \quad (25)$$

with the identification  $u_{\mathbf{k}} = \cos(\theta_{\mathbf{k}}/2)$  and  $v_{\mathbf{k}} = -\sin(\theta_{\mathbf{k}}/2)$ . Note that  $|u_{\mathbf{k}}|^2 + |v_{\mathbf{k}}|^2 = 1$  which is regarded as the normalization condition of the variational wave function. Moreover, a careful look also reveals that  $u_{-\mathbf{k}} = u_{\mathbf{k}}$  while  $v_{-\mathbf{k}} = -v_{\mathbf{k}}$ . The BCS wavefunction, Eq. (20), does not contain a well defined particle number. In particular,  $|\Psi_0\rangle$  contains all possible even particle numbers from 0 to  $\infty$ . This is consistent with the remark made earlier about the non-conservation of no. of particles in the superconducting state.

Note that for  $k \ll k_F$  we have  $\frac{1}{2}\theta_{\mathbf{k}} = \frac{\pi}{2}$  and in this region, it is entirely filled with electrons.

How is the equation (25) related to Cooper pair wave function in real space?

We know that the wave function of Cooper pair is spin-singlet state (zero orbital angular momentum) with symmetrical spatial part.

$$\begin{aligned} \psi(\mathbf{r}_1, \mathbf{r}_2; \uparrow, \downarrow) &= \Phi(|\mathbf{r}_1 - \mathbf{r}_2|) \\ &\times \frac{1}{\sqrt{2}} [|\uparrow\rangle_1 |\downarrow\rangle_2 - |\uparrow\rangle_2 |\downarrow\rangle_1] \end{aligned} \quad (26)$$

where the spatial part  $\Phi(\mathbf{r}) = \Phi(-\mathbf{r})$ . The Fourier transformation of the above wave function can be written as

$$\Phi(\mathbf{r}) = \sum_{\mathbf{k}} g(\mathbf{k}) e^{i\mathbf{k}\cdot\mathbf{r}} \quad (27)$$

Then, we notice that

$$\begin{aligned} &\psi(\mathbf{r}_1, \mathbf{r}_2; \uparrow, \downarrow) \\ &= \frac{1}{\sqrt{2}} [|\uparrow\rangle_1 |\downarrow\rangle_2 - |\uparrow\rangle_2 |\downarrow\rangle_1] \\ &\quad \times \sum_{\mathbf{k}} g(\mathbf{k}) e^{i\mathbf{k}\cdot(\mathbf{r}_1 - \mathbf{r}_2)} \\ &= \sum_{\mathbf{k}} \frac{g(\mathbf{k})}{\sqrt{2}} \{ |\mathbf{k}, \uparrow\rangle_1 | -\mathbf{k}, \downarrow\rangle_2 \\ &\quad - | \mathbf{k}, \downarrow\rangle_1 | -\mathbf{k}, \uparrow\rangle_2 \} \\ &= \sum_{\mathbf{k}} \frac{g(\mathbf{k})}{\sqrt{2}} \{ |\mathbf{k}, \uparrow\rangle_1 | -\mathbf{k}, \downarrow\rangle_2 \\ &\quad - | -\mathbf{k}, \downarrow\rangle_1 | \mathbf{k}, \uparrow\rangle_2 \} \\ &= \sum_{\mathbf{k}} g(\mathbf{k}) \mathbf{b}_{\mathbf{k}}^\dagger | \mathbf{0} \rangle \end{aligned} \quad (28)$$

where we have used  $g(\mathbf{k}) = g(-\mathbf{k})$  to restore the symmetry properties of  $\Phi(\mathbf{r})$ . This

completes the connection of Cooper pair with the spin wave function  $|\Psi_0\rangle$ .

Now we are going to calculate the expectation value of the spin operator.

$$\begin{aligned} \langle S_{\mathbf{k}}^+ \rangle &= \frac{1}{2} \sin \theta_{\mathbf{k}} e^{i\phi_{\mathbf{k}}} \\ \langle S_{\mathbf{k}}^- \rangle &= \frac{1}{2} \sin \theta_{\mathbf{k}} e^{-i\phi_{\mathbf{k}}} \end{aligned} \quad (29)$$

Note that the expectation values (setting  $\phi_{\mathbf{k}} = 0$ ) are non-zero only at  $\theta_{\mathbf{k}} = \frac{\pi}{2}$  and zero at  $\theta_{\mathbf{k}} = 0$ . This serves as an order parameter in the superconducting state to metallic phase transition. As a consequence,

$$\begin{aligned} \langle S_{\mathbf{k}}^x \rangle &= \frac{1}{2} \langle \Psi_0 | (S_{\mathbf{k}}^+ + S_{\mathbf{k}}^-) | \Psi_0 \rangle \\ &= \frac{1}{2} \left( \cos(\theta_{\mathbf{k}}/2) \sin(\theta_{\mathbf{k}}/2) e^{i\phi_{\mathbf{k}}/2} \right. \\ &\quad \left. + \cos(\theta_{\mathbf{k}}/2) \sin(\theta_{\mathbf{k}}/2) e^{-i\phi_{\mathbf{k}}/2} \right) \\ &= \frac{1}{2} \sin(\theta_{\mathbf{k}}) \cos(\phi_{\mathbf{k}}) \end{aligned} \quad (30)$$

In the similar way, we can find the expectation values of the other two operators as

$$\begin{aligned} \langle S_{\mathbf{k}}^y \rangle &= \frac{1}{2i} \langle \Psi_0 | (S_{\mathbf{k}}^+ - S_{\mathbf{k}}^-) | \Psi_0 \rangle \\ &= \frac{1}{2} \sin(\theta_{\mathbf{k}}) \sin(\phi_{\mathbf{k}}) \\ \langle S_{\mathbf{k}}^z \rangle &= \frac{1}{2} \cos(\theta_{\mathbf{k}}) \end{aligned} \quad (31)$$

It is evident that for  $\theta_{\mathbf{k}} = \pi/2$ ,  $\langle S_{\mathbf{k}}^z \rangle = 0$  while  $\langle S_{\mathbf{k}}^x \rangle \neq 0, \langle S_{\mathbf{k}}^y \rangle \neq 0$  (provided  $\phi_{\mathbf{k}} \neq \pi/2$ ). On the other limit,  $\theta_{\mathbf{k}} = 0$ ,  $\langle S_{\mathbf{k}}^z \rangle \neq 0$  while other two expectation values of the spin operator reduce to zero. This observation is important to identify the order parameter of this phase transition of normal metal to superconducting system. Therefore,  $\theta_{\mathbf{k}} = \pi/2$  limit is responsible for occurrence of superconducting state while  $\theta_{\mathbf{k}} = 0$

is the signature of the metallic state. Moreover, the expectation value of the spin operator on the  $|\theta_{\mathbf{k}}, \phi_{\mathbf{k}}\rangle$  state behaves like a classical spin of length  $S = 1/2$ . to yield the length of the spin as  $\frac{1}{2}$ . Further, we notice that

$$\begin{aligned} & \langle (S_{\mathbf{k}}^x)^2 \rangle + \langle (S_{\mathbf{k}}^y)^2 \rangle + \langle (S_{\mathbf{k}}^z)^2 \rangle \\ &= \frac{3}{4} = \frac{1}{2} \left( \frac{1}{2} + 1 \right) \end{aligned} \quad (32)$$

consistent with the spin algebra of spin 1/2 system. We also note that

$$\begin{aligned} & \langle \theta_{\mathbf{k}}, \phi_{\mathbf{k}} | \langle \theta_{\mathbf{q}}, \phi_{\mathbf{q}} | (S_{\mathbf{k}}^x S_{\mathbf{q}}^x \\ & + S_{\mathbf{k}}^y S_{\mathbf{q}}^y | \theta_{\mathbf{k}}, \phi_{\mathbf{k}} \rangle | \theta_{\mathbf{q}}, \phi_{\mathbf{q}} \rangle \\ &= \frac{1}{4} \sin(\theta_{\mathbf{k}}) \sin(\theta_{\mathbf{q}}) [\cos(\phi_{\mathbf{k}}) \cos(\phi_{\mathbf{q}}) \\ & + \sin(\phi_{\mathbf{k}}) \sin(\phi_{\mathbf{q}})] \\ &= \frac{1}{4} \sin(\theta_{\mathbf{k}}) \sin(\theta_{\mathbf{q}}) \cos(\phi_{\mathbf{k}} - \phi_{\mathbf{q}}) \end{aligned} \quad (33)$$

With these expectation values, we are now ready to compute the expectation values of the BCS Hamiltonian in equation (16).

## 5 BCS gap equation

The expectation values of the non-interacting part and interacting parts are respectively

$$\begin{aligned} & \langle \Psi_0 | (H - \mu N)_{non-int} | \Psi_0 \rangle \\ &= \sum_{\mathbf{k}} [2(\epsilon_{\mathbf{k}} - \mu) \\ & - \frac{V_0}{\Omega} \Theta(\epsilon_c - |\epsilon_{k(q)} - \mu|)] \cos(\theta_{\mathbf{k}}) \end{aligned} \quad (34)$$

and

$$\begin{aligned} & \langle \Psi_0 | (H - \mu N)_{int} | \Psi_0 \rangle \\ &= -\frac{V_0}{4\Omega} \sum'_{\mathbf{k} \neq \mathbf{q}} \cos(\phi_{\mathbf{k}} - \phi_{\mathbf{q}}) \sin(\theta_{\mathbf{k}}) \sin(\theta_{\mathbf{q}}) \end{aligned} \quad (35)$$

With these variational energy expressions, we would like to find out the specific spin inclination which minimizes the above energy expression. Now, in this model Hamiltonian  $V_0 > 0$  and  $\theta$  lies between 0 and  $\pi$ , it is evident that  $\phi_{\mathbf{k}} = \phi_{\mathbf{q}} = 0$  minimize the energy expression. Therefore, minimizing the variational energy with respect to  $\theta_{\mathbf{k}}$  for  $|\epsilon_{\mathbf{k}} - \mu| < \epsilon_c$ , we obtain

$$\begin{aligned} & \left( \epsilon_{\mathbf{k}} - \mu - \frac{V_0}{2\Omega} \right) \sin \theta_{\mathbf{k}} \\ &= -\frac{V_0}{2\Omega} \sum'_{\mathbf{k} \neq \mathbf{q}} \sin \theta_{\mathbf{q}} \cos \theta_{\mathbf{k}} \end{aligned} \quad (36)$$

This equation (36) is the central equation of BCS theory from which all the calculations of the physical quantities can be evaluated. Making an error of order  $O(1/\Omega)$ , we can neglect the term  $\frac{V_0}{2\Omega}$  on the left-hand side and then add the term with  $\mathbf{q} = \mathbf{k}$  in the sum on the right-hand side. Introducing then the symbol

$$\Delta = -\frac{V_0}{2\Omega} \sum'_{\mathbf{q}} \sin \theta_{\mathbf{q}} \quad (37)$$

we find

$$\begin{aligned}\tan \theta_{\mathbf{k}} &= \frac{|\Delta|}{(\epsilon_{\mathbf{k}} - \mu)} \\ E_{\mathbf{k}} &= \sqrt{(\epsilon_{\mathbf{k}} - \mu)^2 + \Delta^2} \\ \sin \theta_{\mathbf{k}} &= \frac{|\Delta|}{E_{\mathbf{k}}} \\ \cos \theta_{\mathbf{k}} &= \frac{\mu - \epsilon_{\mathbf{k}}}{E_{\mathbf{k}}}\end{aligned}\quad (38)$$

With these values, we can easily write down the self-consistent energy gap equation as

$$\Delta = \frac{V_0}{2} \sum_{\mathbf{k}} \frac{\Delta}{\sqrt{\xi_{\mathbf{k}}^2 + \Delta^2}} \quad (39)$$

and from which we get the integral equation for solving the gap  $\Delta$  as

$$1 = \frac{V_0}{2} \int_{-\hbar\omega_D}^{\hbar\omega_D} \frac{N(\xi) d\xi}{\sqrt{\xi^2 + \Delta^2}} \quad (40)$$

The above integral can be evaluated under the assumption that the density of states (DOS) within this energy scale ( $\hbar\omega_D \ll E_F$ ) is constant and is given by  $N(0)$ , DOS at the Fermi energy  $E_F$ . Before, we do the exact analysis, let us have a critical look to obtain the approximate value of the integral. The integrand is approximately  $d\xi/\xi$  over most of the range, which is **log** divergent both at  $\xi \rightarrow 0$  and  $\xi \rightarrow \infty$ . The actual integrand however stops diverging and levels off once  $|\xi| < \Delta$  and the upper cutoff is  $\omega_D$ . Thus, the approximated value of the integral is

$$\begin{aligned}1 &\approx N(0)V_0 \left[ \int_{\Delta}^{\hbar\omega_D} + \int_{\hbar\omega_D}^{\Delta} \right] \frac{d\xi}{\xi} \\ 1 &\approx N(0)V_0 \left[ \ln \left( \frac{\hbar\omega_D}{\Delta} \right) + \text{const} \right]\end{aligned}\quad (41)$$

The gap equation in this approximation reads as

$$\Delta \approx \text{const } \hbar\omega_D \exp \left( -\frac{1}{N(0)V_0} \right) \quad (42)$$

The exact final expression for the zero-temperature energy gap is simply

$$\begin{aligned}1 &= N(0)V_0 \sinh^{-1} \left( \frac{\hbar\omega_D}{\Delta} \right) \\ \Delta &= \frac{\hbar\omega_D}{\sinh \left( \frac{1}{N(0)V_0} \right)}\end{aligned}\quad (43)$$

Note that this energy gap is quite different from the energy gap observed in typical semiconductor or insulator. As it is clear that in superconductivity, the energy gap is tied to the Fermi surface where in semiconductor or insulator, it is connected to the lattice itself. The zero-temperature gap equation contains three parameters: one ( $N(0)$ ) characterizing the free-electron energy scale, another ( $\omega_D$ ) characterizing the phonon energy scale, and a third ( $V_0$ ) related to the interaction term (electron-phonon). Using the BCS approximation  $N(0)V_0 \ll 1$ , we find the simple expression of the zero temperature energy gap as

$$\Delta = 2\hbar\omega_D \exp \left( -\frac{1}{N(0)V_0} \right) \quad (44)$$

The dependence of  $\Delta$  on  $V_0$  is non-analytic, indeed it is exactly the function  $\exp(-1/z)$  that is the cautionary example of analytic function theory. Its Taylor series is zero term-by-term. Therefore, the above expression cannot be obtained by perturbation theory [2]. Since  $\omega_D$  is proportional to  $M^{-1/2}$ ,

$M$  being the mass of the ion, thus  $\Delta \approx k_B T_C$  is proportional to  $M^{-1/2}$  establishing the isotope effect in superconductivity.

### 5.1 Finite temperature energy gap equation and Universality

To compute the transition temperature  $T_C$  we generously use the molecular field method used in the study of the theory of ferromagnetism. At a finite temperature  $T$ , the ensemble average spin for this two-state system is directed along the effective field  $\vec{\mathcal{H}}_{\mathbf{k}}$  and has the magnitude,

$$\langle S_{\mathbf{k}} \rangle = \tanh \left( \frac{\mathcal{H}_{\mathbf{k}}}{k_B T} \right) \quad (45)$$

Note that this **tanh** function is a typical characteristic of any two level system. Before we use this result, one small modification is required. This result is correct for the spin analog model which works entirely in the pair subspace. Now, If we extend the space to allow single particle excitations we have to change  $T$  by  $2T$  [8]. Hence, with this variation of the spin component with temperature ( $\xi_{\mathbf{k}}$  remains unchanged ) the new gap equation at finite temperature  $T$  can be obtained by inserting  $\tanh(\frac{E_{\mathbf{k}}}{2k_B T})$  in the right-hand side of equation (39)

$$\Delta = \frac{V_0}{2} \sum_{\mathbf{k}} \frac{\Delta}{\sqrt{\xi_{\mathbf{k}}^2 + \Delta^2}} \tanh \left( \frac{E_{\mathbf{k}}}{2k_B T} \right) \quad (46)$$

This factor correctly reproduces the physics involved in this phase transition. As we raise the temperature  $T$ , the **tanh** factor

gradually takes over the job of suppressing the logarithmic divergence, which was handled by  $\Delta$  in  $\sqrt{\xi_{\mathbf{k}}^2 + \Delta^2}$  in the denominator. As a result,  $\Delta$  will decrease. For  $T > T_C$ , there is only one solution for the self-consistency equation,  $\Delta = 0$ . The transition  $T = T_C$  occurs in this model when  $\Delta = 0$ , i.e. superconductor becomes metal. The integral representation of finite energy gap equation reads as

$$1 = \frac{N(0)V_0}{2} \int_{-\hbar\omega_D}^{\hbar\omega_D} \frac{d\xi \tanh \left( \frac{\sqrt{\xi_{\mathbf{k}}^2 + \Delta^2(T)}}{2k_B T_C} \right)}{\sqrt{\xi_{\mathbf{k}}^2 + \Delta^2(T)}} \quad (47)$$

We would like to approximate the above integral as done in the previous section. The upper cutoff is  $\hbar\omega_D$  again, while the lower cutoff is roughly  $\xi_{\mathbf{k}} \approx k_B T_C$ , since that is where the **tanh** function in (46) crosses over from unity to a linear behavior that eventually cancels the  $1/\xi$  divergence. Thus  $T_C$  is playing the same role in (46) that  $\Delta$  played in the gap equation in (39); as one might anticipate, we have

$$1 \approx N(0)V_0 \left[ \ln \left( \frac{\hbar\omega_D}{k_B T_C} \right) + const \right] \quad (48)$$

and  $k_B T_C \approx \Delta(0)$ . The numerical result consistent with BCS equation ( $N(0)V_0 \ll 1$ , the upper limit is very large) gives us [2, 8]

$$\begin{aligned} \frac{1}{N(0)V_0} &= \int_0^{\hbar\omega_D} \frac{d\xi \tanh \left( \frac{\xi}{2k_B T_C} \right)}{\xi} \\ &= \ln \left( \frac{1.14\hbar\omega_D}{k_B T_C} \right) \\ k_B T_C &= 1.14 \hbar\omega_D \exp \left( -\frac{1}{N(0)V_0} \right) \end{aligned} \quad (49)$$

The critical transition temperature is proportional to the Debye frequency. In addition, it depends on the density of states  $N(0)$  and interaction strength  $V_0$  in a non-analytic way. As the interaction becomes weaker and weaker,  $T_C$  goes down to zero.

Comparing with equation (44) we obtain the final universal result

$$\frac{2\Delta(0)}{k_B T_C} = \frac{4}{1.14} = 3.508 \quad (50)$$

independent of the three parameters  $\omega_D$ ,  $N(0)$  and  $V_0$  and is valid in the weak coupling limit. For strong coupling limit, however, the above ratio can be greater than 3.508. For any BCS type of superconductor, the ratio of zero temperature energy gap and its transition temperature is constant and independent of microscopic interacting parameters relevant for electrons. Any violation of the above relation is termed as non-BCS signature of any superconductor. Most of the high temperature superconductors, however, do not obey the above relation.

At finite temperature  $T < T_C$ , the gap equation can be written as

$$\int_0^\infty d\xi \left[ \frac{\tanh(\frac{E}{2k_B T})}{E} - \frac{\tanh(\frac{\xi}{2k_B T_C})}{\xi} \right] = 0 \quad (51)$$

Notice that since this integral converges, we have extended the upper limit to  $\infty$  without any loss of generality. Then, we can easily

see that the energy gap should be written as

$$\begin{aligned} \Delta(T) &= T_C f\left(\frac{T}{T_C}\right) \\ \frac{\Delta(T)}{\Delta(0)} &= g\left(\frac{T}{T_C}\right) \end{aligned} \quad (52)$$

The numerical integration of equation (51) near transition temperature  $T_C$  yields [2]

$$\frac{\Delta(T)}{\Delta(0)} = 1.74 \left(1 - \frac{T}{T_C}\right)^{1/2} \quad (53)$$

As a result, the coherence length in case superconductor defined as  $\xi(T) = \frac{\hbar v_F}{\pi \Delta(T)}$  varies with  $(T_C - T)^{-1/2}$  consistent with the mean field exponent  $\beta = 1/2$  of GL theory [9]. Further, it is observed that the specific heat shows a discontinuity or jump at  $T_C$  indicating the critical exponent  $\alpha = 0$ . In this sense, Anderson's pseudo-spin approach is a mean field theory as the exponents are classical.

## 6 Magnetization and Average particle number

We define the magnetization as

$$M = \frac{1}{2} \mu_B \sum_{\mathbf{k}} \langle (n_{\mathbf{k}\uparrow} - n_{\mathbf{k}\downarrow}) \rangle \quad (54)$$

In computing this magnetization, we find

$$\begin{aligned} M_{\mathbf{k}}^2 &= \langle (n_{\mathbf{k}\uparrow} - n_{\mathbf{k}\downarrow})^2 \rangle \\ &= \langle (n_{\mathbf{k}\uparrow} + n_{\mathbf{k}\downarrow})^2 - 4n_{\mathbf{k}\uparrow} n_{\mathbf{k}\downarrow} \rangle \\ &= \langle (1 + 2S_{\mathbf{k}}^z)^2 - 4S_{\mathbf{k}}^+ S_{\mathbf{k}}^- \rangle \\ &= (1 + \cos \theta_{\mathbf{k}})^2 - \left(4 \times \frac{1}{4}\right) \sin^2 \theta_{\mathbf{k}} \\ &= 1 + 2 \cos \theta_{\mathbf{k}} + \cos 2\theta_{\mathbf{k}} \end{aligned} \quad (55)$$

It is really nice to see that the square of the magnetization at  $\mathbf{k}$ -th state for superconducting state ( $\theta_{\mathbf{k}} = \frac{\pi}{2}$ ) identically vanishes to zero. However, for the metallic state  $M_{\mathbf{k}}^2 = 4$  since  $\theta_{\mathbf{k}} = 0$ .

The zero magnetization also can be seen easily from the fact that in the superconducting state because either the pairs are empty or occupied. In the zero orbital magnetic moment, since the total spin of the Cooper pairs is zero, thus, the magnetic state of the superconducting material is diamagnetic.

Now let us have a look at how well defined is the average particle number. We define the average particle number as

$$\begin{aligned} \langle N \rangle &= \sum_{\mathbf{k}} \langle n_{\mathbf{k},\uparrow} + n_{-\mathbf{k},\downarrow} \rangle \\ &= \sum_{\mathbf{k}} \langle 1 + 2S_{\mathbf{k}}^z \rangle \\ &= \sum_{\mathbf{k}} (1 + \cos \theta_{\mathbf{k}}) \end{aligned} \quad (56)$$

Similarly, the average square number of particle is calculated as

$$\begin{aligned} \langle N^2 \rangle &= \sum_{\mathbf{k} \neq \mathbf{q}} \langle (n_{\mathbf{k},\uparrow} + n_{-\mathbf{k},\downarrow})(n_{\mathbf{q},\uparrow} + n_{-\mathbf{q},\downarrow}) \rangle \\ &= \left( \sum_{\mathbf{k}} (1 + \cos \theta_{\mathbf{k}}) \right)^2 \\ &\quad + \sum_{\mathbf{k}} (1 + \cos \theta_{\mathbf{k}})(1 - \cos \theta_{\mathbf{k}}) \end{aligned} \quad (57)$$

As a result, we find

$$\begin{aligned} \langle N^2 \rangle - (\langle N \rangle)^2 &= \langle (\Delta N)^2 \rangle \\ &= \sum_{\mathbf{k}} (1 - \cos^2 \theta_{\mathbf{k}}) \end{aligned} \quad (58)$$

Note that for  $\theta_{\mathbf{k}} = 0$  (metallic one), this fluctuation in number of particles is zero while

for the superconducting state this value is non-zero. Again the sum is of the order of  $O(N)$  and hence,

$$\frac{\langle (\Delta N)^2 \rangle}{\langle N \rangle^2} \sim \frac{1}{\langle N \rangle} \quad (59)$$

This implies that the root mean square deviation (RMS) from the average number of particles  $\langle N \rangle$  is of the order of  $\frac{1}{\sqrt{\langle N \rangle}}$ . For a typical  $10^{20} \text{ cm}^{-3}$  value of the average number of particles, this RMS value (relative fluctuation) turns out to be  $10^{-10}$ . Thus, although  $|\Psi_0 \rangle$  does not conserve number of particles however, it does not pose any serious issue in calculating the physical quantity within BCS theory. In such a case we can simply compute the physical quantity with **definite** number of electrons  $\langle N \rangle$  in the  $\mathbf{k}$ -th state.

## 7 Conclusion

In this paper, Anderson's Pseudo-spin analog has been used to obtain BCS gap equation without invoking the complex calculation involving second quantized operators. This formalism points out the existence of soft domain wall in the superconducting state in contrast to sharp one in the metallic one. Besides, the spontaneous symmetry breaking can be identified in this formalism. Finally, this approach finds an easy way to compute the finite temperature energy gap equation, transition temperature and its universality highlighting the mean field theory of statistical mechanics. The formalism has

been also extended to account for the magnetism and the number fluctuation in BCS state. Besides, we have incorporated  $(4 \times 4)$  matrix formulation of BCS Hamiltonia in single electron's Fock space for completeness.

## Acknowledgments

The author would like to acknowledge the post-graduate students of the Dept. of Physics, University of Calcutta for motivating him to write this paper. The author also thanks Mr. Arka Bandyopadhyay and Mr. Supriya Ghosal for critical reading of manuscript.

## References

- [1] L. N. Cooper, *Phys. Rev.*, **104**, 1189 (1956).
- [2] P. G. de Gennes, *Superconductivity of metals and alloys*, W. A. Benjamin, Inc. (New York, Amsterdam), 1966.
- [3] A. Saraiva et. al, *Phys. Rev. Lett.*, **119**, 193603 (2017).
- [4] J. Bardeen, L. N. Cooper and R. Schrieffer, *Phys. Rev.*, **108**, 1175 (1957).
- [5] T. O. Wehling, A. M. Black-Schaffer, and A. V. Balatsky, *Adv. Phys.*, **76**, 1 (2014).
- [6] A. Bandyopadhyay and D. Jana, *Univ. Jour. Mater. Sci.*, **8**, 32 (2020).
- [7] P. W. Anderson, *Phys. Rev.* **112**, 1900 (1958).
- [8] C. Kittel, *Quantum Theory of Solids* (John Wiley and Sons, NY, 1963).
- [9] Philip Phillips, *Advanced Solid State Physics*, (West View, USA, 2003) Page 248-249.
- [10] P. W. Anderson, *Basic Notions of Condensed Matter Physics*, (Addison-Wesley, 1997).
- [11] B. D. Josephson, *Rev. Mod. Phys.*, **46**, 250 (1974).

# Spin Inequality for Energy Computation of Heisenberg Spin Hamiltonian

Debnarayan Jana

Department of Physics, University of Calcutta  
92 A P C Road, Kolkata- 700 009, West Bengal, India.  
djphy@caluniv.ac.in

*Submitted on 17-Jun-2020*

## Abstract

In this paper, we will use a simple spin inequality to compute the ground state energy of nearest neighbour Heisenberg Hamiltonian in one dimension. The implication of this inequality will be highlighted in the thermodynamic properties also. Finally, the utility of this technique is illustrated in Majumdar-Ghosh model.

**Keywords:** Spin algebra, Heisenberg Spin Hamiltonian

## 1. Introduction

The story of magnetism is evergreen and till date can inspire the researcher [1, 2, 3]. Consider the atoms in a crystal with zero orbital quantum number but with non-vanishing spins. It is further assumed that such atoms are separated by sufficiently large distances so that the interaction between them is considered to be weak [4, 5]. In the famous

Heisenberg model, the interaction between two adjacent spins is taken to be as the simple scalar product of spin operators at two different sites  $i$  and  $j$  given by

$$H = \sum_{\langle ij \rangle} J_{ij} \vec{S}_i \cdot \vec{S}_j \quad (1)$$

Here,  $J_{ij}$  is the exchange integral related to the matrix elements of Coulomb interaction of the exchanged two particle wave functions. It is interesting to point out that beyond the usual  $\sum_{\langle ij \rangle} J_{ij} \vec{S}_i \cdot \vec{S}_j$  terms, the *ab-initio* calculations [6] necessarily introduce the four-body spin operators in the  $S = \frac{1}{2}$  case and biquadratic terms in the  $S = 1$  in the effective Hamiltonian formalism. In theoretical computations, this integral  $J_{ij}$  is taken to be constant. In the Heisenberg model, the electronic degrees of freedom are neglected and only the spin degree of freedom plays a key role in controlling the magnetic properties of the solid comprising of the atoms. These spin Hamiltonians not only include Spin -1/2 but also an arbitrary spin

$S \geq 1/2$ . There is indeed rich and quite robust physics from the phase transition point of view and also from the exactly solvable models of quantum many body physics [7, 8, 9, 10].

## 2. Spin Inequality

We will start from a simple quantum mechanical relation about the expectation value of a hermitian operator. Let  $O$  be the hermitian operator and  $\{|\Phi_n\rangle\}$  be its complete set of orthonormal eigenstates with eigenvalues  $O_n$ . Then, we can write the expectation value of the hermitian operator  $O$  in an arbitrary state  $|\Psi\rangle$  ( $|\Psi\rangle = \sum_n C_n |\Phi_n\rangle$  along with  $\langle\Psi|\Psi\rangle = 1; \sum_n |C_n|^2 = 1$ ) as

$$\begin{aligned}\langle O \rangle &= \langle\Psi|O|\Psi\rangle \\ &= \sum_{m,n} C_m^* C_n \langle\Phi_m|O|\Phi_n\rangle \\ &= \sum_n |C_n|^2 O_n \geq O_0\end{aligned}\quad (2)$$

Thus, it is clear from the above equation that the largest value of  $\langle O \rangle$  is given by the largest eigenvalue of  $O$  obtained by taking the  $|\Psi\rangle$  to be the eigenstates of  $O$  with the largest eigenvalue. Even, if we consider the smallest value of  $\langle O \rangle$ , then we have to take the smallest eigenvalue of  $O_0$ . Hence, for an arbitrary hermitian matrix, the largest diagonal element is bounded by the largest eigenvalue. This fact will now be utilized to show that the maximum value of  $\langle\vec{S}_i \cdot \vec{S}_j\rangle = S^2$ . Here, the spins are considered on different sites ( $i \neq j$ ). Now, note that

$$\vec{S}_i \cdot \vec{S}_j = \frac{1}{2} [(\vec{S}_i + \vec{S}_j)^2 - \vec{S}_i^2 - \vec{S}_j^2] \quad (3)$$

Thus, the largest expectation value of  $\vec{S}_i \cdot \vec{S}_j$  is given by the largest eigenvalue of the operator on the rhs of the equation (3). It is interesting to note that the three terms in the rhs of equation (3) commute ( $[H, \vec{S}_i^2] = 0 = [H, \vec{S}_j^2]$ ) with each other which indicates that we can find simultaneous eigenstates for them. The eigenvalues of  $\vec{S}_i^2$  and  $\vec{S}_j^2$  are  $S(S+1)$  while the eigenvalues of  $(\vec{S}_i + \vec{S}_j)^2$  are  $S_{tot}(S_{tot} + 1)$  with  $S_{tot} = |S - S|, \dots, S + S = 0, 1, 2, \dots, 2S$ .

Therefore, the largest expectation value of eigenvalue of  $\vec{S}_i \cdot \vec{S}_j$  is obtained with  $S_{tot} = 2S$  and hence,

$$\begin{aligned}Max \langle\vec{S}_i \cdot \vec{S}_j\rangle &= \frac{\hbar^2}{2} [2S(2S+1) - 2S(S+1)] \\ &= \frac{\hbar^2}{2} \times 2S^2 = \hbar^2 S^2\end{aligned}\quad (4)$$

One might wonder then, the minimum value of the expectation of  $\vec{S}_i \cdot \vec{S}_j$  would be  $-S^2$ . But it is not; as can be seen below by the computation from the equation (2). The minimum value of  $\langle\vec{S}_i \cdot \vec{S}_j\rangle$  is obtained from  $S_{tot} = 0$  as

$$\begin{aligned}Min \langle\vec{S}_i \cdot \vec{S}_j\rangle &= \frac{\hbar^2}{2} [0 - 2S(S+1)] \\ &= -\frac{\hbar^2}{2} \times 2S(S+1) \\ &= -\hbar^2 S(S+1)\end{aligned}\quad (5)$$

Therefore, the expectation value of  $\vec{S}_i \cdot \vec{S}_j$  satisfies the following bounds given by

$$-S(S+1)\hbar^2 \leq \langle\vec{S}_i \cdot \vec{S}_j\rangle \leq S^2\hbar^2 \quad (6)$$

For just two spins with  $S = \frac{1}{2}$ , we have two eigenvalues of  $-\frac{3\hbar^2}{4}$  (triplet state) and

$\frac{\hbar^2}{4}$  (singlet) and the difference between the eigenvalues is  $\hbar^2$ . With the above two expectation values, we now move forward to calculate the ground state energy of Heisenberg models comprising of 2, 3 and 4 spins.

### 3. Two Spin Heisenberg Hamiltonian

The two spins are interacting via the Hamiltonian given by

$$H = J\vec{S}_1 \cdot \vec{S}_2 \quad (7)$$

A straightforward spin algebra yields, there are two eigenvalues one being  $-\frac{3J\hbar^2}{4}$  non-degenerate and other  $\frac{J\hbar^2}{4}$  is three-fold degenerate. These eigenvalues also can be understood from the maximum and minimum values of  $\vec{S}_1 \cdot \vec{S}_2$  as shown in the previous section. The partition function of the system as a function of temperature ( $\beta = \frac{1}{k_B T}$ ) can be written with  $\Delta = \frac{J\hbar^2}{4}$  as

$$Z(\Delta, \beta) = e^{-\beta\Delta}(3 + e^{4\beta\Delta}) \quad (8)$$

The average energy of the above two level system can be written as

$$E_{av} = \Delta - \frac{4\Delta}{1 + 3e^{-4\beta\Delta}} \quad (9)$$

which correctly reproduces the high temperature (0) and low temperature ( $-3\Delta$ ) values. The entropy can be computed as

$$S(\Delta, T) = k_B \log(3 + e^{4\beta\Delta}) - \frac{4\Delta}{T} \frac{1}{(1 + 3e^{-4\beta\Delta})} \quad (10)$$

As  $T \rightarrow 0$ , the entropy  $S \rightarrow 0$  validating the third law of thermodynamics. In the high temperature limit,  $S \rightarrow k_B \log 4$  exploring completely the accessible microstates. Further, one can calculate the specific heat of the system as a function of dimensionless variable  $x = 4\beta\Delta$  given by

$$C(x) = k_B \frac{x^2 e^{-x}}{(1 + 3e^{-x})^2} \quad (11)$$

The specific heat shows a peak at a temperature related to  $\Delta$ , a characteristic signature of a two level system. The three fold degeneracy can be partially broken by incorporating an additional term in the Hamiltonian as

$$H_{new} = J(\vec{S}_1 \cdot \vec{S}_2 - 3S_{1z}S_{2z}) \quad (12)$$

In such a situation, one has doubly degenerate states with energy  $-\frac{J\hbar^2}{2}$  and two other non-degenerate states having energy eigenvalues 0 and  $J\hbar^2$ . Hence, the partition function ( $\Delta_1 = J\hbar^2$ ) can be calculated as

$$Z = 1 + 2e^{\frac{\beta\Delta_1}{2}} + e^{-\beta\Delta_1} \quad (13)$$

In the same tune, the average energy and the specific heat can be written as

$$E_{av} = \frac{\Delta_1 (e^{-\beta\Delta_1} - e^{\frac{\beta\Delta_1}{2}})}{1 + 2e^{\frac{\beta\Delta_1}{2}} + e^{-\beta\Delta_1}}$$

$$C_V(y) = k_B \frac{y^2 e^{-y/2} \left( \frac{13}{2} + \frac{1}{2}e^y + 3e^{-3y/2} \right)}{(1 + 2e^{y/2} + e^{-y})^2} \quad (14)$$

with  $y = \beta\Delta_1$  being a dimensionless variable. In the zero temperature limit, the average energy becomes  $-\Delta_1/2$  while the specific heat vanishes to zero. While in the high

temperature limit, the specific heat as well as the average energy vanish to zero. The zero average energy value is consistent with the fact that

$$E_{av} = \frac{2 \times (-\Delta_1/2) + 1 \times 0 + 1 \times \Delta_1}{1 + 2 + 1} = 0 \quad (15)$$

## 4. Three Spin Heisenberg Hamiltonian

With nearest neighbour interaction, the model Heisenberg Hamiltonian of one dimensional spin chain can be formulated as

$$H = J \sum_{n=1}^N \vec{S}(n) \cdot \vec{S}(n+1) \quad (16)$$

Here  $\vec{S}(n)$  is a quantum spin operator attached to a lattice point  $n = 1, 2, \dots, N$ . Here  $J$  is assumed to be positive. Periodic boundary conditions are adopted by the condition  $\vec{S}_{N+1} = \vec{S}_1$ . As a small subset of three spins system, the above Hamiltonian reduces to

$$H = J [\vec{S}_1 \cdot \vec{S}_2 + \vec{S}_2 \cdot \vec{S}_3 + \vec{S}_3 \cdot \vec{S}_1] \quad (17)$$

Defining  $\vec{S}_{tot} = \vec{S}_1 + \vec{S}_2 + \vec{S}_3$ , we note that the above Hamiltonian can be recast as

$$\begin{aligned} H &= \frac{J}{2} [(\vec{S}_1 + \vec{S}_2 + \vec{S}_3)^2 \\ &\quad - \vec{S}_1^2 - \vec{S}_2^2 - \vec{S}_3^2] \\ &= \frac{J}{2} [\vec{S}_{tot}^2 - \vec{S}_1^2 - \vec{S}_2^2 - \vec{S}_3^2] \quad (18) \end{aligned}$$

It is not always possible to diagonalize such type of nearest neighbour Hamiltonian in this fashion because  $\vec{S}_{tot}^2$  contains terms with

exchange interaction between the spins that are not nearest neighbour such as  $\vec{S}_1 \cdot \vec{S}_3$ . Such terms are not always included in the Hamiltonian.

For an arbitrary  $S$ ,  $S_{total} = 3S$ , hence the maximum energy of the system turns out as  $E_{max} = \frac{J}{2} [3S(3S+1) - 3S(S+1)] = 3JS^2$ . For a special case of spin-1/2 system, this maximum energy reduces to  $\frac{3J\hbar^2}{4}$ . Even, if all the spins are down, then the energy also remains same as  $\frac{3J\hbar^2}{4}$ . Thus, this energy state of the three spin system is doubly degenerate with eigen value  $\frac{3J\hbar^2}{4}$  with  $J > 0$ . One can flip the spins to get the ground states. This flipping of spins generates 6 degenerate states with energy  $-\frac{3J\hbar^2}{4}$ . With  $J > 0$ , this is indeed the ground state of the system. This state corresponds to one "up" spin and two "down" spins. Indeed for the 3 spins system one can have  $2^3 = 8$  possible configurations. With all these energies, we are ready to study the thermodynamic properties [11, 12]. The partition function of the system can now be written as

$$Z(J, T) = 2 e^{-\frac{3J\hbar^2\beta}{4}} + 6 e^{\frac{3J\hbar^2\beta}{4}} \quad (19)$$

The associated free energy can be found as

$$F = -k_B T \log 2 + \frac{3J\hbar^2}{4} - \log \left( 1 + 3 e^{\frac{6\beta J\hbar^2}{4}} \right) \quad (20)$$

The entropy at zero temperature correctly counts the states in the ground state with the result

$$S_{T \rightarrow 0} = k_B \log 6 \quad (21)$$

However, at high enough temperature, entropy translates to  $k_B \log 8$ . The average en-

ergy of the system can be computed from the partition function as

$$\bar{E} = \frac{3J\hbar^2}{4} - \frac{9J\hbar^2}{2} \frac{1}{3 + e^{-\frac{3\beta J\hbar^2}{2}}} \quad (22)$$

The two limits are of interest. At zero temperature it correctly produces  $-\frac{3J\hbar^2}{4}$  energy while at high enough temperature, the average energy stays within the gap given by  $-\frac{3J\hbar^2}{8}$ . This is consistent with the fact (assuming  $\Delta_2 = \frac{3J\hbar^2}{4}$ ) that

$$E_{av} = \frac{6 \times (-\Delta_2) + 2 \times \Delta_2}{6 + 2} = -\frac{\Delta_2}{2} = -\frac{3J\hbar^2}{8} \quad (23)$$

Finally, the specific heat of this two level system can be calculated as

$$C(J, T) = 3k_B \frac{x^2 e^{-x}}{(3 + e^{-x})^2}, \quad x = \frac{3J\hbar^2}{4k_B T} \quad (24)$$

The specific heat remains *positive* throughout the range of its parameter and shows a peak at some temperature characteristic of a two level system.

## 5. Four Spin Heisenberg Hamiltonian

With nearest neighbour interaction, the model Hamiltonian [5] of an antiferromagnetic system can be written as

$$H^{AFM} = J \left[ \vec{S}_1 \cdot \vec{S}_2 + \vec{S}_2 \cdot \vec{S}_3 + \vec{S}_3 \cdot \vec{S}_4 + \vec{S}_4 \cdot \vec{S}_1 \right] \quad (25)$$

The above Hamiltonian can be recast as

$$H^{AFM} = \frac{J}{2} \left[ (\vec{S}_1 + \vec{S}_2 + \vec{S}_3 + \vec{S}_4)^2 - (\vec{S}_1 + \vec{S}_3)^2 - (\vec{S}_2 + \vec{S}_4)^2 \right] \quad (26)$$

Considering the antiferromagnetic interaction  $\vec{S}_{tot} = (\vec{S}_1 + \vec{S}_2 + \vec{S}_3 + \vec{S}_4)$ ,  $\vec{S}_{tot}^{13} = (\vec{S}_1 + \vec{S}_3)$  and  $\vec{S}_{tot}^{24} = (\vec{S}_2 + \vec{S}_4)$ , we note that the minimum value of  $S_{tot}$  is 0 while the maximum values of  $S_{tot}^{13}$  and  $S_{tot}^{24}$  are  $2S$  and  $2S$  respectively. Hence, the ground state of the above antiferromagnetic four spins system can be computed exactly as

$$\begin{aligned} E_0 &= \frac{J\hbar^2}{2} [0 - 4S(2S + 1)] \\ &= -4J\hbar^2 S^2 \left( 1 + \frac{1}{2S} \right) \end{aligned} \quad (27)$$

Again for special case of spin- $\frac{1}{2}$  system, we can get the ground state energy of four spin system as

$$\begin{aligned} E_0^{AFM} &= -4J\hbar^2 (1/2)^2 \left( 1 + \frac{1}{2(1/2)} \right) \\ &= -2J\hbar^2 \end{aligned} \quad (28)$$

For ferromagnetic case, the four spin Hamiltonian written in equation (5) is modified as

$$H^{FM} = -J \left[ \vec{S}_1 \cdot \vec{S}_2 + \vec{S}_2 \cdot \vec{S}_3 + \vec{S}_3 \cdot \vec{S}_4 + \vec{S}_4 \cdot \vec{S}_1 \right] \quad (29)$$

Again considering the parallel spin configuration, we find  $S_{tot} = 4S$  and hence, the ground state energy will be

$$\begin{aligned} E_0^{FM} &= -\frac{J\hbar^2}{2} [4S(4S + 1) - 4S(2S + 1)] \\ &= -4J\hbar^2 S^2 \end{aligned} \quad (30)$$

For Ising system where  $S = \pm 1$ , we obtain  $E_0^{FM} = -4J\hbar^2$  ( $J > 0$ ).

## 6. Majumdar-Ghosh Chain

It is again a one dimensional quantum spin model [13, 14, 15] with the nearest and next

nearest neighbour exchange interactions as

$$H = 2J \sum_{i=1}^N \vec{S}_i \cdot \vec{S}_{i+1} + J \sum_{i=1}^N \vec{S}_i \cdot \vec{S}_{i+2} \quad (31)$$

with periodic boundary conditions  $\vec{S}_{N+1} = \vec{S}_1$  and  $\vec{S}_{N+2} = \vec{S}_2$ . A careful look into the above Hamiltonian reveals that it can be written in a very nice form as

$$\begin{aligned} H &= J \sum_{i=1}^N \left[ \vec{S}_i \cdot \vec{S}_{i+1} + \vec{S}_i \cdot \vec{S}_{i+2} + \vec{S}_{i+1} \cdot \vec{S}_{i+2} \right] \\ &= \frac{J}{2} \sum_{i=1}^N \left[ (\vec{S}_i + \vec{S}_{i+1} + \vec{S}_{i+2})^2 - \vec{S}_i^2 \right. \\ &\quad \left. - \vec{S}_{i+1}^2 - \vec{S}_{i+2}^2 \right] \end{aligned} \quad (32)$$

The rearrangement of the terms ensures that the connectivity of the three spins in a block. Like in three spin case, the minimum energy configuration corresponds to one free spin and the rest two spins forming a singlet. For example, one can have the eigenstate

$$|\Psi_0\rangle = (|\uparrow_i \downarrow_{i+1}\rangle - |\downarrow_i \uparrow_{i+1}\rangle) \times |\uparrow_{i+2}\rangle \quad (33)$$

There are two linearly independent ways of forming such configurations. For spin  $-1/2$  system, the minimum energy per spin [16] is simply

$$\epsilon_{min} = -\frac{3J\hbar^2}{4} \quad (34)$$

Prof. Pasupathy [17] gave an elegant variational argument regarding the minimum bound state of the above Hamiltonian as

$$\frac{3J\hbar^2}{4} \leq \frac{9J\hbar^2}{4} + 2 \langle H \rangle \quad (35)$$

by noting the fact that the triad of spin can have either  $S = (1/2)\hbar$  or  $S = (3/2)\hbar$ . As a

result, we can have

$$\langle H \rangle \geq -\frac{3J\hbar^2}{4} \quad (36)$$

Using the spin inequality equation (6) in the second section, it is easy to notice that the energy per spin satisfies the equation given by

$$-\frac{3J\hbar^2}{4} \leq \epsilon_{min} \leq \frac{3J\hbar^2}{4} \quad (37)$$

Again, from the variational principle,

$$\begin{aligned} \langle \Phi | H | \Phi \rangle &\geq E_g \\ &= J \sum_{i=1}^N \text{Min}_{\Phi} [\langle \Phi | (\vec{S}_i \cdot \vec{S}_{i+1} \\ &\quad + \vec{S}_i \cdot \vec{S}_{i+2} + \vec{S}_{i+1} \cdot \vec{S}_{i+2}) | \Phi \rangle] \\ &\geq -\frac{3J\hbar^2}{4} \end{aligned} \quad (38)$$

If  $|\Phi\rangle$  is such an eigen state of the Hamiltonian so that the upper bound equals to the lower bound, then the eigenstate  $|\Phi\rangle$  must be the ground state. This rigorously proves that the ground state energy per spin  $\epsilon_{min}$  is indeed  $-\frac{3J\hbar^2}{4}$  for Majumdar-Ghosh chain model. In fact, the exact solution of the Majumdar-Ghosh model has inspired the researcher [18] to frame a family of one-dimensional translationally invariant spin Hamiltonians having degenerate dimer ground states. Another well-known technique Jordan-Wigner transformation is used to compute the degeneracy and ground state of various spin chains [19].

## 6. Conclusions

In this paper, we have used a very simple spin inequality to compute the bounds

on the ground state of Heisenberg Hamiltonian. This identity also can be used to identify the ground state energy of Majumdar-Ghosh model in one dimensional interacting many body system.

## Acknowledgments

The author would like to acknowledge the post-graduate students for asking several interesting questions related to this subject which prompted him to write this paper.

## References

- [1] N. Singh, *The story of magnetism: from Heisenberg, Slater, and Stoner to Van Vleck, and the issues of exchange and correlation*, arXiv:cond-mat/1807.11291.v1; N. Singh and A. M. Jayannavar, arXiv:1903.07031.
- [2] H. Li, S. Ruan and Y.-J Zeng, *Adv. Material*, **31**, 19000965 (2019).
- [3] S. Chatterjee, *Resonance*, **August**, 57 (2004).
- [4] A. Lichtenstein, in *Emergent Phenomena in Correlated Matter Modeling and Simulation* Edited by E. Pavarini, E. Koch, and U. Schollwöck, **3**, chapter 5 (Forschungszentrum Julich, 2013), ISBN 978-3-89336-884-6
- [5] N. W. Ashcroft and N. D. Mermin, *Solid State Physics* (Hott, Rinehart and Winston, 1976).
- [6] I. de P. R. Moreira et al., *Phys. Rev. B*, **66**, 134430 (2002).
- [7] D. Pines, *Elementary Excitations in Solids* ( Benjamin, 1968).
- [8] T. Giamarchi, *Quantum Physics in One Dimension*( Oxford University, 2003)
- [9] *Articles in Mathematical Physics in One Dimension*, edited by E. H. Lieb and D. C. Mattis, (Academic Press (1966)).
- [10] A. Auerbach, *Interacting Electrons and Quantum Magnetism*, (New York : Springer-Verlag) (1994).
- [11] D. Jana, *Phys. Edu.*, **21**, 153 (2005).
- [12] D. Jana, *Phys. Edu.*, **24**, 23 (2007).
- [13] C. K. Majumdar and D. K. Ghosh, *J. Math. Phys.*, **10**, 1388 (1969); *ibid*, **10**, 1399 (1969).
- [14] C. K. Majumdar, *J. Phys. C* , **3**, 911 (1970).
- [15] W. J. Caspers et al, *J. Phys. A: Math. Gen.*, **17**, 2687 (1984).
- [16] D. K. Ghosh, *Indian J. Phys.*, **80 (6)**, 577 (2006)
- [17] J. Pasupathy, *Proc. DAE Nucl. Phys. and Solid State Phys. Symp. (Bombay, India)*, **13C**, 753 (1970).
- [18] B. Kumar, *Phys. Rev. B*, **66**, 024406 (2002).
- [19] S. Fan, *Condens. Matter*, **3**, 32 (2018).

# Revisiting Lees and Chorlton Disc Experiment

Deepak Jain

Deen Dayal Upadhyaya College  
(University of Delhi)  
Dwarka, New Delhi 110078

djain@ddu.du.ac.in

*Submitted on 13-Jun-2020*

## 1 Introduction

The conduction of heat is basically the transfer of heat energy through matter from high temperature to low temperature. In this process no part of the material medium is moving itself. In 1822, Jean B. J. Fourier laid the foundation of the rate of flow of heat by the conduction method. He quantified this process with the "thermal conductivity" of the medium through which the heat energy propagates.

**Conduction of Heat :** Consider the heat flows normally across thin slab of cross-sectional area  $A$ , thickness  $\delta x$ , with one face maintained at temperature  $T + \delta T$  and other face at  $T$  ( see Fig 1). The temperature gradient, the temperature per unit distance, across the slab is  $\frac{\delta T}{\delta x}$ . The rate of flow heat normally across the slab is given by:

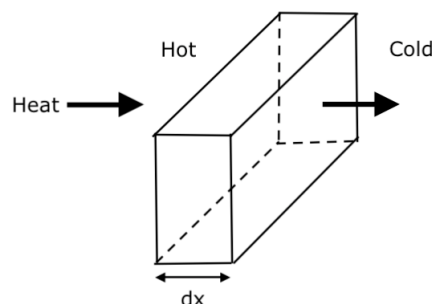


Figure 1: Flow of heat across thin slab

The negative sign indicates that the heat flows in the direction from the high temperature to lower one and  $K$  is a constant for the material known as *coefficient of thermal conductivity*. If both the parallel faces of the slab are closed enough ( $\delta x$  is very small), then the temperature gradient,  $\frac{\delta T}{\delta x}$ , can be written as  $\frac{dT}{dx}$  ( by using the calculus notation). Hence the rate of flow of heat, in the limit of small time interval, can be written as:

$$\text{rate of flow of heat} = -K A \frac{\delta T}{\delta x} \qquad \frac{dQ}{dt} = -K A \frac{dT}{dx} \qquad (1)$$

Where  $dQ$  is the amount of heat passes through the slab in the time  $dt$ . The above equation can be used to define the coefficient of thermal conductivity of given material,  $K$ : it is the amount of heat flows per second normal to the faces of thin parallel-sided slab of a given material of unit area, when the opposite faces of the slab are maintained at unit temperature difference under the steady state condition. Its C.G.S. unit is  $\text{cal.cm}^{-1}\text{sec}^{-1}(\text{°C})^{-1}$ . Copper is an excellent conductor of heat and its coefficient of thermal conductivity is  $0.92 \text{ cal/cm/sec/°C}$ . On the other hand, air is a very poor conductor of heat, its value of  $K$  in the C.G.S. unit is  $0.000058$ .

**Rate of flow of heat:** In order to understand the concept of rate of flow of heat, first we will consider the conduction of heat in a metallic rod heated at one end and cooled at the other end. Assume that there is no loss of heat from the sides of the rod. This is possible if one uses the thick good conducting rod. As the fraction of heat which is lost from the sides of the rod is proportional to  $1/r$ , hence the thick rod can develop the steady flow of heat (ratio of surface area / cross section area =  $2\pi rl / \pi r^2$ , where  $r$  and  $l$  are the radius and length of the rod respectively). In the steady state, the temperature gradient remain the same for all the cross-sections (see Fig 2a). This implies that the amount of heat flows through each cross section of the rod in the given time is same. It also indicates that the temperature distribution along the length of the rod is

a straight line as shown in the Fig 2b. The same behaviour is also shown by the perfectly lagged rod (no loss of heat from its sides) which is heated at one end and cooled at the other. Therefore due to the uniformity of the temperature gradient in the steady state, we can calculate the heat flow through the good conductor by using eq.(1).

Similarly, the temperature gradient can be maintained uniform in a thin sheet whose area is large compare to its thickness. The lines of flow of heat in thin sheet will be identical to the flow of heat in the perfectly lagged rod (rod covered completely with cotton-wool so that no heat is lost from its surface) or thick rod. (see Fig 3). The flow of heat lines near the edges of thin plate may not be straight but the flow of heat lines passes through the rest of the major portion of the plate are straight. So one can approximately assume that there is no loss of heat from the edges and the temperature gradient is uniform. Therefore, we can summarize the main conclusion: The study of rate of flow of heat through (i) a uniform rod whose sides are perfectly lagged (Searl's method of calculation of  $K$  for good conductor) and (ii) a sheet of material whose area is large compare to its thickness (Calculation of  $K$  for a bad conductor by using Lees and Chorlton method) can be described by using the eq. (1) (For more details see ref[1]). In both the above experiments, steady state must be achieved otherwise coefficient of thermal diffusivity may be involved which measures the rate of change of temperature

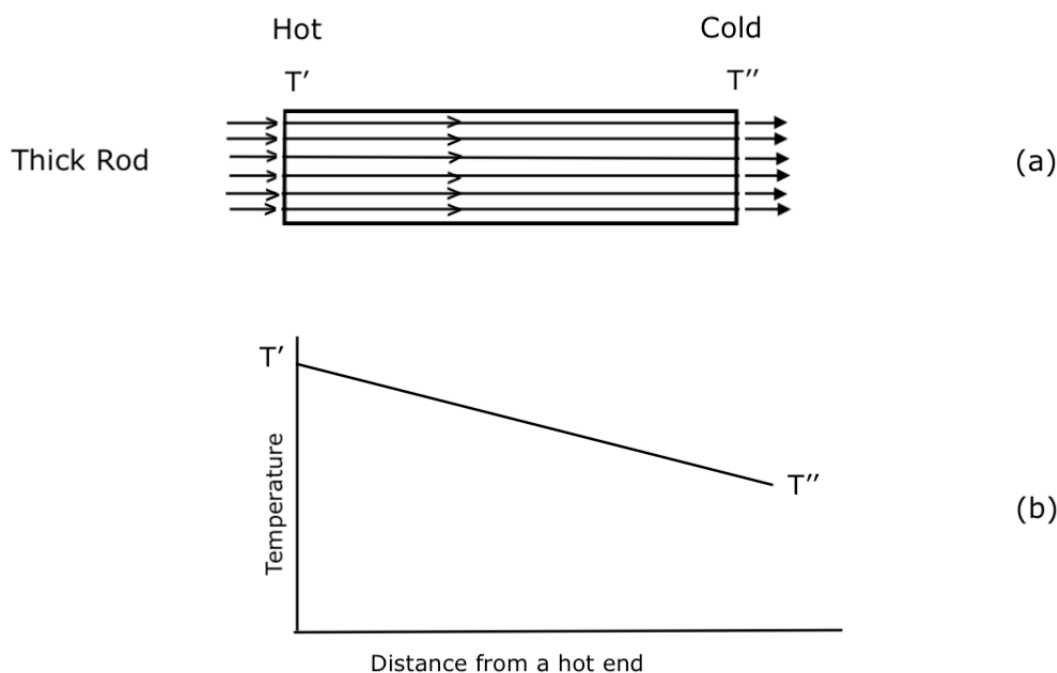


Figure 2: (a) Uniform flow of heat in the thick rod. (b) The temperature distribution along the length of the thick rod.

in the medium.

**Lees and Chorlton Set up:** In this experiment, a bad conductor (X) in the form of thin circular disc is placed between the hollow circular cylinder (C) and the copper or brass disc (B). Usually in the Lab, the cardboard sheet whose  $K = 0.00035$  in C.G.S. unit, is used. A hollow cylinder (C) which is placed over the bad conductor has the same diameter as B and X. The bottom of the hollow cylinder has thick brass or copper block with a hole bored in it to place the thermometers (See Fig.4).

The hollow circular cylinder has the

provision to allow the steam to enter and exit from it. The lower disc B received the heat by the means of conduction. If the area of the disc X is  $A$  and its thickness is  $d$ , then rate of flow of heat through the bad conductor (X) is :

$$\frac{dQ}{dt} = \frac{K(T_1 - T_2)A}{d}$$

where  $T_1$  and  $T_2$  are the steady temperature of Block C and B. Since brass is a good conductor, therefore the temperature recorded in the thermometers fixed in the Disc C and B actually measures the temperature of the upper and lower face of the bad conductor (X). If the emissivity of the disc B is  $\epsilon$  then the heat radiated per unit time by the lower

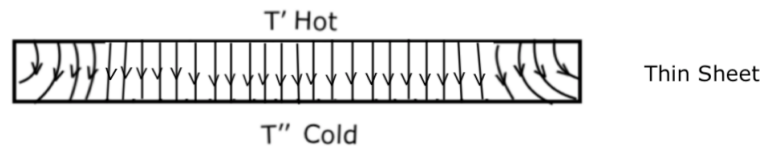


Figure 3: The passage of flow of heat through a thin sheet having a small thickness and large area.

disc B is

$$\frac{dQ'}{dt} = (A + S) \epsilon$$

where A and S are the area of lower surface and curved surface of disc B respectively. (Remember both the disc B and bad conductor have the same area A) Now in steady

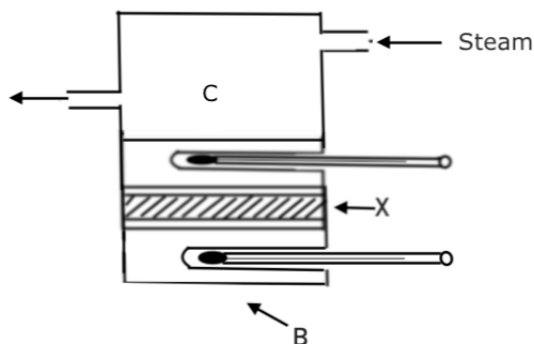


Figure 4: Lees and Chorlton set-up.

state

$$\frac{dQ}{dt} = \frac{dQ'}{dt}$$

$$\frac{K(T_1 - T_2)A}{d} = (A + S) \epsilon$$

Hence

$$K = \frac{A + S}{A} \frac{d}{(T_1 - T_2)} \epsilon \quad (2)$$

There are two special cases for the calculation of K which crucially depend on the procedure followed in the evaluation of emissivity.

**Case I: Top surface of disc B is covered with bad conductor (X) :**

The emissivity ( amount of heat radiated per unit area per unit time) of lower disc B can be defined as:

$$\epsilon = \frac{\text{rate of heat loss}}{\text{Area}} = \frac{M s (dT/dt)}{(A + S)}$$

The rate of heat loss from the conductor B is proportional to the rate of change of temperature w.r.t. time ( dT/dt). When the upper surface of B is covered with the bad conductor, the heat will be lost by the lower portion and from the curved surface area of B only. After substitution of the value of emissivity, eq. (2) becomes

$$K = \frac{d}{(T_1 - T_2)} \frac{M s}{A} \left( \frac{dT}{dt} \right)_{T_2} \quad (3)$$

where M is the mass of the disc B and s

is the specific heat of the material of the disc B.

**Case II:** Top surface of disc B is **not covered with bad conductor (X)** : In this case both upper as well as lower surface of disc B

along with the curved surface area of it will radiate the heat. Hence the  $\epsilon$  becomes:

$$\epsilon = \frac{M s (dT/dt)}{(2A + S)}$$

After substituting the value of  $\epsilon$  in eq. (2), it becomes.

$$K = \left( \frac{A + S}{2A + S} \right) \frac{d}{(T_1 - T_2)} \frac{M s}{A} \left( \frac{dT}{dt} \right)_{T_2} \quad (4)$$

the extra factor  $(A + S)/(2A + S)$  in the above equation is called Bedford's correction.

In both the above cases, the important part is to measure the rate of heat loss,  $dT/dt$  from the disc B.

## 2 Calculation of rate of heat loss

The major source of error in the calculation of  $K$  lies in the measurement of rate of cooling of lower disc B at the temperature  $T_2$ . In order to draw the cooling curve, first heat the lower copper disc B at  $10^\circ \text{C}$  above its steady temperature. Record the fall in temperature after every 30 seconds until it falls  $10^\circ \text{C}$  below the steady state temperature. There are two methods to evaluate the rate of cooling,  $dT/dt$ , at the temperature  $T_2$ .

### Method I : Slope at a given point on the curve

In this method, first plot the fall in temperature ( $T$ ) of lower disc B w.r.t. time ( $t$ ). In order to measure the  $dT/dt$  at the steady temperature  $T_2$ , draw the tangent at this temperature  $T_2$  in the temperature versus time curve. The common mistake that the student usually does that they draw a tangent at the steady temperature  $T_2$  by simply using the scale only. One must follow the correct procedure for drawing the tangent at the given point on the curve (Here it is rate of cooling curve). The correct method for drawing the tangent at given point is as follows:

(i) First, place the plane mirror strip perpendicular to the plane of paper. The mirror should be placed in such a way that it should pass through the given point on the curve at which tangent is to be drawn.

(ii) Now If we orient the mirror at  $TT'$  position then the image PQ of the part of

given curve NP in the plane mirror doesn't appear as the smooth curve ( See Fig 5a ).

(iii) Again rotate a plane mirror such that the curve NPN' appear as smooth and continuous ( without any kink) and the mirror must pass through the point P. ( See Fig 5b). One should try this procedure 2- 3 times in order to get the correct position of plane mirror.

(iv) At this position of mirror , draw the line RPR ' along the edge of the mirror. Now we can easily draw the perpendicular LPL' with the help of protractor or compass at point P which lies on the given curve NPN'.

(v) The line LPL', is the tangent to curve NPN' at the given point P.

(vi) Calculate the slope of the line LPL',  $\Delta Y/\Delta X$ , which measures the  $dT/dt$  at the temperature  $T_2$ .

**Method II**

In this method , one can calculate cooling rate ,  $dT/dt$  by dividing the difference between the two consecutive temperatures ( say  $dT = T_i - T_{i+1}$ ) by the corresponding time interval ( $dt = t_i - t_{i+1}$ ). Now plot the  $dT/dt$  w.r.t the average temperature ,  $\bar{T}$

(where  $\bar{T} = \frac{T_i + T_{i+1}}{2}$ ) [2].

From the the graph which is straight line ( see Fig. 6), one can easily find the rate of cooling,  $dT/dt$ , at the steady temperature of the lower block B ( $T_2$ ).

**3 Calculation of Errors**

**Case I ( Top surface of the conductor B is covered with bad conductor X)**

The coefficient of thermal conductivity is given as:

$$K = \frac{M s d}{A(T_1 - T_2)} \left( \frac{dT}{dt} \right)_{T_2}$$

Now rate of heat loss by disc B , (  $dT/dt$ ), can be calculated by two methods as explained in the previous section. If we use the **method I** , by drawing the tangent in the cooling curve at the point  $T_2$ , the above formula can be rewritten as:

$$K = \frac{M s d}{\pi r^2(T_1 - T_2)} \left( \frac{T' - T''}{t} \right)$$

Where area  $A = \pi r^2$  and  $r$  is the radius of the disc. The disc B is to be cooled from  $T'$  ( $T_2 + 10^\circ\text{C}$ ) to  $T''$  ( $T_2 - 10^\circ\text{C}$ ) through  $T_2$  in  $t$  seconds. The error in  $K$  is calculated as:

$$\sigma_K = K \left[ \frac{\sigma_M^2}{M^2} + \frac{\sigma_{T'-T''}^2}{(T' - T'')^2} + \frac{\sigma_d^2}{d^2} + \frac{\sigma_t^2}{t^2} + \frac{4\sigma_r^2}{r^2} + \frac{\sigma_{T_1-T_2}^2}{(T_1 - T_2)^2} \right]^{1/2} \tag{5}$$

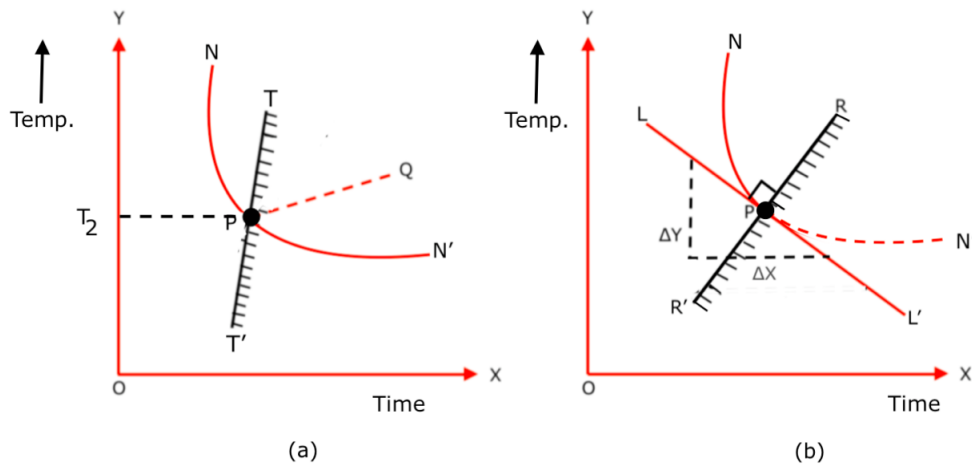


Figure 5: Method of drawing a tangent at given point ( Here P) on the curve by using a plane mirror

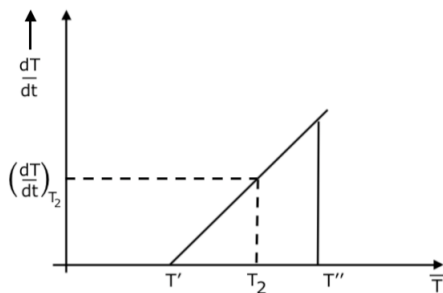


Figure 6: Rate of change of temperature versus average temperature

The mass of disc is very large as compare to other quantities in this experiment and hence the relative error due to this term is very small and may be neglected. The error in  $\sigma_{T'-T''}^2$  is equal to  $\sigma_{T'}^2 + \sigma_{T''}^2$ , which is the sum of the squares of the least count of

the thermometer used to measure the temperature of disc B . Similarly the  $\sigma_t$  is the least measured time from the stop watch and again  $t$  is the total time taken in seconds by the disc B when its temperature changes from  $T'$  to  $T''$ . The error  $\sigma_{T_1-T_2}^2$  should be  $\sigma_{T_1}^2 + \sigma_{T_2}^2$ , where  $\sigma_{T_1}$  and  $\sigma_{T_2}$  are the least count of both the thermometers. The vernier constants of screw gauge and vernier caliper are expressed as  $\sigma_r$  and  $\sigma_d$  respectively. Since specific heat of the disc B is a constant quantity , so it will not contribute to the error budget.

If we use **method II** ( by plotting the graph between  $dT/dt$  versus average temperature,  $\bar{T}$ ), the error in the coefficient of thermal conductivity can be written as:

$$\sigma_K = K \left[ \frac{\sigma_M^2}{M^2} + \frac{\sigma_Y^2}{Y^2} + \frac{\sigma_d^2}{d^2} + \frac{4\sigma_r^2}{r^2} + \frac{\sigma_{T_1-T_2}^2}{(T_1 - T_2)^2} \right]^{1/2} \tag{6}$$

where  $Y = \left( \frac{dT}{dt} \right)_{T_2}$ . The uncertainty in  $Y$  is given as:

$$\sigma_Y = \sqrt{\frac{1}{n-2} \sum_i (Y_i - c - m \bar{T}_i)^2}$$

Where  $c$  and  $m$  are the best fit values of  $C$  and  $M$  obtained after fitting the data  $(\bar{T}, dT/dt)$  by using the relation  $Y = C + M\bar{T}$  and  $n$  is the total number of data points used to plot the graph between  $dT/dt$  and  $\bar{T}$  ( For more details see ref.[3]). The method to obtain  $Y_i = dT/dt$  and  $\bar{T}_i$  is already explained in the previous section. Here one can again ignore the error due to the mass of the disc B as the mass of the disc is very large.

**Case II ( Top surface of the B is not covered with bad conductor X),**

In this case the coefficient of thermal conductivity is given by eq (4). There is one extra term present in this expression called Bedford correction i.e.  $G = \frac{A+S}{(2A+S)} = \frac{r+2d}{(2r+2d)}$ . The error due to this correction term can be written as

$$\sigma_G = G \left[ \left( \frac{\sigma_r + 2\sigma_d}{r + 2d} \right)^2 + \left( \frac{2\sigma_r + 2\sigma_d}{2r + 2d} \right)^2 \right]^{1/2}$$

The error due to this correction term is added in either eq. (5) or eq. (6) depending

upon which method is used for calculating the rate of heat loss.

**4 Possible modification**

One possible change that can be incorporated in this set up is to replace the lower copper disc B with the copper block . The rate of flow of heat which passes through the copper block can be measured with the help of cooling system. It consist of several turns of copper tube wound helically around the copper block tightly (see Fig 7). By measuring the rate of flow of water and the temperature difference of the inlet and the outlet water, one can calculate the rate of flow of heat into the copper block. It is also essential to use the 'constant head' for the water supply into the cooling system [5].

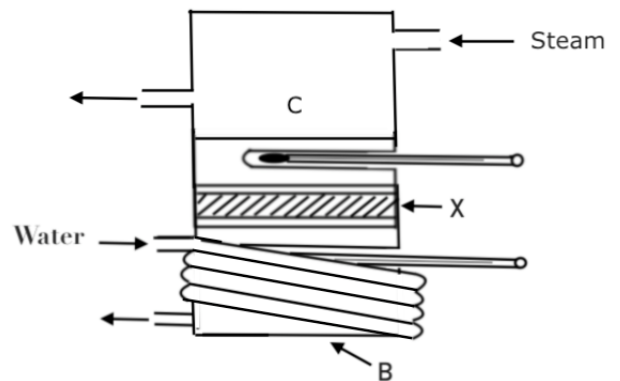


Figure 7: Possible modification of Lees and Chorlton set-up

## 5 Precautions

1. After removing the steam chamber ( C) from the metallic disc ( B), at-least wait for 2 – 3 minutes so that heat gets uniformly distributed over the disc B. It is important to ensure that the temperature of disc B is still  $10^{\circ}\text{C}$  above the steady state temperature before noting down the change of temperature w.r.t time.
2. It is important to check that both the thermometers are displaying same readings at room temperature. If it is not, then note down the difference between the two readings. This difference should be added to the term  $(T_1 - T_2)$ , mentioned in the formula of K ( see eq.2).
3. Use the thermometers which have least count less than  $1^{\circ}\text{C}$  ( i.e  $0.5^{\circ}\text{C}$  or  $0.2^{\circ}\text{C}$  ). This will provide more data points near the steady temperature  $T_2$  and cooling curve may become smooth.
4. Both the steady state ( Calculation of  $T_1$  and  $T_2$ ) and the dynamical part ( calculation of cooling curve) of this experiment must be done successively as it depend crucially on the room temperature.

5. The outer surfaces of C and B should be nickel plated so that both should have the same emissive power.
6. There should be good thermal contact between the metal disc and the bad conductor (X). In order to achieve this, the glycerine should be smeared between the specimen and the metallic disc.
7. Record the steady temperature  $T_1$  and  $T_2$  of the disc C and B only when it remain stable for more than 10 - 15 minutes.

## References

- [1] Textbook of Heat: G. R. Noakes ( Macmillan)
- [2] Advanced Practical Physics for Students , B.L. Worsnop and H.T. Flint. ( Methuen & Co. Ltd.)
- [3] An Introduction to Error Analysis, J. R. Taylor, ( University Science Books)
- [4] Heat: R. C. Brown
- [5] Heat : A . J. Woodall

---

# Elements of Electrical Safety for Physics Students

Emanuel Gluskin

Ruppin Academic Center Israel, Emek Hefer, 40250 Israel

emanuel15@bezeqint.net

*Submitted 28-12-2017*

## Abstract

Starting from J.D. Jackson's definition [1] of the topic of grounding, we present some knowledge of electrical safety, essential for every physics student.

---

**Keywords:** Electrodynamics, Electrical Safety, Grounding (Earthing), Human Health, Education.

## 1. Introduction

Importance of the topic of Electrical Safety for students working in a laboratory, or for future engineers, empirical scientists, and even simple householders, is obvious. We widely use electrical supply, generated by very powerful power plants with furnace burning natural gas, oil, coal, nuclear reactors, or with hydro, solar, wind and other renewable energy sources. Through the supply of the electricity via the wires, the power sources offer us numerous possibilities of having very serious injuries, if we do not use the advantage of having the power supply with reasonable care. Here, we shall mainly focus on the topic of grounding – one of the central and educationally interesting topics of Electrical Safety.

Wishing to avoid the very unsuccessful term "general resistance of the earth mass" found, e.g., in Israeli official instructive book "Electrical Law" [2], let us start from the definition of grounding found in the classical text [1]:

"When a conducting object is said to be grounded, it is assumed to be connected by a very fine conducting filament to a remote reservoir of charge that serves as a common zero of potential. Objects held at fixed potentials are similarly connected to one side of a voltage source, such as a battery, the other side of which is connected to the common 'ground'. Then, when initially electrified objects are moved relative to one another in such a way that their distributions of electricity are altered, but their potentials remain fixed, the appropriate amount of charge flow from or to the remote reservoir, assumed to have an inexhaustible supply. The idea of grounding something is a well-defined concept in electrostatics where time is not a factor, but for oscillating fields the finite speed of propagation blurs the concept. In other words, stray inductive and capacitive effects can enter significantly. Great care is then necessary to ensure a 'good ground'."

The concept "remote reservoir of charge" of [1], is definitely much better than the concept of "general resistance of the earth mass" of [2]. The latter concept is even misleading, because the very concept of resistance [3] is associated with the way of the measurement, for which the geometrical presentation of the relevant piece (sample) of material must be given. Just assume that you measure the resistance of a material ball, while the electrodes are connected to the North's and the South's poles of the ball. Then, move one of the contacts towards the other; the measured resistance is obviously reduced, with the limiting value of zero, obtained when the contacts touch each other.

However, the words "very fine conducting filament" of [1] are generally wrong. No realistic grounding can be "very fine" -- a mistake that has to be pinpointed just because of the wide use of [1]. Presumably, Jackson would like to have the "very fine" filament exclusively because of the field problem, that is, for suitability in the calculation of the fields, not considering the main purpose of the grounding. In order to see the mentioned suitability, consider a spherical capacitor (two concentric conducting spheres), with the internal sphere having its potential zero. The theory of such capacitor is quite simple, and one easily obtains, via the radiuses of the spheres, the formula for the capacitance [3]

$$C = \frac{4\pi\epsilon}{\frac{1}{r_1} - \frac{1}{r_2}}, \quad r_1 < r_2 \quad (1)$$

However, in order to ground the internal sphere, one has to make a hole in the external sphere for the grounding wire with a possible current in it to pass via the hole. The simple picture of the field, which led to (1), will be less disturbed, if the diameter of the grounding wire (the "conducting filament" in [1]) is much smaller than the diameter of the hole, because the magnetic field of the current in the wire is stronger near the wire. Note that since the grounding wire has to supply the charge, we cannot ignore the current, whose pulses cause time varying magnetic field, resulting in some electrical field.

Nevertheless, the thinness of the grounding wire represents a problem from the positions of the electrical safety -- one should not forget an important reason why grounding is really needed!

According to the formula for resistance of a piece of wire of length  $l$ , and cross-section  $S$ , [3]

$$R = \frac{\rho l}{S} \quad (2)$$

as the diameter of the wire tends to zero (and so  $S$  does),  $R$  becomes large.

Let us give an example showing how the latter is dangerous for the grounding. This example is taken from [4], where we also dealt with finding a relation between the internal resistance of the generator and its power, here we assume that the internal resistance  $R_{int}$  is given.

## 2. A case from students' power laboratory

Thus, we speak about a teaching laboratory where a student studies a generator, and it may occur that a defective 220 volts generator might electrify its metal body that the student touches. Since the metal body is grounded, there is a "competition" between the source of 220 volt and the source (the ground) of 0 volt – which one will define the body's potential? Electrical safety requires that the potential of the metal body that can be touched by the student to be less than 30 volts. The actual potential obviously (see Fig.1) depends on the ratio

$$\frac{R_{gr}}{R_{int}} \quad (3)$$

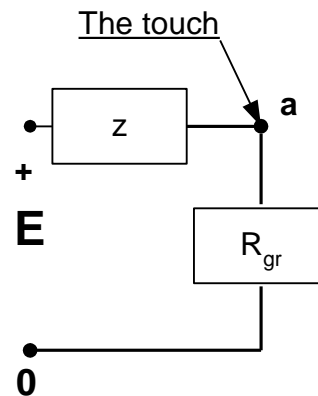


Fig. 1: Our equivalent scheme. "Z" is our "R<sub>int</sub>". The generator is thus {E,Z}. E here is 220V. Point a denotes the metal body of the generator, which can be touched by the student, and where, in the case of the fault, a dangerous voltage arises.

Since the resistance of the human body is much larger than  $R_{gr}$ , in the parallel connection of the two, the resistance of the body can be ignored, and the voltage divider, seen in Fig. 1, defines the voltage on the generator's body as

$$V = 220 \frac{R_{gr}}{R_{int} + R_{gr}} \approx 220 \frac{R_{gr}}{R_{int}} \text{ volt.} \quad (4)$$

(As we shall immediately see, the assumption of  $R_{gr} \ll R_{int}$  is justified). In order to have this be less than 30 volts, we require that

$$\frac{R_{gr}}{R_{int}} < \frac{30}{220} \quad (5)$$

that is, approximately,

$$R_{gr} < \frac{R_{int}}{7} \quad (6)$$

Since the more powerful the generator, the smaller  $R_{int}$  is (i.e. the generator is "more ideal"), and since we are interested, in the laboratory, to study generators that are as powerful as possible -- actually  $R_{int}$  is rather small (say, a half ohm). Obviously,  $R_{gr}$  must be very small. The latter excludes using a "very fine filament", and if one also considers that it is necessary to have very firm mechanical connections of all the pieces of the grounding path (for the reliability of the grounding) – then one sees that the grounding connections are actually made of a wide (massive) pieces of wire.

Works [5-31] are advised for more conceptual (and history, e.g. [31]) reading.

### 3. A commonly asked question

Which is more lethal to the electrical shock: voltage or current?

Finally – the current. Of course, without any voltage no current can arise, just as without pressure of a knife on the skin there will be no penetration of the

knife into the body, but finally it is the movement of the knife in the body which is killing.

It is widely accepted to consider human as a linear resistor (of the value about 1 kilohm). The resistance of skin is involved, which can be changed from 700 ohm for wet skin, up to 14 kohm for a dry skin. If one is a long time under voltage stress, then feeling the danger, he becomes nervous, and his skin becomes covered by sweat, resulting in decrease of its resistance, and the current is strongly increased. It is clear from the said, that for woman and children it is more dangerous to be under electrification than for adults. It is also clear that working in the conditions of high humidity is unwanted as re electrical safety.

Any damage requires certain energy. The expression for the electrical power  $P$  is

$$P = vi$$

Thinking in terms of a linear resistor, i.e. using

$$v = Ri ,$$

we have for  $P$  either

$$P = Ri^2, \text{ or } P = \frac{v^2}{R}$$

Since power systems are given by voltage sources, i.e.  $v$ , not  $i$  is given, we should choose the latter expression for  $P$ , from which it is clear that smaller  $R$ , the higher is  $P$ , and the damage. Also for  $i(t)$ ,

$$i = \frac{v}{R} \sim \frac{1}{R}.$$

It has to be known that: we sense one or few mA, 10 mA causes pain, 60mA causes cramps of the muscles, and 100 mA is almost surely lethal. The danger depends, however, on the path of the current inside the body, and directly through the heart, even 10 microampere may be lethal.

One walking on electrified soil, when the current through the body is from one lag to another (seemingly, not a dangerous path), *is in danger* – if this current will reach the value about 60 mA, the

cramp of the muscles occurs, and the human may fall because of the cramp, and then the current might be through the chest. We can roughly estimate the dangerous "step voltage" as

$$V_{step} \geq 1k\Omega \cdot 60mA = 60V$$

However, the topic of parameters of human body is not at all simple. We shall make two comments. The first includes a warning – using even a common textbook, one should check the parameters given in the book.

The initiative of [20] to include safety considerations (chapter 9 there) into a standard course of circuit analysis is highly appreciated, and some of the examples there are very interesting. However, reading in [20]: "In his book "Medical Instrumentation" (Boston: Houghton Mifflin, 1978), John G. Webster suggests the following values for resistance of the human body:

$$R_{skin}(dry) = 15k\Omega, R_{skin}(wet) = 150\Omega,$$

$$R_{limb}(arm\ or\ leg) = 100\Omega, R_{trunk} = 200\Omega.$$

I had a problem, because trunk is wider than either arm or leg -- thus its resistance should be lower. Thus, I found in the library of Ben Gurion University Webster's book, and indeed saw in it that the figures were just opposite:

$$R_{limb}(arm\ or\ leg) = 200\Omega, R_{trunk} = 100\Omega.$$

Thus, some answers in [20] has to be recalculated - nota bene!

The second comment relates to the attempts to find a good equivalent circuit imitating the current response of the body. That it is widely accepted (see the references in [23]) that such a scheme should include linear resistors and capacitors, and no inductors, seems to us problematic.

Indeed, consider that we can expect in the body some diffusion processes for the current that flows via the life tissue/medium. This means a delay of the current with respect to applied voltage.

However, in the macroscopic view of a lumped circuit, a delay of  $i(t)$  with respect to  $v(t)$  is an inductive feature. Indeed, substituting into

$$v = L \frac{di}{dt}$$

$i(t)$  as some positive pulse, one finds the maximum of  $v(t)$  on the initial slope of the pulse, i.e. before the maximum  $i(t)$ . The connection of the delay with the inductance is also seen in the following manner. Assume the model

$$v(t) = Ri(t + \tau), \quad \tau > 0$$

for which  $v(-\tau) = Ri(0)$  -- obvious forestalling the current by the voltage. Assuming that  $\tau$  is small, we expand  $i(t)$  and write this equation as

$$v(t) \approx Ri(t) + R\tau \frac{di}{dt}$$

which is the equation of a series R-L circuit with

$$L = R\tau.$$

Such, an inductance should not be ignored.

Of course, *nonlinear modeling* should be much more complicated.

In order to avoid electrical shock, any repairing of the electrical equipment should be done only when the equipment is not electrified. You never make any such work when you are alone, i.e. and never see you. If you are under voltage stress, somebody has, first of all turn down the switch that interrupts the voltage supply in the whole room. Of course, one has to know a priori where this switch is.

#### 4. Some questions for additional consideration

The following questions show how multifold and complicated is the topic of electrical safety, and how

easily we can meet the associated hazards. Though some of the questions are simple, their list outlines the scope of the topics one should keep in mind when considering electrical safety, and this gives a correct orientation.

Does the reader know (and for what reason) that:

1. powder, e.g. flour, can be explosive,
2. when a liquid flows in a plastic pipe, an electrostatic charge is accumulated on the pipe walls, and this is the static charge which can cause a dangerous spark,
3. the water that is pouring from a faucet to a bucket may be positively charged, and the fact that the bucket may be metal and then left for some time on the ground does not eliminate the charge in the water quickly enough; because of the charge, the water may lead (see [17] for an interesting example) to a spark,
4. it is prohibited to turn on or off a light if the switch is located in an area (say the kitchen) where a strong smell of gas is detected,
5. in order to cause ignition or explosion of a certain gas, powder or liquid, the spark has to possess some minimal energy; which is somewhat similar to the medical fact that in order to be infected by a virus and became ill, a certain amount (dose) of the virus is necessary.
6. regarding the possibly of causing explosions, a corona-type discharge is less dangerous, than a spark-type discharge.
7. by saying that a flammable liquid is ignited, we mean that the vapor (gas) of the liquid, over its surface, is ignited,
8. a flammable gas may be ignited only at a certain concentration, and at a higher concentration it becomes explosive; the explosive concentration is usually about twice the flammable concentration,
9. the dangerous "step" voltage caused by lightning can be distributed both in the horizontal and the vertical direction (on buildings),
10. there have been cases of injury by lightning through a telephone cable,
11. if a car is staying on a junction during a storm, and an electrical wire falls on the car, no passenger should emerge from the car, but rather wait for an electrician to remove the wire,
12. kite-flying by children near voltage lines is dangerous,
13. static charge is dangerous not only in the chemical industry but also in the integrated circuit industry, where the discharge can cause damage to the thin layers of the microcircuits,
14. today there are instruments in the chemical and electronic industries, made from special plastic materials that have a low triboelectric ability (i.e. the ability to absorb static charge) allowing to reduce the risk of a spark; the development of such materials is a challenging field of material science,
15. one can be shocked while holding a well-grounded frame of a drill if the floor is electrified by a motor with faulty isolation,
16. one can be shocked by the line voltage when connecting one of the wires of an unlit bulb to the zero-potential wire of the line, while not directly touching the phase-wire of the line, which is because the wires in the switch are inter-placed, and the switch does not interrupt the hot wire -- thus the voltage can come to one's hands via the lamp,
17. the large metallic foundation of a high-voltage line column (post, tower) has to be grounded at each of its corners (think about one lying on the ground, touching the electrified foundation by his shoulder),
18. new buildings have their grounding electrode systems organically included in the building's foundations,
19. in the conditions when even a short-time overvoltage of power equipment is dangerous, the grounding of the equipment may be unwanted or even prohibited, because of the possibility of the electrification of the soil around the grounding electrodes, caused by a lightning stroke (a high voltage can come to the equipment via the grounding); this is relevant to the regions where lightnings are usual,
20. in order to improve the quality of grounding, in some cases special salts are introduced into the soil – this reduces  $\rho$  in (2),

21. there have been cases where plumbers working near old houses received electric shocks when disconnecting a water pipe from the underground water system,
22. when starting to work, electricians sometimes first touch an open electric wire with the back of a hand.

## Acknowledgement

I am grateful to Yinnon Stav and Shlomo Engelberg for their kind attention to my research efforts, to Leonid Minkin for some style corrections, and to unknown Referee for some interesting suggestions regarding the examples.

## Appendix: Some historical background

The lightning-rod for lightning protection was proposed by Benjamin Franklin approximately in 1750.

The use of a "Faraday cage" for lightning protection of buildings was introduced by James Clerk Maxwell in 1876.

Luigi Galvani conducted the first experiments on the influence of an electrical current on a live (animal's) body in 1791. Galvani could have answered question 22 of Section 3.

Approximately one hundred years after Galvani's experiments, the pioneer of heavy-current and high-frequency current engineering, Nikola Tesla, started a systematic study of the influence of electrical current on the human body, which was necessary for the safe application of his inventions. It was Tesla who discovered that at very high frequencies one can touch a very high voltage, and in his lecture in Philadelphia in 1893 Tesla personally demonstrated

touching the terminals of a 200 kV source. Tesla had proved that the 50 - 60 Hz line is the most dangerous among the alternating current supplies, and that contrary to Edison's opinion, up to about 500 volts, the constant-voltage current is more dangerous for people than alternating current of 50 or 60 Hz. The proofs were experimental and demonstrated on very few individuals, often Tesla himself. Even today we do not know enough about the electrical parameters of the human body that allow to calculate precisely the distribution of the density of electrical current, which is passing through it, and this is a subject of biophysical investigations. Tesla's experiments, motivated by his interests in electrical safety, also led to the medical applications which are called today electrotherapy.

The "Fire Protection Handbook", which included important rules of electrical safety, named the National Electrical Code (NEC) appeared in the USA in 1897. It is now published by the American National Fire Protection Association (NFPA) with many improvements.

NEC is a very extended and complete list of instructions for electrical safety arrangements. This document has influenced electrical safety rules in many countries outside the USA, though in England, Germany, Switzerland, Russia and some other countries there are their own detailed and very useful regulations.

The NEC is readily available today (including a CDROM version). Even just a study of the classification of hazardous areas given in the NEC provides an understanding of some basic electrical safety problems.

## References

- [1] J.D. Jackson, "Classical Electrodynamics," John Wiley, New York, 1975. (See p. 23)
- [2] Hok ve Takanot be Nose Hashmal ("The Law and Rules Regarding Electricity," in Hebrew) The Office of Safety and Health, 1919
- [3] R.P. Feynman, R. Leighton, M. Sands, "Feynman Lectures of Physics," Addison Wesley, vol. 2, New York, 1965.
- [4] E. Gluskin, "The parameter of order for estimation of the needed grounding resistor," FJEC

- (Far East Journal of Electronics and Communications), Volume 22 No. 1-2 (2019).
- [5] R. Artdej, "Investigating undergraduate student's scientific understanding of laboratory safety", *Procedia Social and behavioral sciences*, Vol. 46, pp. 5058-5062, New York, 2012.
- [6] C.O. Ponferrada, J.G. Daque, D.C.L. Buadlart, E.J.L. Cabigon, V.R.K.R. Galarpe, "Laboratory Safety Awareness Among General Physics Undergraduate Students", *Engineering Technology & Applied Science research*, vol. 7, no 6 (2017)
- [7] Ashley R. Carter, "On building a research Laboratory, not starting one", *American Journal of Physics*, 87, 413 (2019)
- [8] Beryl Lieff Benderly, "Danger in School Labs: Accident count Experimental Science", *Scientific American*, August 1, 2010.
- [9] E. Leonard Jossem, "The education of physics graduate assistants", *American Journal of Physics*, vol. 68, no 6, June 2000
- [10] Science lab safety – <http://www.youtube.com/watch?v=5g>
- [11] Todd Campbell, Drew Nelson, and Phil Seak Oh, "Grounding instruction around scientifically rich, often complex phenomena", *Science Teacher (Normal III)*, September 2013, pp. 35-41.
- [12] "Grounding – the removal of charge", *The physics classroom*, <http://www.physicsclassroom/class>;
- [13] I.A. Jamieson, S.S. Jamieson, H.M. ApSimon, and J.N.B. Bell, "Grounding and Human Health – a Review", *Journal of Physics, Conference Series*, volume 301, number 1.
- [14] G. Chevalier, R. Mori, and Oschman, "The effect of earthing (grounding) on human physiology", *European Biology Bioelectromagnetic*, 2007, 1, 600-621.
- [15] G. Chevalier, S.N. Sinatra, J.L. Oschman, K. Sokol and P. Sokol, *J. Environ, Public Health* 2012, 291541; doi: 10.1155/2012/291541
- [16] K. Sokol and P. Sokol, "Earthing the human body influences physiological processes", *Journal of Alternative and Complementary Medicine*, 2011; 17(4):301-308.
- [17] W. F. Cooper, "Electrical Safety Engineering," *Newnes-Butterworth*, London, 1982. (In particular, Section 10.21)
- [18] L. B. Gordon, "Electrical hazards in the high energy laboratory," *IEEE Transactions on Education*, Vol. 34, No. 8 (Aug. 1991), pp. 231-242.
- [19] E. Gluskin, "Betichut Hashmalit," (Lecture Notes on Electrical Safety, in Hebrew), *The British Library*, Shelfmark HEC 1998 a 508.
- [20] J.D. Irwin & R. M. Nelms, "Basic Engineering Circuit Analysis", *Wiley*, New York, 2008.
- [21] G. McPherson & R.D. Laramore, "An introduction to Electrical Machines and Transformers", *Wiley*, New York, 1990.
- [22] <http://www.hit.ac.il/staff/gluskin/full.pdf>
- [23] E. Gluskin, "On the human body's inductive features: A comment on 'Bioelectrical parameters...' by A.L. Lafargue et al., " *Bioelectromagnetics*, 24(4), 2003 (292-293)
- [24] *National Electrical Code*, NFPA (National Power Protection Association) Quincy, Mass., 2010.
- [25] S. Corsi, G.N. Taranto, "Voltage instability, -- the different shapes of the nose", from *Bulk Power System Dynamics and Control - VII. Revitalizing Operational Reliability*, 2007 iREP

---

Symposium (19-24 Aug. 2007, Charleston, SC), DOI: 10.1109/IREP.2007.4410582.

[26] E. Gluskin, "An Extended Frame for Thevenin (Norton) Theorem", IEEE CASS Newsletter, vol. 5, issue 6 (the "Forum" section), Dec. 2011.

[27] E. Gluskin, "An Extended Frame for applications of Helmholtz-Thevenin-Norton Theorem", J Electr Eng Electron Technol (JEEET), 2013, 2:2. [http://www.scitechnol.com/extended-frame-for-applications-of-the-helmholtztheveninnorton-theorem-8nCB.php?article\\_id=1419](http://www.scitechnol.com/extended-frame-for-applications-of-the-helmholtztheveninnorton-theorem-8nCB.php?article_id=1419).

[28] <http://hyperphysics.phy-astr.gsu.edu/hbase/electric/gfi.html>

[29] Ch.A. Desoer, E.S. Kuh, "Basic Circuit Theory", McGraw Hill, New York, 1969.

[30] W.H.J. Childs, "Physical Constants", London, Methuen & Co. LTD; (also New York. John Wiley & Sons).

[31] "A Short History of Circuits and Systems" IEEE CAS book (Editors: Franco Maloberti and Anthony C. Davies), River Publishers, Danmark, 2016: [https://ieeecas.org/sites/default/files/a\\_short\\_history\\_of\\_circuits\\_and\\_systems-\\_ebook-\\_web.pdf](https://ieeecas.org/sites/default/files/a_short_history_of_circuits_and_systems-_ebook-_web.pdf)

[32] Practical Electronics for Inventors by Paul Scherz, Simon Monk, 4th Ed. McGraw Hill, New York, 2012.

[33] Electrical Safety Handbook by John Cadick, Mary Capelli-Schellpfeffer, Dennis K. Neitzel and Al Winfield, Kindle, New York, 2012/

---

# Graphical Pedagogy of Teaching Reciprocal Space

Adarsh Singh and Mitushi Gupta

Department of Physics, Hindu College,  
University of Delhi, Delhi-110007

asingh@hinducollege.du.ac.in

*Submitted 05-08-2020*

## Abstract

The present work proposes a graphical method of obtaining reciprocal lattice from direct lattice while at the same time demarcating those reciprocal points which correspond to real planes thus establishing the connection of reciprocal space to the diffraction pattern of the given lattice. The said approach acquaints the students with the origin and physical significance of the reciprocal lattice in a more conceivable way. This has been done using programming through an open-source software SCILAB which helps the students to develop and experiment with different forms of 2D and 3D reciprocal lattices.

about the pedagogy of teaching and explaining reciprocal lattice is mostly analytical in approach where the mathematical construct and equivalence of direct lattice with reciprocal lattice is demonstrated.<sup>4–8</sup>

It is a fact that what can be visualized, can be better conceptualized. This is especially true in the early stages of the introduction of a new concept where learning through visualization can help build a better connection to the physical aspect of the problem and hence provide better clarity and understanding as compared to analytical methods. Also, the use of Information Technology and programming methods in teaching open wide avenues of generalizing a basic oversimplified physical problem done in texts to approach more realistic conditions, while also being able to depict the results using 2D and 3D plots. The present work proposes the methodology of going step by step in generating the reciprocal lattice from the direct lattice graphically and plotting the points along the way in each step using open source software SCILAB, as a better way of introducing the origin and physical significance of the reciprocal space.

The work presented considers an orthogonal  $10 \times 10$  square lattice in real space for simplicity. This simple lattice may be viewed as stacked parallel planes along various orientations. The idea is to represent each of the family of parallel planes by a single point in a new coordinate plane called the reciprocal space. The reciprocal space has the dimensions of wave number  $k$  just as the real space has the dimensions of distance. The work

---

## 1. Introduction

Reciprocal lattice, which is one of the most important and basic concepts in Solid State Physics, also happens to be the most baffling for students encountering it for the first time. The construction of the reciprocal lattice from a direct lattice is an enigma to most students and the said evolution as given in most textbooks leaves a lot unexplained and open to doubts.<sup>1–3</sup> The treatment of the subject is mostly mathematical with only the construction of reciprocal basis lattice vectors from the direct basis vectors demonstrated graphically. These reciprocal basis vectors are then made to extend throughout in 2D or 3D to make up the entire reciprocal space just as a unit cell in a direct lattice may be extended to make up the entire real lattice.<sup>1–3</sup> Also, the reported work

describes a step-by-step graphical method of obtaining the reciprocal points corresponding to each family of parallel planes in a direct lattice. It is these graphically obtained points which correspond to the diffraction spots obtained from the given lattice, thus presenting a visually clear picture of how some points on the reciprocal space correspond to real planes and hence the diffraction pattern, thus emphasizing the physical origin, need and importance of the reciprocal space.

The generation and plotting of the reciprocal points have been done using the open- source software SCILAB, thus leaving huge scope for students to modify the chosen direct lattice and generate its corresponding reciprocal lattice for better understanding. The work may be extended to simulate 3D plots of the reciprocal lattices as well as generating their corresponding Brillouin Zones for different direct lattices.

### I. IDENTIFYING THE PLANES

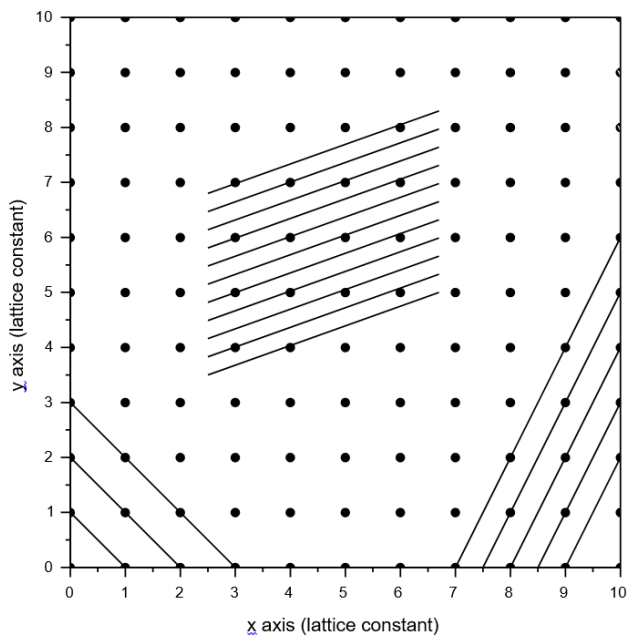


FIG. 1: Direct lattice in real space with three families of planes Consider a 10 x 10 orthogonal

For example, the family {1,1} consists of planes (1,1), (2,2), (3,3), . . . (10,10), as shown in Fig. 2 but the entire family may be represented by a single plane (1,1) which is the plane closest to the

square lattice in 2D such that the lattice constant is one unit dimension along both x and y-axis as shown in Fig. 1.

The given lattice is viewed by any external agency as “families of parallel planes”, stacked along varying orientations. These families of parallel planes are labeled using Miller Indices such as {1,1}, {1,2}, {6,1} to name a few. Each family of parallel planes in any given lattice can be uniquely identified with two physical parameters, i) a specific orientation with respect to the origin, namely, the direction normal to the planes and ii) the inter-planar distance between any two adjacent planes. Since all planes in each family are equivalent, hence an entire family of parallel planes may be represented by only one plane which is closest to the origin i.e., has the smallest perpendicular distance from the origin. This one plane is sufficient to provide both the inter-planar distance and the normal direction for the entire family of parallel planes.

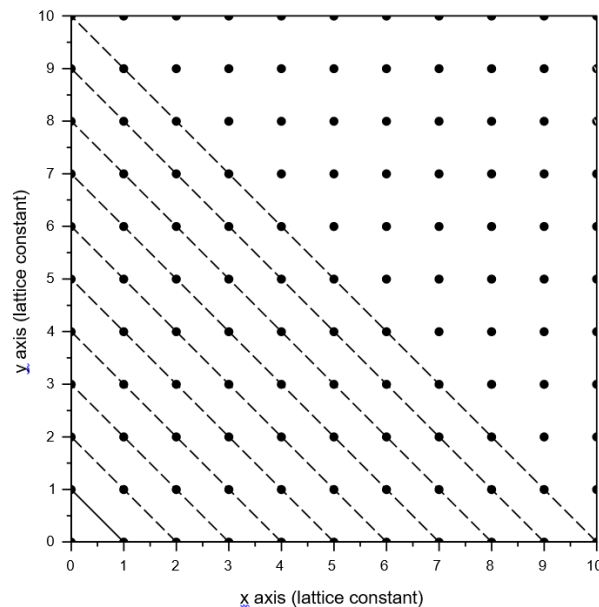
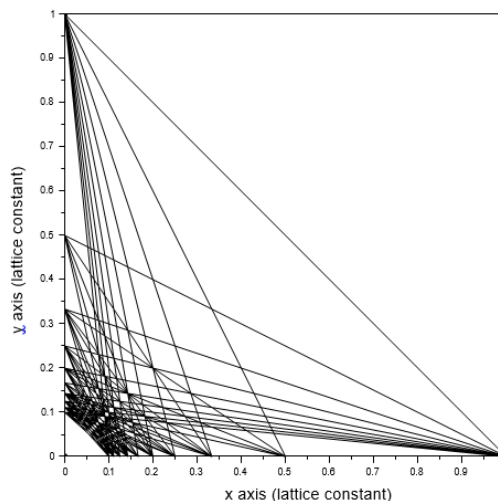
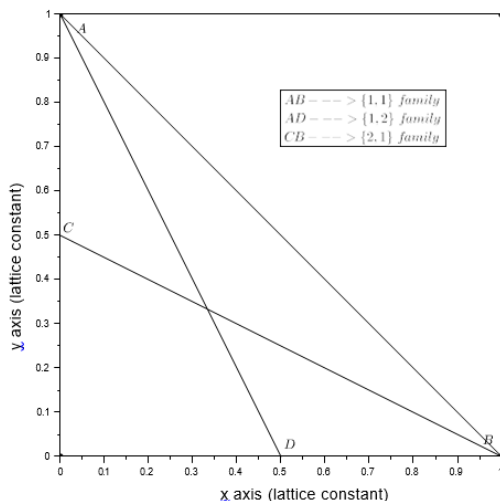


FIG. 2: Family of planes {1,1} with plane (1,1) shown by solid line

origin. Thus, extending the argument, all families of planes in the 10 x 10 direct lattice can be represented by one plane each. These single, closest to origin planes for {1,1}, {1,2} and {2,1} families are shown in Fig. 3(a), while Fig. 3(b)

shows the nearest planes for all families in 10 x 10 lattices under consideration. One may note that the closest to origin planes corresponding to all families of planes may be represented within one unit cell, by dividing the Miller indices (h,k) of the

plane by the least common multiple of the indices h and k, thus implying that all information regarding the geometric arrangement, symmetry and hence the physical properties of the given lattice is contained in a single unit cell.



(a) Planes closest to origin corresponding to families {1,1}, {1,2}, {2,1}

(b) Closest to origin planes for all families of a 10 x 10 lattice

FIG. 3

## II. RECIPROCAL LATTICE POINTS FROM DIRECT LATTICE PLANES

Reciprocal space is a reproduction of direct lattice in wave number or  $k$  space. Direct lattice, as shown in Fig. 1, is a plot of points in a coordinate plane which has dimensions of distance with one unit being equal to the lattice constant along each axis. The new

reference plane called  $k$  space or reciprocal space is a plot of points in a coordinate plane which has dimensions of wave number or inverse of length as  $k = 2\pi/\lambda$ . The unit dimension in this plane is  $2\pi/(\text{lattice constant})$ . Since for simplicity we have chosen the lattice constant as one unit, the  $k$  space is marked as  $2\pi, 2 \cdot 2\pi, 3 \cdot 2\pi \dots$  as shown in Fig. 4.

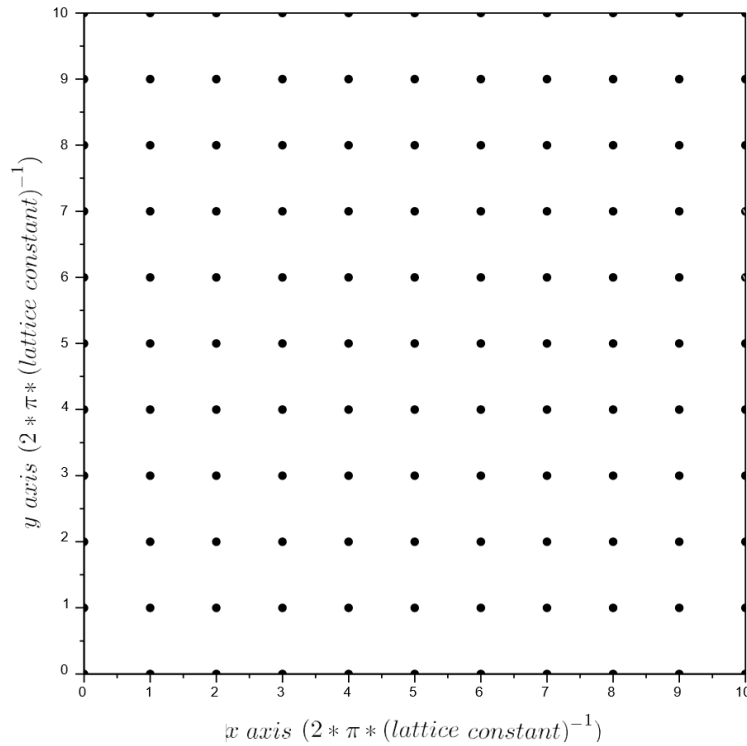
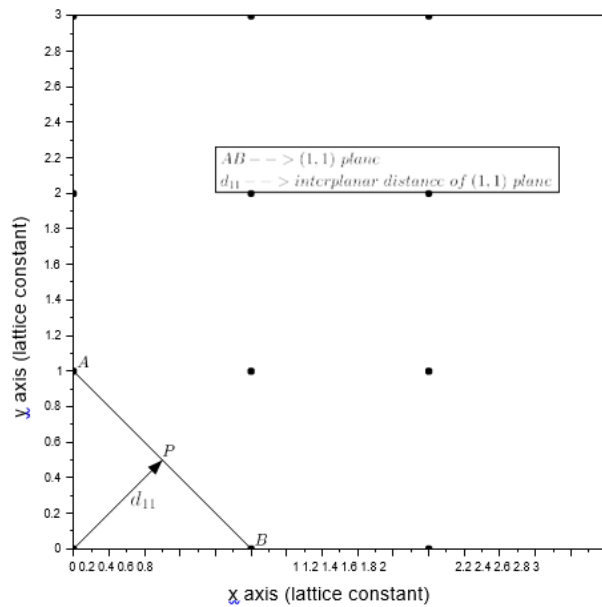


FIG. 4: Reciprocal space for 10 x 10 direct lattice

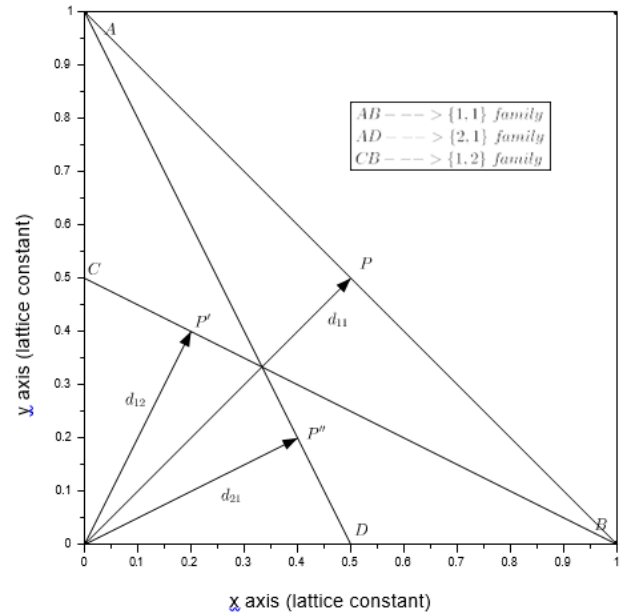
The idea is to convert each family of parallel planes in the real lattice to a single point in the reciprocal lattice, so that all perceivable families of planes in the real lattice may be replaced by one point each in the reciprocal space. Also, as discussed above, each family of planes can be represented by one single plane, therefore the next step would be to represent this single plane in the direct lattice by a single point in the reciprocal space.

Consider the plane (1,1) in Fig. 5(a). This plane represents the family {1,1} and can be uniquely

identified by the vector  $OP$ , whose direction is normal to (1,1) and whose magnitude is the inter-planar spacing,  $d_{11}$ , which is the smallest perpendicular distance to the plane (1,1) from the origin. Figure 5(b) shows the vectors  $OP, OPJ, OPJJ$  normal to the planes (1,1), (1,2) and (2,1) whose magnitudes are  $d_{11}, d_{12}, d_{21}$  and directions are  $O^{\wedge}P, O^{\wedge}PJ, O^{\wedge}PJJ$ . This may be repeated for all planes in Fig. 3(b) such that a similar normal vector is obtained for each of these planes.



(a) The normal vector  $OP$  to plane  $(1,1)$  with inter-planar spacing  $d_{11}$

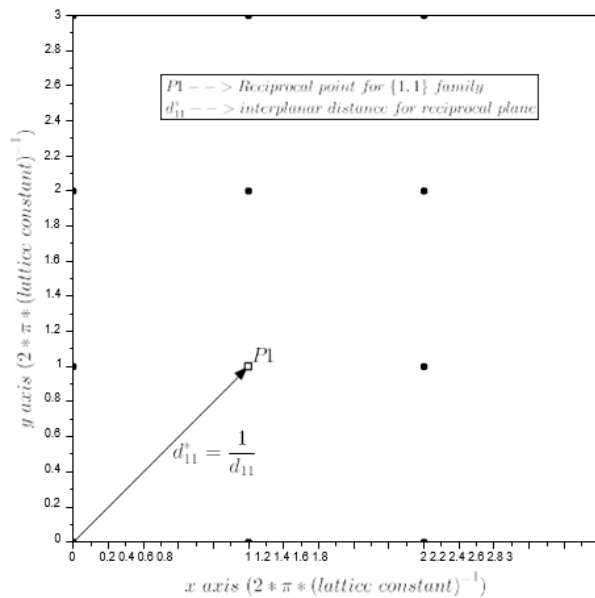


(b) Normal vectors  $OP$ ,  $OP'$  and  $OP''$  to planes  $(1,1)$ ,  $(1,2)$ ,  $(2,1)$  respectively with corresponding inter-planar spacings  $d_{11}$ ,  $d_{12}$  and  $d_{21}$

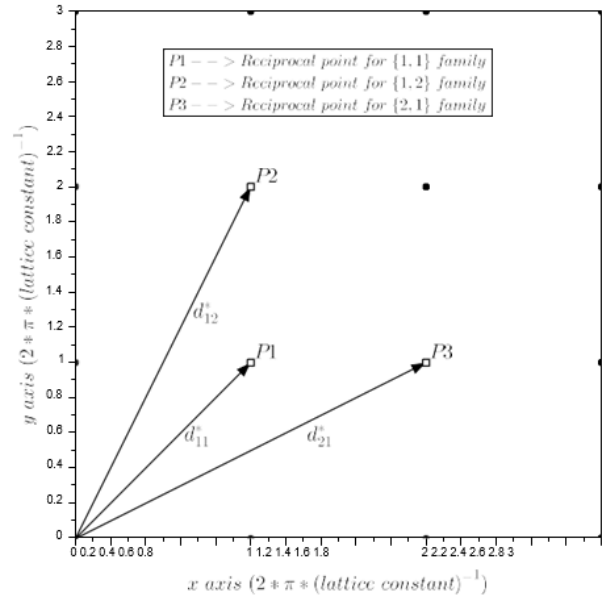
FIG. 5

Each normal vector is then converted to a single point in the reciprocal space. This is done for the vector  $OP$  in Fig. 6(a), by marking a point  $P1$  in the reciprocal space of Fig. 4, at a distance of  $1/d_{11}$  from the origin along the direction of  $O^{\wedge}P$ . Now this single point  $P1$  in the reciprocal space

represents the entire family of planes  $\{1,1\}$  as it contains the information about the orientation of the family of planes with respect to the origin as well as the inter-planar spacing between them. Figure 6(b) shows the reciprocal points for the families  $\{1,1\}$ ,  $\{1,2\}$  and  $\{2,1\}$ .



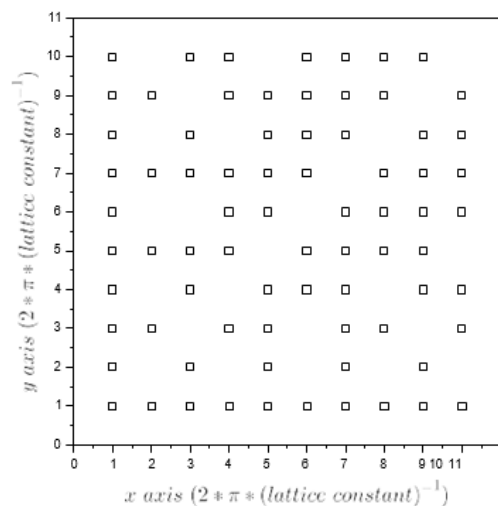
(a) Reciprocal point P1 in k space representing family of planes {1,1}



(b) Reciprocal points P1, P2 and P3 in k space representing families of planes {1,1}, {1,2} and {2,1}

FIG. 6

Generating the reciprocal points for all planes of 10 x 10 lattices which are shown in Fig. 3(b), one obtains a set of reciprocal points spread out in the k space as in Fig. 7(a). Each of these points corresponds to real planes in the direct lattice. Figure 7(b) shows these points superimposed on



the reciprocal lattice of Fig. 4. Thus, it may be observed that of all the reciprocal points in the entire reciprocal space, only some (marked as squares) correspond to real planes of the direct lattice.

- (a) The reciprocal points corresponding to real planes in the direct lattice.
- (b) Reciprocal space with the points corresponding to real planes shown as squares.

FIG. 7

### III. RECIPROCAL POINTS AND DIFFRACTION SPOTS

When a wave falls on a lattice, each family of parallel planes appears to it as a “diffraction grating” with grating constant being the interplanar spacing. Refer to Fig. 1, where each set

of parallel lines represents a diffraction grating.

Provided the wavelength of the incoming wave is of the order of the inter-planar spacings, those planes for which the angle of incidence satisfies the Bragg's Law, would produce a first-order diffraction spot on a photographic plate. The location of the diffraction spot on the photographic plate is analogous to finding the location of the reciprocal point P1 corresponding to the family of planes  $\{1,1\}$  on the reciprocal space. Just as the location of the reciprocal point P1 depends on the orientation of the family of planes and their inter-planar spacing, so does the location of diffraction spot on the photographic plate. Each family of planes will lead to one first-order diffraction spot, in the same manner as each family of

planes corresponds to one reciprocal point in  $k$  space. Thus, the reciprocal points obtained graphically in Fig. 7(a) from the real set of parallel planes of the direct lattice are a representation of the diffraction spots or the diffraction pattern obtained from the  $10 \times 10$  direct lattices.

Consequently, the reciprocal space provides a map of possible  $k$  values or wavelengths that can interact with a given direct lattice. The values of wave number  $k$  (or wavelength) that will interact with the direct lattice planes have a special significance as they are a spread of the diffraction pattern that would be obtained from the given direct lattice, thus establishing a connection between the reciprocal lattice and the diffraction pattern of a given direct lattice.

## References:

- <sup>1</sup> Kittel, C., McEuen, P., & McEuen, P., *Introduction to Solid State Physics*, (New York: Wiley., Vol. 8, 1996, pp. 105-130).
- <sup>2</sup> Ashcroft, N. W., and N. D. Mermin., *Solid State Physics Int. ed.*, (Holt-Saunders, Philadelphia 16, 1976).
- <sup>3</sup> Dekker, A. J., *Solid State Physics*, Vol. 6, (Seitz and D. Turnbull, eds., Academic Press, New York, 1958).
- <sup>4</sup> Morten Hannibal Madsen, Louise Høpfner, Nina Rasmussen, Mikkel Stolborg, Jesper Nygård, Robert Feidenhans'l, Jan W. Thomsen. "A classroom demonstration of reciprocal space", *American Journal of Physics*, **81**:4, pp. 274-279, (2013).
- <sup>5</sup> Thompson, D., "The reciprocal lattice as the Fourier transform of the direct lattice", *American Journal of Physics*, **64**, pp. 333-336, (1996).
- <sup>6</sup> Chen, N. X., "An elementary method for introducing the concept of reciprocal lattice", *American Journal of Physics*, **54** (11), pp. 1000-1002, (1986).
- <sup>7</sup> Smirnova, E. N., Pikhtilkova, O. A., Dobrovol'skii, N. N., & Dobrovol'skii, N. M., "Algebraic lattice in a metric space lattices", *Chebyshevskii Sbornik*, **18** (4), pp. 326-338, (2017).
- <sup>8</sup> Foadi, J., & Evans, G., "Elucidations on the reciprocal lattice and the Ewald sphere",

